JOURNAL OF APPLIED PHYSICS

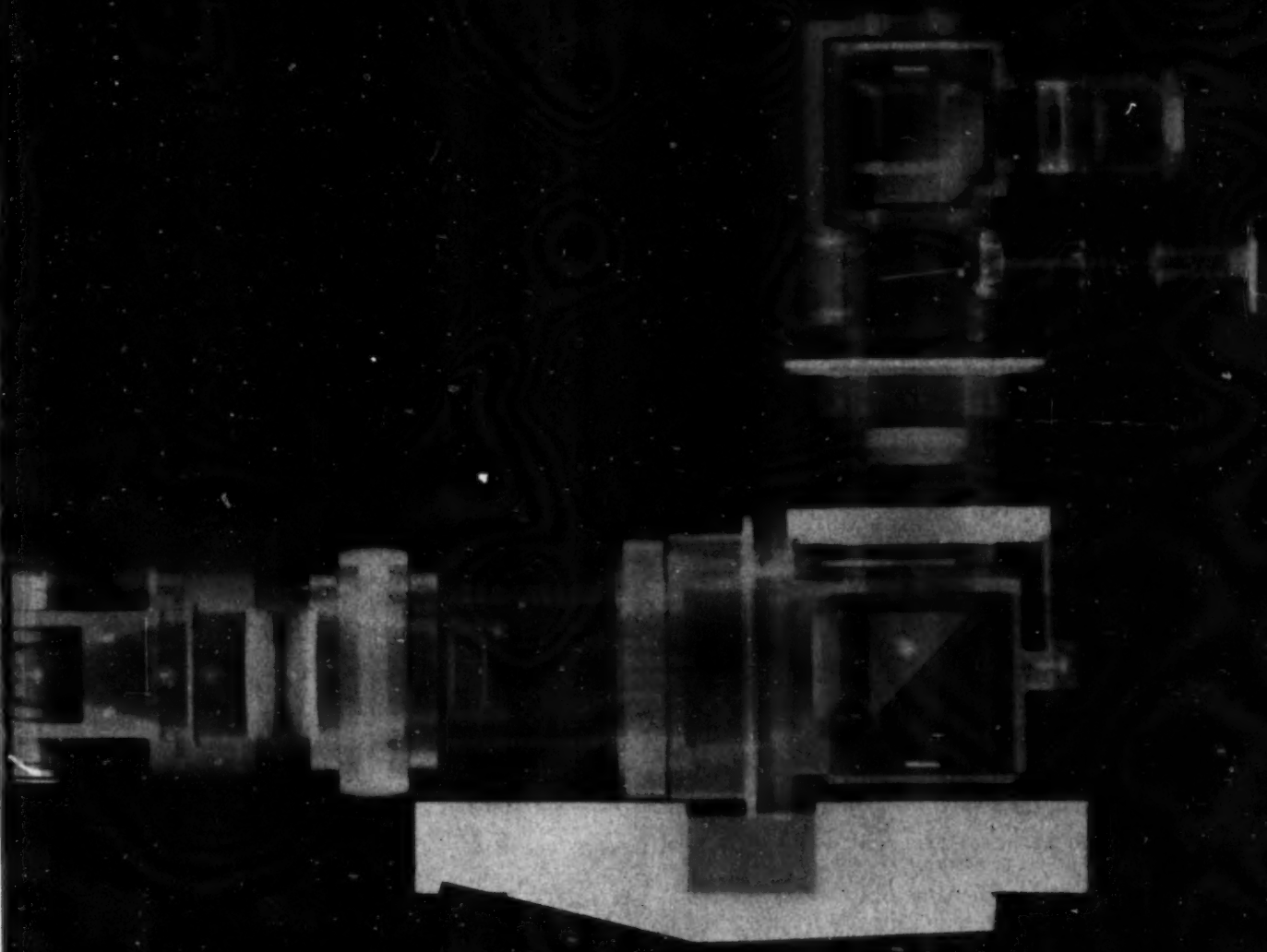

JOURNAL OF APPLIED PHYSICS

Vol. 16, No. 1 JANUARY, 1945

In This Issue

Page

Revised Publication Plans for the Papers from the Inaugural Meeting of the Division of High-Polymer Physics of the American Physical Society 1

Some Physical Properties of Elastomers at Low Temperature H. E. GREENE AND D. L. LOUGHBOROUGH 3

Retraction and Stress Propagation in Natural and Synthetic Gum and Tread Stocks B. A. MROWCA, S. L. DART, AND EUGENE GUTH 8

Theory of Filler Reinforcement EUGENE GUTH 20

Kinematic Errors in Bobbin Drives on Roving Frames S. L. GERHARD 26

Control of Elongation in Highly Stretched Cotton Tire Cord HOWARD J. PHILIPP AND CARL M. CONRAD 32

Ultraviolet Spectra of Biologically Important Molecules GLADYS A. ANSLOW 41

Thermodynamics of Rubber at Small Extensions D. R. ELLIOTT AND S. A. LIPPMANN 50

Contributed Original Research

Magnetic Permeability of Iron Wires at Radiofrequencies ALVA W. SMITH, F. P. DICKEY, AND S. W. FOOR 57

Letters to the Editor:

Theory of Filler Reinforcement JANE M. DEWEY 55

Etymology of the Word Microradiograph L. V. CHILTON 55

In Every Issue

Calendar of Meetings 2

Here and There 56

Recent Applications of Physics xviii

New Booklets xx

Index to Advertisers xxx

BOARD OF EDITORS

ELMER HUTCHISSON, *Editor*

Associate Editors

R. B. BARNES
OTTO BEECK
W. F. BUSSE
S. H. CALDWELL
CLARK GOODMAN
SELIG HECHT
W. J. LYONS
MORRIS MUSKAT
THOMAS H. OSGOOD
PAUL E. SABINE
FREDERICK SEITZ
J. R. TOWNSEND

Publication of the
American Institute of Physics

ADMINISTRATIVE STAFF

HENRY A. BARTON, *Director*

MADELINE M. MITCHELL, *Publications Manager*

JOHN T. TATE, *Adviser on Publications*

GOVERNING BOARD

PAUL E. KLOPSTEG, *Chairman*

GEORGE B. PEGRAM, *Secretary*

T. D. COPE
R. B. DOW
L. A. DUBRIDGE
FLOYD A. FIRESTONE
HARVEY FLETCHER
R. C. GIBBS
K. S. GIBSON
HERMANN MARK
A. G. WORTHING
JOHN T. TATE
L. W. TAYLOR
N. W. TAYLOR
WALLACE WATERFALL

The JOURNAL OF APPLIED PHYSICS, published monthly at Prince and Lemon Sts., Lancaster, Pa., is devoted to physics in its role as the science basic to other natural sciences and to the arts and industries. Previous to 1937 this publication was known as PHYSICS. The JOURNAL OF APPLIED PHYSICS publishes editorials, news of physicists, and reviews, as well as technical papers of applied physics.

Manuscripts should be submitted to Elmer Hutchisson, Editor, Case School of Applied Science, Cleveland 6, Ohio.

Subscriptions and orders for back numbers should be addressed to Prince and Lemon Streets, Lancaster, Pa. or to the American Institute of Physics, 57 East 55 Street, New York 22, N. Y.

Subscription Price

	U. S. AND CANADA	ELSEWHERE
To members of scientific societies	$5.00	$5.70
To all others	7.00	7.70

Back Number Prices

Complete set: Vol. 1, July, 1931–Vol. 15, 1944—**$94.50**
Yearly back number rate: **$7.70**
Single copies: **$0.70** each.

Changes of address and proofs should be addressed to the Publications Manager.

Advertising rates supplied on request. Orders, advertising copy, and cuts should be sent to the American Institute of Physics.

Entered as second class matter January 22, 1937, at the Post Office at Lancaster, Pennsylvania, under the Act of March 3, 1879
Accepted for mailing at the special rate of postage provided for in the Act of February 28, 1925, authorized May 2, 1932.

Copyright 1945, by the American Institute of Physics.

W.M

Journal of Applied Physics

Board of Editors

ELMER HUTCHISSON, *Editor*

Associate Editors

R. B. BARNES
OTTO BEECK
W. F. BUSSE
S. H. CALDWELL
CLARK GOODMAN
SELIG HECHT
W. J. LYONS
MORRIS MUSKAT
THOMAS H. OSGOOD
PAUL E. SABINE
FREDERICK SEITZ
J. R. TOWNSEND

VOLUME 16

JANUARY–DECEMBER, 1945

Published by the

AMERICAN INSTITUTE OF PHYSICS
Incorporated

INFORMATION FOR CONTRIBUTORS

Manuscripts

Send manuscripts to Elmer Hutchisson, Case School of Applied Science, Cleveland 6, Ohio.

Papers must be in English, typewritten double spaced with wide margins on a durable white paper, preferably lettersize. The original copy, not the carbon, should be submitted.

For general style, spellings, abbreviations, and form, recent issues of this journal should be consulted.

Abstracts

An abstract must accompany each article. It should be adequate as an *index* and as a *summary*. As an index it should give all subjects, major and minor, concerning which new information is presented. As a summary it should give the conclusions of the article and all numerical results of general interest.

Mathematical Expressions

Make all expressions clear to the typesetter. Identify in the margin of the manuscript Greek letters and unusual symbols.

Use fractional exponents instead of root signs.

Avoid complicated exponents and subscripts. Should it be necessary to repeat a complicated expression a number of times it should be represented by some convenient symbol.

The solidus (/) should be used wherever possible for fractions.

References

References should appear as footnotes, numbered consecutively, and arranged thus:

[1] A. B. Smith, Phys. Rev. **41**, 852 (1932).

[2] G. R. Harrison, *Atoms in Action* (William Morrow & Company, New York, 1939), first edition, p. 30.

Figures and Tables

Legends for figures must accompany manuscript. Each table should have a caption. These in all cases should be complete in themselves so as to make the data intelligible to the reader without reference to the text. Each figure and table should be cited in sequence in the text.

Line Drawings and Photographs

Plan figures for approximately one-half reduction. Wherever possible arrange figures so that after reduction they will not be wider than three inches. Lettering must be large enough to be readable after reduction.

Line drawings must be made with India ink on white paper or tracing cloth. Coordinate paper is not desirable, but if used must be blue-lined and all coordinates to be reproduced drawn with India ink.

Drawings which cannot be used will be returned to the author.

Photographs should show clear black and white contrasts.

Avoid round and oval photographs.

Alterations

Take great care that each manuscript is typographically accurate. A limited number of alterations in proof are unavoidable, but the cost of making extensive alterations after the article has been set in type will be charged to the author.

Proof and all correspondence concerning papers in the process of publication should be addressed to the Publications Manager, American Institute of Physics, 57 East 55 Street, New York 22, New York.

INFORMATION FOR SUBSCRIBERS

The JOURNAL OF APPLIED PHYSICS is devoted to physics in its role as the science basic to other natural sciences and to the arts and industries. Previous to 1937 this publication was known as PHYSICS. It aims to be of service not only in physical laboratories, but also in the laboratories of industrial, chemical, geological, geophysical, meteorological, radio, and similar concerns. The JOURNAL OF APPLIED PHYSICS publishes editorials, news of physicists, and reviews, as well as technical papers of applied physics.

Subscriptions and orders for back numbers should be addressed to the American Institute of Physics, 57 East 55 Street, New York 22, New York.

SUBSCRIPTION PRICE

	U. S. AND CANADA	ELSEWHERE
To members of scientific societies ..	$5.00	$5.70
To all others	7.00	7.70

BACK NUMBER PRICE

Complete set: Vol. 1, July, 1931—Vol. 15, 1944—$94.50.
Yearly back number rate: $7.70.
Single copies: $0.70 each.

Advertising rates will be supplied on request.

American Institute of Physics

57 East 55 Street **New York 22, New York**

Physics
Taylor

CONTENTS

JANUARY, 1945

Revised Publication Plans for the Papers from the Inaugural Meeting of the Division of High-Polymer Physics of the American Physical Society 1
Some Physical Properties of Elastomers at Low Temperature . . . . . H. E. GREENE AND D. L. LOUGHBOROUGH 3
Retraction and Stress Propagation in Natural and Synthetic Gum and Tread Stocks . . . . . B. A. MROWCA, S. L. DART, AND EUGENE GUTH 8
Theory of Filler Reinforcement . . . . . EUGENE GUTH 20
Kinematic Errors in Bobbin Drives on Roving Frames . . . . . S. L. GERHARD 26
Control of Elongation in Highly Stretched Cotton Tire Cord . . . . . HOWARD J. PHILIPP AND CARL M. CONRAD 32
Ultraviolet Spectra of Biologically Important Molecules . . . . . GLADYS A. ANSLOW 41
Thermodynamics of Rubber at Small Extensions . . D. R. ELLIOTT AND S. A. LIPPMANN 50
Magnetic Permeability of Iron Wires at Radiofrequencies . . . . . ALVA W. SMITH, F. P. DICKEY, AND S. W. FOOR 57

Letters to the Editor:

Theory of Filler Reinforcement . . . . . JANE M. DEWEY 55
Etymology of the Word Microradiograph . . . . . L. V. CHILTON 55
Calendar of Meetings 2
Here and There 56
Recent Applications of Physics xviii
New Booklets xx

FEBRUARY, 1945

Physics in 1944 . . . . . THOMAS H. OSGOOD 61
Small Prism Infra-Red Spectrometry . . . . . R. BOWLING BARNES, ROBERT S. MCDONALD, VAN ZANDT WILLIAMS, AND RICHARD F. KINNAIRD 77
General Theory of Stresses and Displacements in Layered Systems. I . D. M. BURMISTER 89
Use of the Electron Diffraction Camera to Detect Insulating Films . EILEEN I. ALESSANDRINI 94
Crystal Interference Phenomena in Electron Microscope Images . . . . . R. D. HEIDENREICH AND L. STURKEY 97
Sustained Subharmonic Response in Non-Linear Series Circuits . . . CHARLES F. SPITZER 105
X-Ray Diffraction Study of the Fatigue in Metals at High Stresses . . ARTHUR G. BARKOW 111
Erratum: Fatigue of Fabrics . . . . . W. F. BUSSE, E. T. LESSIG, D. L. LOUGHBOROUGH, AND L. LARRICK 120

Here and There 87
New Books 87
New Booklets 88

MARCH, 1945

Electrical Research in the U.S.S.R. . . . . GERALD OSTER 121
General Theory of Stresses and Displacements in Layered Soil Systems. II . D. M. BURMISTER 126
Electrical Charging of Electron Diffraction Specimens . D. G. BRUBAKER AND M. L. FULLER 128
100-kv Electron Microscope . . . . . L. MARTON 131
Solution of the Diffusion Equation Applicable to the Edgewise Growth of Pearlite . . . . . W. H. BRANDT 139
Production Histories of Oil Producing Gas-Drive Reservoirs . . . . . MORRIS MUSKAT 147
Effects of Temperature and Humidity on the Physical Properties of Tire Cords . . . . . J. H. DILLON AND I. B. PRETTYMAN 159
Numerical Solution of Ordinary and Partial Differential Equations by Means of Equivalent Circuits . . . . . GABRIEL KRON 172
Erratum: Physical Aspects of Foaming in Steam Generation . . . . . HANS M. CASSEL 186

Letter to the Editor: . . . . . W. JAMES LYONS 187

Here and There 125
New Book 125
Recent Applications of Physics 188

APRIL, 1945

Mobilization of Scientific Resources—V, The U. S. Army 189
Organization of the War Department and Coordination of the General Staff with Operating Divisions of the Army 190
Army Research and Development . . . . . BRIGADIER GENERAL W. A. BORDEN 195
Research and Development at Wright Field . . . . . BRIGADIER GENERAL F. O. CARROLL 199
Development for Army Ground Forces . . . . . MAJOR GENERAL A. W. WALDRON 203
Research and Development Division, Headquarters, Army Service Forces . . . . . COLONEL R. M. OSBORNE 207
Research in the Technical Division, Chemical Warfare Service . . . . . BRIGADIER GENERAL W. C. KABRICH 211
Research in the Corps of Engineers . . . . . BRIGADIER GENERAL JOHN W. N. SCHULZ 216
Research Program of the Office of the Surgeon General, U. S. Army . . . . . LT. COLONEL LEON H. WARREN 227
Research in the Military Planning Division, Quartermaster Corps . . . . . COLONEL GEORGES F. DORIOT 235
Research in the Engineering and Technical Service, Signal Corps . . . . . MAJOR GENERAL G. L. VAN DEUSEN, COLONEL VICTOR A. CONRAD, COLONEL WILLIAM L. BAYER, LIEUTENANT GEORGE OWEN, AND COLONEL GORDON G. IRWIN 244
Letter to the Editor . . . . . WESLEY E. BRITTIN AND MAYNARD G. ARSOVE 262
Proceedings of the Electron Microscope Society of America 263
Erratum: Some Physical Properties of Elastomers at Low Temperatures . . . . . H. E. GREENE AND D. L. LOUGHBOROUGH 266
Here and There 257
New Booklets 257
New Books 258
Recent Applications of Physics xviii

MAY, 1945

Mechanics of the Metal Cutting Process. I. Orthogonal Cutting and a Type 2 Chip . . . . . M. EUGENE MERCHANT 267
Optimum Height of Flight of Winged Rocket- or Jet-Bomb . M. ZBIGNIEW L. KRZYWOBLOCKI 275
Deflection Sensitivity of Parallel-Wire Lines in Cathode-Ray Oscillographs . . . . . H. GUNTHER RUDENBERG 279
Novel Form of Refrigerator . . . . . J. R. ROEBUCK 285
General Theory of Stresses and Displacements in Layered Soil Systems. III. . . . . D. M. BURMISTER 296
Stability of Low Pressure Mercury Arcs as a Function of Current . . . . . PAUL COPELAND AND W. H. SPARING 302
Validity of the Pole Figure . . . . . BEULAH FIELD DECKER 309
Message to All Interested in Physics . . . . . HOMER L. DODGE 310
Letter to the Editor:
Wave Equation for Finite Elastic Strains . . . . . A. NADAI 313
Here and There 311
New Booklets 311
New Books 312
Recent Applications of Physics 314

JUNE, 1945

Mechanics of the Metal Cutting Process. II. Plasticity Conditions in Orthogonal Cutting . . . . . M. EUGENE MERCHANT 318
Frictional Properties of Some White Metal Bearing Alloys: The Role of the Matrix and the Hard Particles . . . . . D. TABOR 325
High Temperature, High Pressure Rheometer for Plastics . . . . . H. K. NASON 338
Relationship between the Rheological Properties and Working Properties of Printing Inks . . . . . ROLF BUCHDAHL AND JOAN E. THIMM 344
Electromagnetic Field Inside a Cylinder with a Gap . . . . . C. C. WANG 351
Convection Currents in a Porous Medium . . . . . C. W. HORTON AND F. T. ROGERS, JR. 367
Pigment Dispersion Methods for Electron Microscopy . . . . . H. C. O'BRIEN, JR. 370
News from Here and There 315
New Booklets 317
New Books 317

JULY, 1945

Bibliography of Electron Microscopy. III. . . . . CLAIRE MARTON AND SAMUEL SASS 373
Hipersil—A Greatly Improved Transformer Iron . . . . . T. D. YENSEN 379
Comparison of Some Elastic Properties of Tire Cords . . . . . HELMUT WAKEHAM, EDITH HONOLD, AND EVALD L. SKAU 388
On the Distribution of Current along Asymmetrical Antennas . . . . . LT. COMMANDER CHARLES W. HARRISON, JR. 402
Correction of X-Ray Diffraction Intensities for Lorentz and Polarization Factors . . . . . M. J. BUERGER AND GILBERT E. KLEIN 408
Determination of Molecular-Weight Distribution in High Polymers by Means of Solubility Limits . . . . . D. R. MOREY AND J. W. TAMBLYN 419
Techniques for Evaporation of Metals . . . . . LEONARD O. OLSEN, CHARLES S. SMITH, AND E. C. CRITTENDEN, JR. 425

Letter to the Editor:

Adaptation of Special Specimen Holders to Commercial Electron Microscopes . . . . . L. MARTON 387
Here and There 386
Recent Applications of Physics 434

AUGUST, 1945

Microwave Impedance Measurements with Application to Antennas. I . . . . . D. D. KING 435
Microwave Impedance Measurements with Application to Antennas. II . . . . . RONOLD KING AND D. D. KING 445
Secondary Electron Emission of Pyrex Glass . . . . . C. W. MUELLER 453
Structure of Certain Muscle Fibrils as Revealed by the Use of Electron Stains . . . . . C. E. HALL, M. A. JAKUS, AND F. O. SCHMITT 459
Wave Guides and the Special Theory of Relativity . . . . . W. D. HERSHBERGER 465
Discussion of the Illuminating System of the Electron Microscope . . . . . JAMES HILLIER AND R. F. BAKER 469

Here and There 484
New Booklets 485
New Books 485
Recent Applications of Physics 486

SEPTEMBER, 1945

News of the Hour 487
Design of X-Ray Powder Cameras . . . . . M. J. BUERGER 501
Extension of the Beam Theory to Tapered Beams and Conical Shells . . . . . LEON BESKIN 511
On Maximum Gain-Band Width Product in Amplifiers . . . . . W. W. HANSEN 528
"Power Function" for the Determination of Lagrangian Generalized Forces . D. A. WELLS 535
Flow Orientation in Isotropic Fluids . . . . . A. BONDI 539
Three-Dimensional Fourier Transforms and Their Application to Maxwell's Equations . . . . . F. T. ADLER 545
Erratum: "On the Representation of Rigid Rotations" . . . . . E. T. BENEDIKT 551

Letter to the Editor . . . . . ARTHUR M. G. MOODY 551

New Booklets 550
New Book 550
Here and There 552

OCTOBER, 1945

Basic Principles of Semi-Conductors . . . . . FREDERICK SEITZ 553
Electrical Properties of Semi-Conductors . . . . . ROBERT J. MAURER 563
On the Representation of Rigid Rotations . . . . . H. SCHWERDTFEGER 571
100-Million Volt Induction Electron Accelerator . W. F. WESTENDORP AND E. E. CHARLTON 581
Thermal Expansion and Second-Order Transition Effects in High Polymers . . . . . R. F. BOYER AND R. S. SPENCER 594
Method of Measuring the Radiofrequency Resistance of Wires . . CHANDLER STEWART, JR. 608
Absorption Displacement in X-Ray Diffraction by Cylindrical Samples . . . . B. E. WARREN 614
Molecular Weight Studies on High Polymers with the Electron Microscope . . . . . R. F. BOYER AND R. D. HEIDENREICH 621
Conversion Diagrams for Triode Tube Mixers . . . . . HARRY STOCKMAN 639

Letters to the Editor:

On a Novel Form of Refrigerator . . . W. D. Hayes 642
Wave Equations for Finite Elastic Strains . . . Hubert M. James and Eugene Guth 643
Here and There . . . 577
New Booklets . . . 580
Recent Applications of Physics . . . 644

November, 1945

Proposed "Atomic Energy Act of 1945" . . . 645
Gas Flow in the Mass Spectrometer . . . Richard E. Honig 646
Use of Direct Current in Induction Electron Accelerators . . . W. F. Westendorp 657
Crucible Failure in the Induction Melting Process . Andrew Gemant and Joseph Sticher 661
Double-Solenoid Coil System for Magnetic Measurements . . . E. W. Frowe and C. J. Aronson 667
Class of Electron Lenses Which Satisfy Newton's Image Relation . . . R. G. E. Hutter 670
Rigorous Treatment of the Electrostatic Immersion Lens Whose Axial Potential Distribution is Given by: $\phi(z) = \phi_0 e^{K \arctan z}$ . . . R. G. E. Hutter 678
Methods of Specifying the Properties of Viscoelastic Materials . . . Turner Alfrey and Paul Doty 700
Double-Yoke Plate Permeameter . . . William F. Brown, Jr. and Sidney M. Rubens 713
Electron Diffraction Camera for the Study of High Temperature Surface Reactions . . . Earl A. Gulbransen 718
Virtual Masses of Rectangular Plates and Parallelepipeds in Water . . . Yee-Tak Yu 724
Electron Microscopical Replica Techniques for the Study of Organic Surfaces . . . R. Bowling Barnes, Charles J. Burton, and Robert G. Scott 730
Stability of the Low Pressure Mercury Arc as a Function of Area at the Cathode Pool . . . Carroll W. Lufcy and Paul L. Copeland 740

Here and There . . . 655
New Booklets . . . 656

December, 1945

Research and Development in the Ordnance Department, U. S. Army

Research and Development Service . . . Major General G. M. Barnes 745
Research—Its Coordination and Application in the Development of Ordnance Materiel . . . Colonel Scott B. Ritchie 747
Ammunition Research and Development . . . Colonel I. A. Luke 751
Artillery Materiel Research and Development . . . Colonel W. R. Gerhardt 757
Small Arms and Small Arms Ammunition Research and Development . . . Colonel R. R. Studler 760
Rockets and Missiles . . . Colonel G. W. Trichel 764
Tank and Automotive Development . . . Colonel Joseph M. Colby 767
Aircraft Armament . . . Lt. Colonel George C. Gentry 771
Some Recent Advances in Ballistics . . . The Staff of the Ballistic Research Laboratory 773
Ferrous Metallurgical Research . . . Lt. Colonel N. A. Matthews 780
Non-Ferrous Metallurgical Research at Frankford Arsenal . . . Lt. Colonel C. H. Greenall 787
Research and Development, Military Explosives and Propellants . . . Colonel Miles W. Kresge 792
Research and Development of Materials for Ordnance Materiel . . . Colonel J. H. Frye 797
Fuels and Lubricants . . . Lt. Colonel R. E. Jeffrey, Jr. 801

Determination of Coexisting Phases in Heterogeneous Systems of Many Components . . . Paul A. Beck 808
Production and Decomposition of Ozone by Low Pressure Mercury Vapor Lamps . . . L. R. Koller 816
Flexural Vibration of Unrestrained Cylinders and Disks . . . Gerald Pickett 820
High Dispersion Electron Diffraction by Primary Magnification . . . G. L. Simard, Charles J. Burton, and R. Bowling Barnes 832
Strain Hardening Under Combined Stresses . . . W. Prager 837
Coil Systems for Producing Transverse and Longitudinal Magnetic Gradients . . . George H. Shortley and Albert May 841
Data on Rate of Capillary Rise . . . Elmo J. LeGrand and William A. Rense 843
Letter to the Editor: A Novel Form of Refrigerator . . . J. R. Roebuck 846

Author Index to Volume 16 . . . 849
Subject Index to Volume 16 . . . 852
Volume Table of Contents . . . III
Here and There . . . 806
New Booklets . . . 847
Recent Applications of Physics . . . 848

Journal
of
Applied Physics

Volume 16, Number 1 January, 1945

Revised Publication Plans for the Papers from the Inaugural Meeting of the Division of High-Polymer Physics of the American Physical Society

THE WPB restrictions on the use of paper apply equally to journals publishing scientific research and those publishing comic strips or love stories. Because of these restrictions, the initial plans to publish all of the papers from the Inaugural Meeting on June 23–24 of the Division of High-Polymer Physics of the American Physical Society in the November, 1944 issue of this journal had to be abandoned. Also because of the large number of manuscripts now being submitted for 1945 and in anticipation of the restrictions applying during the coming year, the size of the January, 1945 issue of the *Journal of Applied Physics* cannot materially exceed the average during the past year. Realizing these circumstances, the Editor has appealed for assistance to the Editor of *The Journal of Chemical Physics* in the publication of this series of papers. This assistance has kindly been provided and we are, therefore, dividing most of the papers which were not published in November between the January issues of *The Journal of Chemical Physics* and the *Journal of Applied Physics*. A complete list of the papers presented at the meeting is given below together with the present publication schedule. It is hoped that the authors of the papers and the members of the Division of High-Polymer Physics will be patient with the changes which have had to be made in publication plans.

Publication Schedule of Papers from June 23–24 Meeting of Division of High-Polymer Physics

1. A. V. Tobolsky and R. D. Andrews—"Systems Manifesting Superposed Elastic and Viscous Behavior"	January, J. Chem. Phys. **13**, 3 (1945).
2. W. O. Baker—"Transition Phenomena in High Polymers"	Paper not now available.
3. T. Alfrey—"A Contribution to the Kinematic Theory of Rubber Elasticity" (Publication title "Molecular Theory of the Viscoelastic Behavior of an Amorphous Linear Polymer")	September, J. Chem. Phys. **12**, 374 (1945).
4. B. A. Mrowca, S. L. Dart, and E. Guth—"Retraction and Stress Propagation in Natural and Synthetic Gum and Tread Stocks"	January, J. App. Phys. **16**, 8 (1945).
5. R. S. Havenhill, H. C. O'Brien, and J. J. Rankin—"Electrostatic Properties of Rubber and GR-S"	November, J. App. Phys. **15**, 731 (1944).
6. R. B. Stambaugh, M. Rohner, and S. D. Gehman—"Speed of Retraction of Rubber"	November, J. App. Phys. **15**, 740 (1944).
7. S. L. Dart and E. Guth—"Rise of Temperature on Fast Stretching of Butyl Rubber"	January, J. Chem. Phys. **13**, 28 (1945).
8. H. M. Smallwood—"Limiting Law of the Reinforcement of Rubber"	November, J. App. Phys. **15**, 758 (1944).
9. F. L. Roth and L. A. Wood—"Some Relations Between Stress, Strain, and Temperature in a Pure-Gum Vulcanizate of GR-S Synthetic Rubber"	November, J. App. Phys. **15**, 749 (1944).
10. F. S. Conant and J. W. Liska—"Some Low Temperature Properties of Elastomers"	November, J. App. Phys. **15**, 767 (1944).

11. H. E. Greene and D. L. Loughborough—"Some Physical Properties of Elastomers at Low Temperatures"	January, J. App. Phys. **16**, 3 (1945).
12. H. Mark, P. M. Doty, and B. H. Zimm—"Molecular Weight and Molecular Weight Distribution of High Polymers by Light Scattering Measurements"	Paper not now available.
13. E. Guth—"Theory of Filler Reinforcement"	January, J. App. Phys. **16**, 20 (1945).
14. R. S. Spencer and R. F. Boyer—"Factors Influencing the Brittle Point of High Polymers"	Paper not now available.
15. S. L. Gerhard—"Kinematic Errors in Bobbin Drives on Roving Frames"	January, J. App. Phys. **16**, 26 (1945).
16. H. J. Philipp and C. M. Conrad—"Control of Elongation in Highly Stretched Cotton Tire Cord"	January, J. App. Phys. **16**, 32 (1945).
17. W. J. Lyons—"The Influence of Velocity Gradient on the Relation Between Viscosity and Concentration in Cuprammonium Solutions of Cellulose"	January, J. Chem. Phys. **13**, 43 (1945).
18. S. E. Sheppard and P. T. Newsome—"Orientation of Hydrophile Xerogels in an Electric Field"	Part I published in June, J. Chem. Phys. **12**, 244 (1944). Part II, December, J. Chem. Phys. **12**, 513 (1944).
19. D. R. Morey and J. W. Tamblyn—"Determination of Molecular Weights of High Polymers by Solubility Methods"	Paper has been submitted to Ind. Eng. Chem.
20. M. L. Huggins—"Comparison of the Structures of Stretched Linear Polymers"	January, J. Chem. Phys. **13**, 37 (1945).
21. J. W. Tamblyn, R. L. Tichener, D. R. Morey, and R. H. Wagner—"Fractionation, Viscosity, and Osmotic Pressure Studies on Cellulose Esters"	Paper not now available.
22. G. A. Anslow—"Ultraviolet Spectra of Biologically Important Molecules"	January, J. App. Phys. **16**, 41 (1945).
23. D. R. Elliott and S. A. Lippmann—"The Thermodynamics of Rubber at Small Extensions"	January, J. App. Phys. **16**, 50 (1945).

Calendar of Meetings

January

17–19	American Society of Civil Engineers, Hotel Commodore, New York, New York
19–20	American Physical Society, Columbia University, New York, New York
19–20	American Association of Physics Teachers, Columbia University, New York, New York
22–24	American Society of Heating and Ventilating Engineers, Boston, Massachusetts
22–26	American Institute of Electrical Engineers, New York, New York
24–27	Institute of Radio Engineers, Hotel Commodore, New York, New York
30 to Feb. 1	Institute of Aeronautical Sciences, Columbia University, New York, New York

February

13	Physics Club of Chicago, Chicago, Illinois
18–22	American Institute of Mining and Metallurgical Engineers, New York, New York
19–22	Technical Association of the Pulp and Paper Industry, Hotel Commodore, New York, New York
23–24	Inter-Society Color Council, Hotel Pennsylvania, New York, New York
24	American Mathematical Society, New York, New York
24	American Physical Society, Metropolitan Section, Columbia University, New York, New York
27–28	American Astronomical Society, Columbia University, New York, New York
28	American Society for Testing Materials, Pittsburgh, Pennsylvania

March

13	Physics Club of Chicago, Chicago, Illinois

April

1–3	American Institute of Chemical Engineers, Houston, Texas
4–6	Society of Automotive Engineers, New Yorker Hotel, New York, New York (National Aeronautic Meeting)
10	Physics Club of Chicago, Chicago, Illinois
12–14	Optical Society of America, Hotel Statler, Cleveland, Ohio
15–19	American Ceramic Society, Buffalo, New York
16–18	American Society of Mechanical Engineers, Boston, Massachusetts
19–21	American Philosophical Society, Philadelphia, Pennsylvania
25–26	American Institute of Electrical Engineers, Buffalo, New York
25–27	American Institute of Mining and Metallurgical Engineers, Chicago, Illinois
27–28	American Mathematical Society, New York, New York
28	American Mathematical Society, Chicago, Illinois
28	American Mathematical Society, Stanford University, California

May

2–3	Society of Automotive Engineers, Hotel William Penn, Pittsburgh, Pennsylvania
14–18	Society of Motion Picture Engineers, Hollywood-Roosevelt Hotel, Hollywood, California
16–17	Society of Automotive Engineers, Carter Hotel, Cleveland, Ohio
16–19	Institute of Aeronautical Sciences, Buffalo, New York

June

18–21	American Society of Mechanical Engineers, Chicago, Illinois
18–22	American Society for Testing Materials, Buffalo, New York
23	Mathematical Association of America, Montreal, Canada
25–29	American Institute of Electrical Engineers, Detroit, Michigan

Some Physical Properties of Elastomers at Low Temperature*

BY H. E. GREENE AND D. L. LOUGHBOROUGH

The B. F. Goodrich Company, Akron, Ohio

(Received Sept. 20, 1944)

Little has been published concerning the effect of low temperature on the elasticity of rubbers. Since in many applications this is the only property which justifies their use, some attention must be paid to this problem. Rubbers can be characterized by the temperature at which they become brittle and by the width of the transition region. The sharpness of the transition between the elastic and the glassy states is greatest when the testing time is long compared to the molecular relaxation times. Other physical factors such as sample shape, stress at which the modulus is calculated, and the previous history of the sample affect the absolute nature of the elastic properties measured. A test is described which gives the values of the elastic constants at slow rates of extension, at moderate extensions, on previously flexed samples. For these conditions the superiority of gum stocks at low temperature decrease in the order polybutadiene, natural rubber, Butyl, Neoprene FR. The comparative values of the stocks can be changed by compounding variations. Addition of plasticizer shifts the relative modulus vs. temperature curve down the temperature scale without producing a significant change in shape. Addition of reinforcing materials decreases the sharpness of the transition without changing the position of the curve.

INTRODUCTION

THE design of a laboratory test to duplicate the service performance of a product is always difficult. When carried out carefully it becomes as involved as a direct use test. To circumvent these difficulties in low temperature measurements we have chosen to measure well-defined constants over a range of independent variables. From an interpretation of these data one can predict performance in a way not possible by service-simulating tests. The analysis does, however, demand an understanding of the physical nature of stress-strain properties including at least a qualitative understanding of the mechanism involved.

Below the second-order transition temperature[1] an elastomer is hard and brittle. This glassy state is characterized by an elastic modulus in the neighborhood of 10^7 p.s.i.[2] As the temperature increases the modulus decreases rapidly along a sigmoidal curve until the modulus has reached a value of approximately 10^2 p.s.i. With further increase in temperature the modulus increases linearly with absolute temperature in a manner successfully explained by the kinetic thermodynamic approach.[3–7] The modulus-temperature curve consists, then, of three parts: (1) a glassy region, (2) a transition, (3) an elastic region.

The value of the stress for a given strain at any temperature depends upon the ratio of the test interval to the time required for equilibrium to be established. The ratio decreases as the temperature decreases until in the transition region equilibrium is not established in an interval at all comparable with the testing time. Here, the values of the modulus, or any other elastic property, depend greatly on the testing rate as shown in Fig. 1. To obtain these data the samples were stressed at the test temperature and the strain measured at different times.

For short time tests the transition curve is less

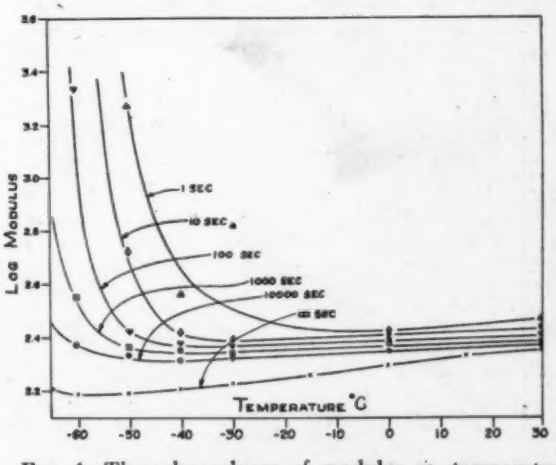

FIG. 1. Time dependence of modulus *vs.* temperature curve for a pure gum natural rubber stock. Modulus calculated from strain after recorded times have elapsed.

* Presented on June 24, 1944 before the Inaugural Meeting of the Division of High-Polymer Physics of the American Physical Society at Rochester, New York.

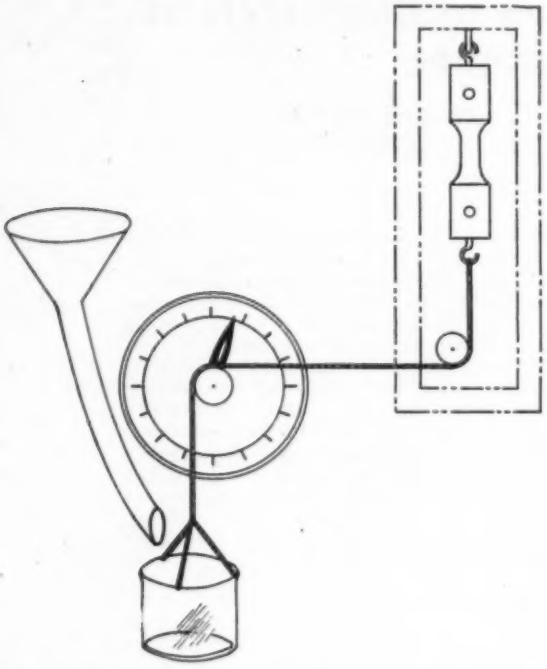

FIG. 2. Diagram of the apparatus used for the single-point method of determining modulus.

abrupt, and stiffening begins at relatively high temperatures. For long time tests the modulus decreases with decreasing temperature as predicted by thermodynamic theories. The infinite time curve of Fig. 1 was taken at true thermodynamic equilibrium by measuring the stress required to hold the sample at fixed length as the temperature is decreased slowly—a so-called isometric.[8] No correction was made for the thermal expansion of the supporting structure.

The physical mechanism associated with the transition region has never been described completely, but it is clear that the phenomenon is associated with a change in molecular relaxation times.[9–12]

In many uses a rubberlike material with a modulus greater than five times its value at room temperature is unsuitable. In these cases the temperature at which the material becomes glassy is not useful for evaluation. Measurements of the physical properties as a function of temperature are required.

EXPERIMENTAL

Very little of the work in the literature[13] deals with such variations and there is almost none that records values for moderate elongations (about 100 percent) and low testing rate (around 100 p.s.i./min.), determined on previously flexed samples measured in tension.

To supply the required data a simple test apparatus has been designed. In general the sample is extended by means of force applied to the free end through a cable extending out of the test chamber to a measuring head. Either of two methods can be used for the determination of the stress and strain. One is for exploratory work in which a large number of samples are involved; the other is valuable when complete curves are required.

The first device is indicated in Fig. 2. To the free end of the sample is attached a cable which extends around a pulley, out of the refrigerator, and over another pulley to a weight pan. Attached to the external pulley and in front of a scale is a pointer which indicates the length of

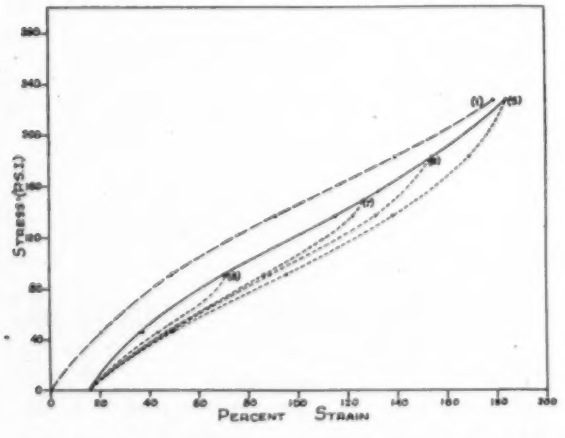

FIG. 3. The complete stress-strain curve of the first, fifth, sixth, seventh, and eighth cycles. Pure gum rubber stock at −42°C.

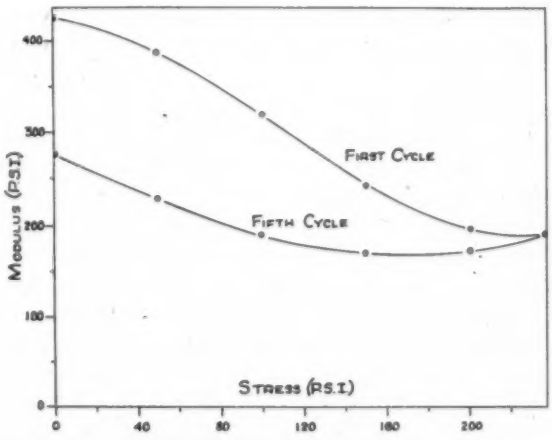

FIG. 4. Modulus at different stresses for first and fifth cycles. A GR-S stock at 24°C.

wire which passes, and hence, the sample elongation.

With this set-up the grips are attached and the sample is flexed to 100 percent several times by hand at room temperature, and then placed in the refrigerator at −70°C. When the conditioning time has elapsed, the sample is moved into position, and enough granulated lead is added, at a fixed rate of 1 lb./min., to the pan to produce 100 p.s.i. stress above the tare weight. The resulting extension is read on the scale and the modulus calculated. The experiment is repeated at 10° intervals up to 30°C, allowing approximately one-half hour conditioning time at each temperature.* The relaxed sample length used for calculating percent strain is then measured.

In the second method the entire stress-strain curve is recorded by a simple device designed to measure both stress and strain on a single wire from the test chamber.[15]

When complete information on one stock is desired, this machine is used. The sample is placed in the refrigerator unflexed and given a definitely prescribed history. The most common procedure is to extend the samples at the testing rate to 100 p.s.i. and back to zero stress four times without pause before recording the stress-strain curve. Further cycles give almost reproducible curves (Fig. 3). A different sample is used at each temperature when the modulus on the first cycle is also desired. The equilibrium cycle at a number of temperatures is shown in Fig. 4.

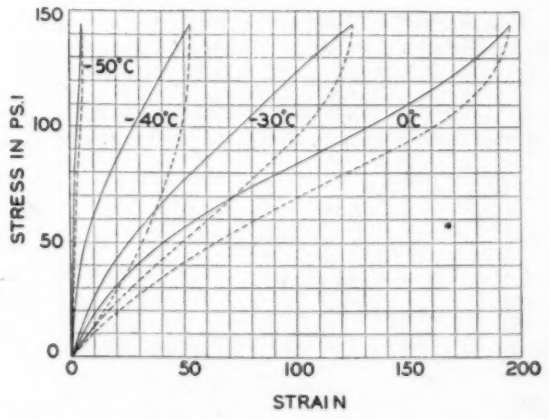

FIG. 5. The fifth-cycle hysteresis loop at four temperatures. Neoprene-rubber stock.

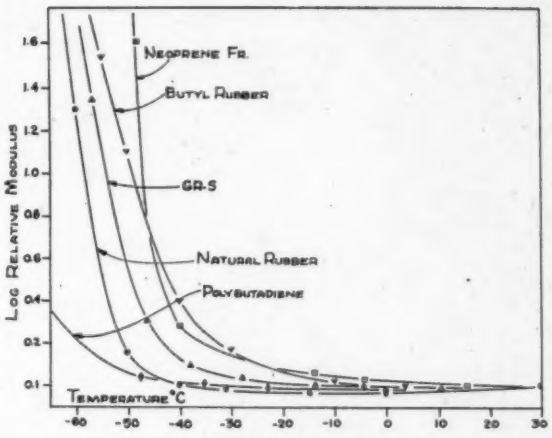

FIG. 6. Modulus *vs.* temperature curve for six pure gum elastomers as determined by single-point method. Ordinate is log of ratio of the modulus to modulus at 30°C.

EFFECT OF SOME INDEPENDENT VARIABLES

For the preliminary evaluation of stocks it is usually sufficient to determine the modulus at a single stress. The first method gives this value with sufficient accuracy as is shown in Table I.

In both methods the elongation is determined by measuring the separation between grips. The error introduced in the strain values is shown in Table II.

The flared ends of the sample necessary for satisfactory gripping account for this correctable error.

By recording the stress-strain curve through several cycles by the use of the single-wire stress-strain machine most of the desired properties of

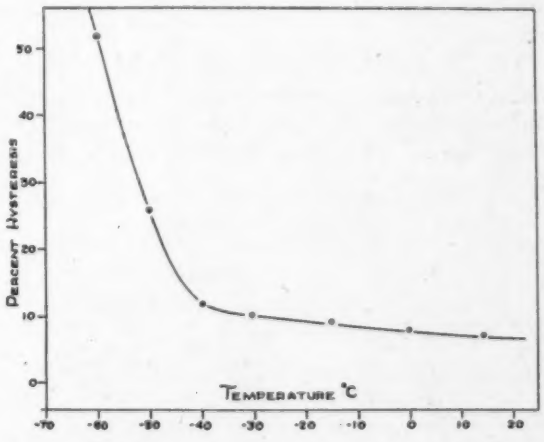

FIG. 7. Hysteresis of a pure gum natural rubber stock at a number of temperatures.

* Other workers in the field (reference 14) have been concerned with crystallization. Certain elastomers when held at specific temperatures for a period of time of a few hours crystallize. Modulus increases result. For normal rubber service this phenomenon is not important and will not be considered in this paper. The modulus *vs.* temperature curve of the crystallized rubber would, however, be interesting from a physical point of view.

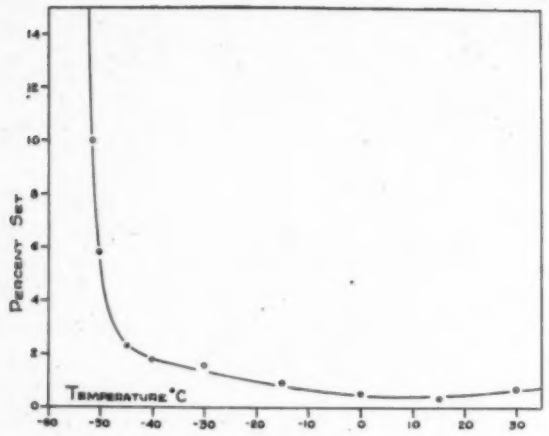

FIG. 8. Set for a pure gum natural rubber stock at a number of temperatures. Set equals final elongation divided by original elongation (five minutes under 100 percent strain, recovery after 100 sec.).

the elastomers can be measured. Such a complete set at one temperature is shown in Fig. 3. From these curves the modulus at any low stress for any cycle, the hysteresis, the set, and the effect of stress on modulus or hysteresis may be determined.

For a material which does not follow Hooke's law some care must be used in specifying the meaning attached to the modulus of elasticity. In this work the ratio of the stress to the strain calculated at a stress of 100 p.s.i. is used. In the recorded curves this is equivalent to the secant of the curve. The single-point technique gives the strain at 100 p.s.i., and hence, a similar measure of modulus. To conform with the customs of the rubber industry the strain is given as the ratio of the increase in length to the original length, and thus the modulus may be said to be the stress required to double the length if Hooke's law were obeyed.

The hysteresis is here defined as a percent energy loss in a cycle; i.e., the ratio of the area in the loop to the area under the ascending stress-strain curve. The set is recorded as the ratio of

TABLE I. Comparison of two ways to measure modulus of a rubber stock.

	Modulus (p.s.i.)	
Temperature °C	First method	Second method
31	177	162
0	165	165
−15	169	170
−31	174	175
−40	178	180
−50	257	252
−60	3570	3000

TABLE II. Error in strain measured by separation of grips.

Percent separation of grips	Elongation between gauge marks divided by elongation between grips
0	1.00
10	0.985
20	0.975
30	0.968
40	0.962
50	0.956
60	0.952
80	0.944
100	0.937
140	0.932
180	0.931
200	0.930

the remaining elongation to the initial elongation. It is not a permanent set, but applies to one testing speed only.

The absolute values of the properties defined depend very greatly on the testing technique. The effect of speed of testing was shown in Fig. 1. The effect of sample shape is shown in Table III.

The effect of the previous history was shown in part in Fig. 3, but is shown in a different way in Fig. 4.

By proper attention to the factors considered above it is possible to learn much about low temperature properties of stocks. Figure 5 shows the fifth or equilibrium cycle for a stock at a number of temperatures.

RESULTS

Figure 6 shows the temperature dependence of the modulus of elasticity in tension for a number of pure gum stocks as determined by the single-point method. Relative modulus, used as the ordinate, is defined as the ratio of the modulus at

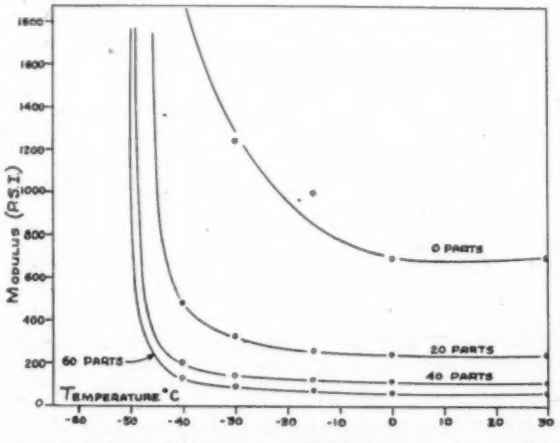

FIG. 9. Effect of the amount of plasticizer on the modulus *vs.* temperature curve. Neoprene FR with 100 parts of Thermax and indicated amounts of Circo light process oil.

TABLE III. Effect of sample width on modulus.

Pure gum rubber—3" long—0.1" thick				
		Modulus (p.s.i.)		
Temperature, °C	Width—¼"	1"	2"	3"
30	80	118	134	146
0	79	120	129	139
−15	83	131	132	143
−30	93	177	142	155
−40	119	196	159	166
−50	247	277	190	302
−60	2360	2770	2820	2870

any temperature to that at +30°C. It may be observed that a natural rubber stock has approximately its designed modulus to within a few degrees of its "critical" temperature, while a GR-S stock begins stiffening gradually just below room temperature. Yet both stocks have about the same "brittle point." The effect is even more strikingly shown by the comparison between natural rubber and Butyl. Methyl methacrylate has been shown to give the same type of modulus increase at 71°C.[2] The flexibility of polybutadiene at low temperatures has been explained by Bunn[16] on the basis of lack of steric hindrance. Hysteresis and set increase approximately according to the same law as that followed by the modulus as a function of temperature. Figures 7 and 8 show typical curves. The set was measured by holding the sample under 100 percent elongation at the temperature for five minutes, releasing it and measuring the length after 100 seconds. The values given are the ratio of the elongation remaining after 100 seconds to the initial elongation.

Figure 9 shows the effect of plasticizer on the modulus variation. Figure 10 gives the effect of

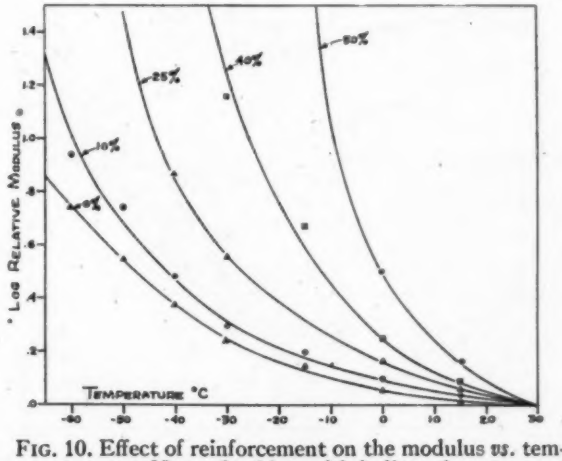

FIG. 10. Effect of reinforcement on the modulus *vs.* temperature curve. Natural rubber with indicated amounts of Gastex (PHR).

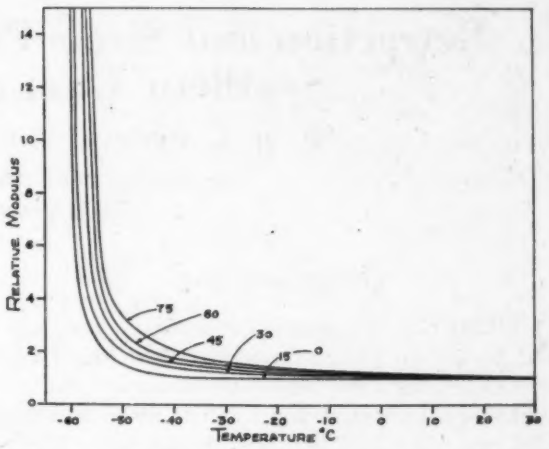

FIG. 11. Effect of temperature on the modulus of butadiene-styrene copolymers. Figures represent percentage of styrene charged.

reinforcing black. Plasticizers alter the shape of the relative modulus *vs.* temperature curve very little, but translate the entire curve down the temperature axis. Increasing the plasticizer content has an effect very similar to that produced by raising the temperature. Loading changes the shape of the curve in the transition range. Other interesting effects can be observed by varying the polymer. A study of the butadiene-styrene copolymers of different compositions gives results shown in Fig. 11. Increasing the styrene content of the copolymer has the combination effect of increasing the sharpness of the transition and raising the brittle point.

BIBLIOGRAPHY

(1) N. Bekkedahl, J. Research Nat. Bur. Stand. **13**, 411 (1934).
(2) R. A. Robinson, R. Ruggy, and E. Slantz, J. App. Phys. **15**, 344.
(3) W. Kuhn, Kolloid Zeits. **68**, 2 (1934).
(4) L. R. G. Treoloar, Trans. Faraday Soc. **39**, 36 (1943); **38**, 293 (1942).
(5) L. E. Peterson, R. L. Anthony, and E. Guth, Ind. Eng. Chem. **34**, 1349 (1942).
(6) F. T. Wall, J. Chem. Phys. **10**, 132, 485 (1942); F. T. Wall, J. Chem. Phys. **11**, 67, 527 (1943).
(7) P. J. Flory and J. Rehner, J. Chem. Phys. **11**, 512, 521 (1943).
(8) K. H. Meyer and C. Ferri, Helv. Chem. Acta **18**, 570 (1935).
(9) A. P. Aleksandrov and Y. S. Lazurkin, J. Tech. Phys. (USSR) **9**, 1249, 1261, 1267 (1939).
(10) H. Leaderman, *Elastic and Creep Properties of Filamentous Materials and Other High Polymers* (Textile Foundation, Washington, D. C.).
(11) L. R. G. Treoloar, Reports on Progress in Physics **9**, 123 (1942–1943).
(12) D. D. Eley, Trans. Faraday Soc. **38**, 299 (1942).
(13) J. W. Liska, Ind. Eng. Chem. **36**, 40 (1944).
(14) N. Bekkedahl and L. A. Wood, Ind. Eng. Chem. **33**, 381 (1941).
(15) C. W. Harris, Rev. Sci. Inst. (in press).
(16) C. W. Bunn, Proc. Roy. Soc. **180**, 88 (1942).

Retraction and Stress Propagation in Natural and Synthetic Gum and Tread Stocks*

BY B. A. MROWCA, S. L. DART, AND EUGENE GUTH
University of Notre Dame, Notre Dame, Indiana
(Received August 24, 1944)

I. INTRODUCTION

RUBBERS (elastomers), natural and synthetic, are characterized by their long range reversible elasticity. More particularly, the existence of a retractive force distinguishes rubbers from materials like beeswax, which may be extended but do not snap back.

Whereas all rubbers show a snapback, the *good* rubbers show a *fast* snapback. Thus the speed of the snapback is an outstanding index to the quality of the rubber. For instance, both Hevea and Butyl show a snapback, but Butyl snaps back much more slowly than Hevea. This is the reason for the poor rebound in Butyl. Incidentally, the speed of snapback may be, and actually is, used as a simple "hand test" for progress of cure. One bends a cured sheet and observes how fast it straightens out again. In this example the speed of recovery after bending is observed. The speed of snapback may be studied, of course, for any deformation: bending, torsion, shear, compression, extension, etc. Since stress-strain data are used so extensively in rubber technology, the snapback after extension was studied first. Snapback will be used in this restricted sense in the following text.

Besides characterizing the quality of a polymer, the speed of snapback is of great direct importance for tire construction. Sluggish snapback may lead to increased flexing, i.e., increased heat generation. In addition, slow snapback means less grip of the tire on the road assuming equal wetting conditions.

II. EXPERIMENTAL METHOD

Stylus on Recording Drum

The speed of snapback can be obtained if the change of length with time of a freely retracting rubber bar can be recorded. The speed of snapback may be obtained by taking the slopes of the length *versus* time curves. The upper limit for the velocity of the tip of a freely retracting natural rubber band was calculated to be larger than 200 miles per hour (9000 cm/sec.) for 450 percent elongation. Therefore, the whole snapback must take place in a time interval of the order of 10 milliseconds or less. Recognizing these facts, an obvious method of recording the length-time curve is high speed photography as perfected by Edgerton. The photographic method will be discussed in Section V.

In the apparatus used the rubber sample was clamped at one end. A light stylus was fastened to the other end. The stylus was connected with a light frame which was kept in a straight line during its motion by two guide wires. The weight

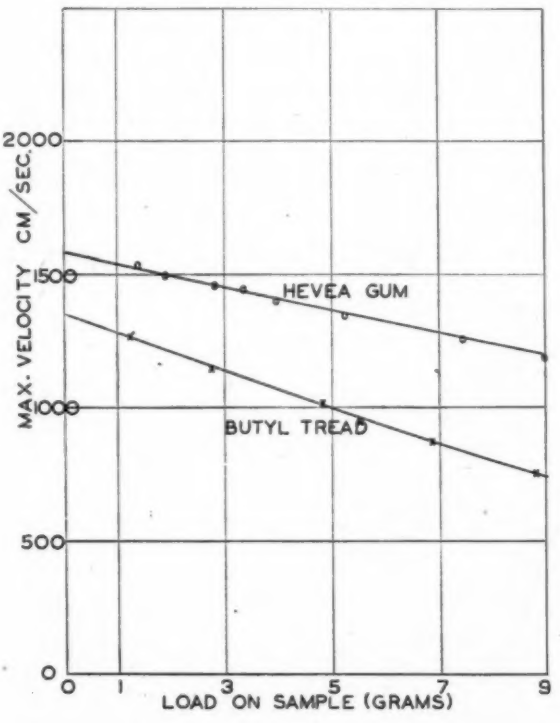

FIG. 1.

* Presented on June 23, 1944 before the Inaugural Meeting of the Division of High-Polymer Physics of the American Physical Society at Rochester, New York. This paper was substituted for another one originally scheduled entitled, "A recent development in the theory of rubber elasticity," by H. M. James and E. Guth.

of the frame and stylus was less than one gram. The weight of the rubber bar of $\frac{1}{4}$ inch-square cross section and 10-inch length was about 10 grams. The motion of the stylus during the retraction of the sample was recorded on a revolving smoked drum (25 in. in circumference and 20 in. in length) which was driven by a synchronous motor at 1800 r.p.m. Thus a record of the length-time curves was obtained for the determination of the slopes and recognition of details.

III. INFLUENCE OF STYLUS

In order to study the influence of the weight of the stylus (and of the weight of the unstretched rubber in the grip) weights of increasing size were attached to the stylus to permit an extrapolation to zero weight. In Fig. 1 the maximum velocity of the tip is plotted against the weight for the two extreme cases of Hevea gum and Butyl tread for 50 percent initial elongation. Straight lines were obtained for both stocks within the experimental accuracy. This fact permits a simple extrapolation. The first point on each of the curves represents the velocity with the stylus and the unstretched rubber, but without any additional weight. The extrapolated velocities are about $3\frac{1}{2}$ and 6 percent higher than the original values for Hevea gum and Butyl tread, respectively.

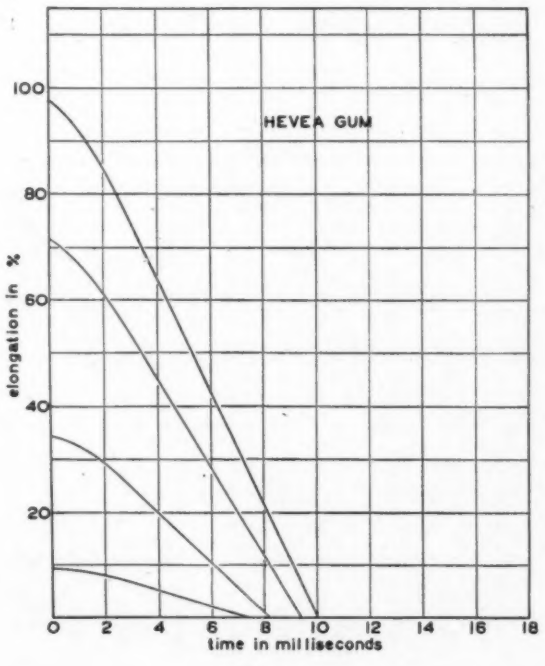

FIG. 2.

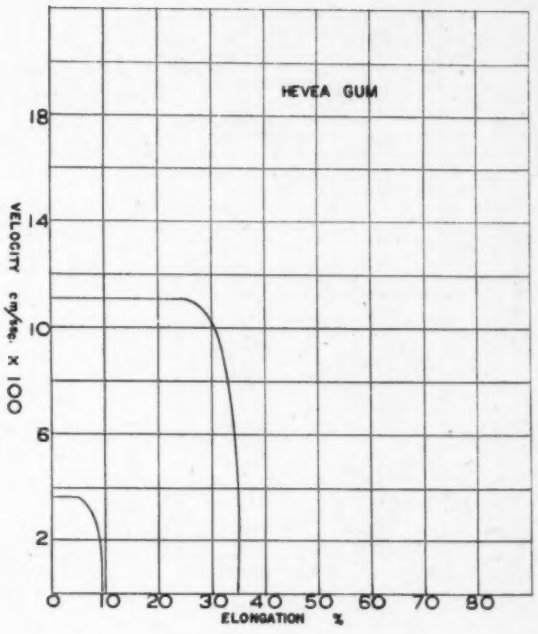

FIG. 3.

IV. RESULTS BY STYLUS METHOD

Hevea, GR-S, and GR-I gum and tread stocks were investigated.[1] For Hevea and GR-S, gum and tread stocks differ only in that the tread stocks contain carbon black, the gum stocks containing a softener. Butyl tread is obtained from the gum stock by the addition of Captax and carbon black. The cures were optimum, based on maximum tensile strength tests.

Figure 2 gives the elongation as a function of the time for four different elongations. The duration of the snapback increases from about 7 to 10 milliseconds for the range of elongations covered. All these elongation curves meet the time axis, without showing inflexion points. Figure 3 represents the negative of the slopes of the two lowest elongation curves, plotted against the successive elongations on retraction (velocity curves). These slopes were not taken from Fig. 2, but directly from the original records in order to obtain greater accuracy. For the upper curve it took about a third of the initial elongation (and a third of the duration as Fig. 2 shows) to attain the final maximum velocity represented by the horizontal line. The straightness of that line indicates that the final maximum velocity once attained will persist over the rest of the retraction.

Figure 4 shows a surprising and important result, which was obtained to check theoretical considerations outlined in Part VI. In Fig. 4, the

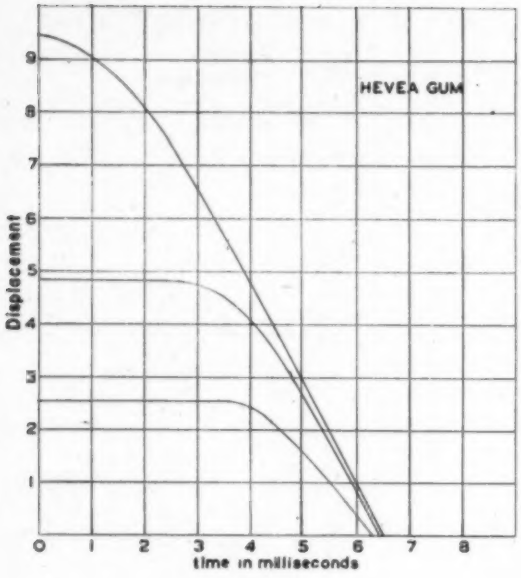

FIG. 4.

actual change in length of the sample is plotted against the time. The top curve describes the path of the tip of the sample and is, of course, almost identical with the top curve of Fig. 2. The sample in Fig. 4 was only half as long as that of Fig. 2. This accounts for the longer duration in Fig. 2. The middle curve describes the retraction of the middle of the bar and shows quite a different behavior. The middle of the bar starts to move only after the first half has retracted. The lower curve describes the motion of an element at a quarter-length position. Again it lags behind the end, and somewhat behind the middle. The final maximum velocity of the middle is only slightly smaller than that of the tip, and only slightly larger than that of the quarter. The top and middle curves were obtained by fastening a stylus to the tip and another one to the middle of the bar.

Figure 5 shows elongation curves for the Hevea tread stock. Whereas the three upper curves show qualitatively the same behavior, the bottom curve shows two new effects. First, it does not go to zero, but to a minimum. This indicates a permanent or a temporary set. Secondly, after reaching a minimum, it rises again. This rise may be ascribed to the compression of the bar.

Figure 6 shows a two-stylus run (one at the tip and one at the middle of the sample) with essentially the same results as for the gum stock; cf. Fig. 4. It should be pointed out that in the three upper curves of Fig. 5 this tread stock showed an inflection point which is not indicated on the scale of Figs. 5 and 6. Consequently, the velocity curve for any of these upper curves would show a dip at the velocity axis, similar to that of Fig. 11 for GR-S tread, but the dip would be much smaller. The dip is visible, of course, for the bottom curve of Fig. 5.

Figure 7 gives the elongation curves for a GR-S gum stock. The bottom curve (for the lowest elongation used) is similar to the bottom curve for Hevea tread in Fig. 5. Here the set is quite pronounced and slows the sample up before it buckles. One notices that GR-S gum needs about twice as long to snap back as Hevea gum.

Figure 8 shows the velocity curve with a dip corresponding to the S-shape of the elongation curves.

Figure 9 gives the results of a two-stylus run. Just as for Hevea, the middle of the bar exhibits a delayed snapback.

Figure 10 gives the elongation curves for a GR-S tread stock. The two lowest curves show damped vibrations more developed than for Hevea tread or for GR-S gum. The three upper curves have the same character as the corresponding elongation curves for Hevea tread (cf. Fig. 5) and reveal the remarkable speeding up of the snapback of GR-S by carbon black reinforcement.

Figure 11 shows a velocity curve with a single dip caused by the single inflection point.

Figure 12 shows the result of two-stylus ex-

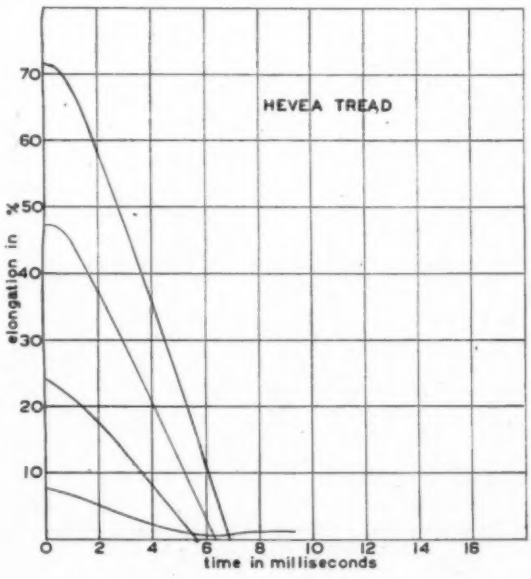

FIG. 5.

periment. Again the middle is delayed and moves only with a slightly smaller velocity than the tip of the bar.

Figure 13 shows elongation curves for a Butyl gum stock. All curves show a single S-shape (single inflection point). Even at the lowest elongation used, overdamping is apparent in the last half of the elongation curve.

Figure 14 exhibits a velocity curve with a single dip, like in Fig. 11 for GR-S tread, caused by the single inflection point in the elongation curves.

Figure 15 represents elongation curves for a Butyl tread stock. Except for the higher elongation used, all the curves show the inflection point very markedly, i.e., are strongly overdamped. The lower elongation curves reveal considerable temporary or permanent set.

Figure 16 shows a velocity curve. Because of the strong damping the final velocity is not only smaller than the maximum velocity but goes to zero, as an almost linear function of the elongation.

Figures 17 and 18 show the maximum velocities plotted against initial elongation for Hevea gum, Butyl gum and tread. Butyl tread, while quite sluggish at lower extensions, catches up with Hevea gum above 200 percent. GR-S gum without softener* is much more snappy than one containing Bardol B. Another noteworthy feature is the crossing of the Hevea tread curve by the GR-S tread curve. However, at lower elongations (the range important for tires) Hevea is superior to GR-S.

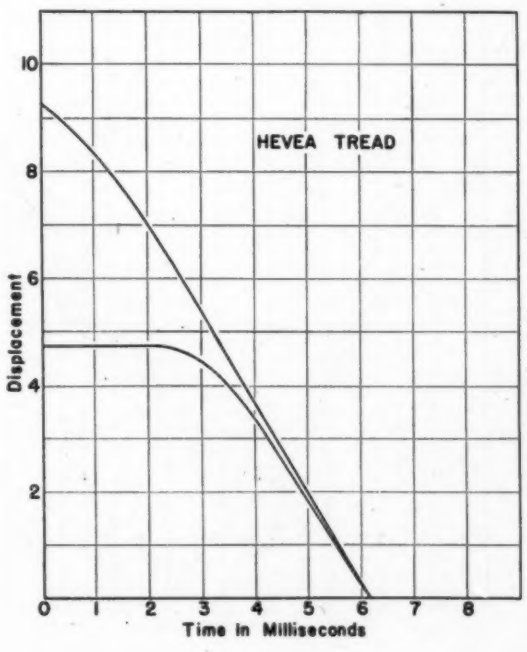

FIG. 6.

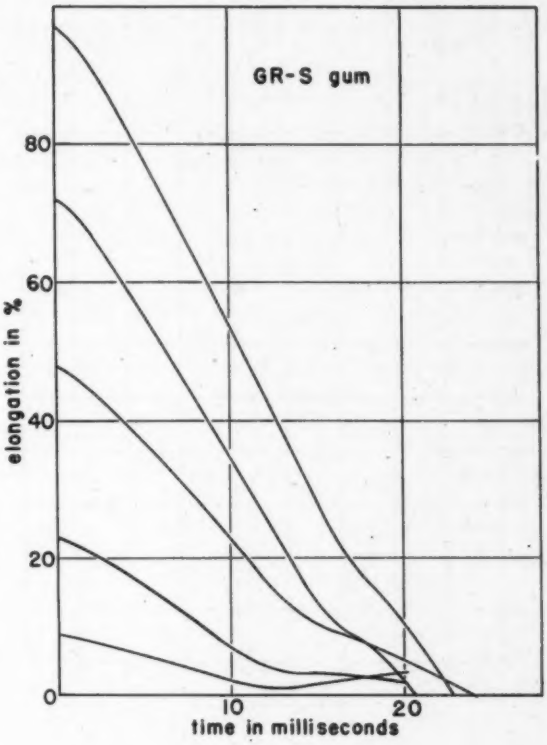

FIG. 7.

V. PHOTOGRAPHIC STUDY OF THE RETRACTION PROCESS

Instantaneous photographs[2] of the retraction were taken by an ordinary camera in the illumination of a stroboscopic lamp (strobolux). This simple method (strobolux photography), however, does not provide a time scale and therefore had to be supplemented by the use of Edgerton high speed photography method.

Figure 19 shows a set of instantaneous photos of Hevea gum at different stages (elongations) of the snapback. The initial elongation was 100 percent. One sees very clearly the wave pulse progressing along the sample. The white dots are equidistant at the start of the retraction and their separation indicates the progressive retraction of the sample. In Hevea tread the wave pulse

* This stock had the same composition as that used by F. L. Roth and L. A. Wood, J. App. Phys. 15, 749 (1944).

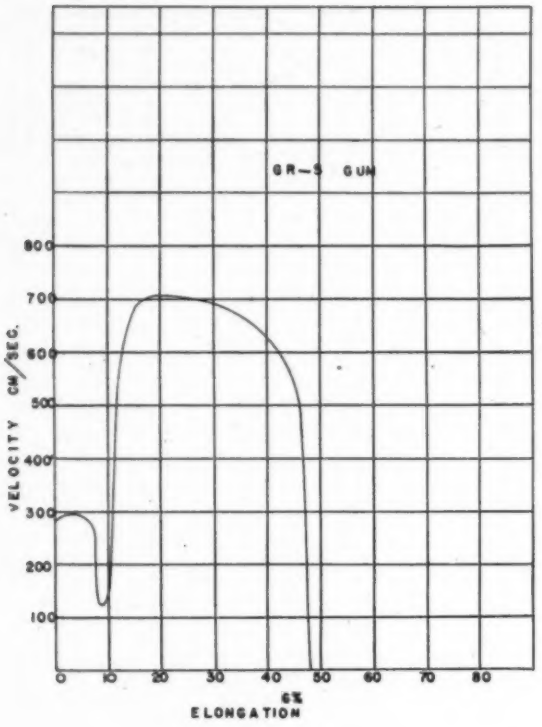

FIG. 8.

is visible but is less sharp than for the case of Hevea gum. This diffuseness is caused by the larger internal friction of the tread stock as compared with the gum stock. Some buckling takes place in the last phase of the retraction, in accordance with the elongation-time curves of Fig. 6.

Figure 20 shows a set of instantaneous photos for GR-S. The moving pulse is still visible, but is more diffuse than for the Hevea tread. The GR-S tread shows a behavior similar to that of Hevea tread. This similarity of the tread stocks is well known from other data. The wave pulse is more diffuse for GR-S because of its larger internal friction.

Figure 21 exhibits the snap of Butyl gum and tread, and their sluggish character. The wave pulse is too diffuse to be seen. In addition, the retraction is slowed down so much by internal friction, that the pulse arrives at the fixed end, before the sample is completely contracted.

In principle, most of the information which can be obtained from smoked drum records could be derived from timed high speed movies which we took (the time was recorded on the film by a spark at 1/120 second intervals). The motion of the tip as a function of the time may be plotted, i.e., the elongation-time curves. Also, from the same photos, the motion of any point behind the tip as a function of the time may be obtained corresponding to the results of the two-stylus experiments. The accuracy depends upon the sharpness of the system of marks (dots or lines) put on the sample to indicate the element positions.

From the instantaneous photos alone, without knowing the time of retraction (which we could take from the elongation-time curves) one could plot the extension of each element (differential extension) as a function of the distance from the fixed end. This was done in Fig. 22 for Hevea gum and for Butyl tread at two different times. These curves show what we know already from the photos, namely, the motion of a comparatively sharp wave pulse or "necking" for Hevea gum and of a quite diffuse pulse for Butyl tread. We notice that increasing time shifts the curve for Hevea gum parallel to the ordinate axis, but the shift is parallel to the abscissa axis for Butyl tread.

VI. DISCUSSION AND EXPLANATION OF THE RESULTS

A theory of the retraction of rubber has been developed by James and Guth[3] and the results are as follows:

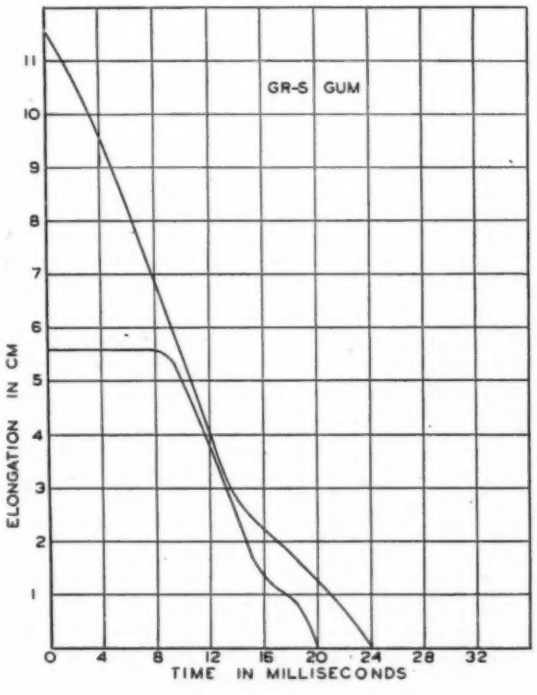

FIG. 9.

We consider a uniform elastic rod of length l_0 fixed at one end, with linear density ρ in the unstretched state. We assume that Hooke's law holds, with Young's modulus E, and that frictional forces are proportional to the rate of deformation. Let x be a measure of distance in the material of the unstretched rod, starting at the fixed end, and let $u(x)$ be the displacement of the material corresponding to the indicated value of x. In the absence of body forces, the behavior of the rod in extension and retraction is governed by the wave equation

$$\rho\frac{\partial^2 u}{\partial t^2}=f\frac{\partial^3 u}{\partial x^2\partial t}+E\frac{\partial^2 u}{\partial x^2}. \tag{1}$$

If the rod is initially uniformly stretched with fractional extension ϵ, and is released at time $t=0$, the boundary conditions are:

$$\begin{aligned} &\partial u/\partial x=\epsilon, \quad \partial u/\partial t=0 \quad \text{for all } x \text{ at } t=0,\\ &u=0 \quad \text{for all } t \text{ at } x=0,\\ &f\frac{\partial^2 u}{\partial x\partial t}+E\frac{\partial u}{\partial x}=0 \quad \text{for } x=l_0 \text{ when } t>0. \end{aligned} \tag{2}$$

In the limiting case of small friction, $f=0$, the solution becomes, with $v=(E/\rho)^{\frac{1}{2}}$

$$\begin{aligned} u(x,t)&=\epsilon x & l_0-x>vt,\\ u(x,t)&=\epsilon(l_0-vt) & l_0-x<vt<1. \end{aligned} \tag{3}$$

According to this solution a pulse of acceleration arises at the free end at the moment it is released, and travels, with respect to the unstretched material, at a rate v; its rate of transmission in space is $v_p=(\epsilon+1)v$. Each portion of the bar is stationary until it is reached by this pulse. The velocity of the tip of the bar is $v_t=-\partial u/\partial t=\epsilon v$. As the pulse passes over it the stress is completely relaxed, and the material reaches its final velocity ϵv. When the acceleration pulse reaches the fixed end of the material, after time $t_c=l_0/v$, the bar is unstretched and in uniform motion at the rate ϵv, the original potential energy is completely converted into kinetic energy. After this time a solution other than Eq. (3) begins to apply. The wave pulse is reflected at the fixed end and a pulse of deceleration begins to progress back down the bar. In the case of a rod in which transverse motion is not prevented, as in the case of a retracting rubber band, buckling begins at the moment of reflection of the pulse.

This motion is shown schematically in Fig. 23. This plot shows the change in the position of various points on the sample during the time of

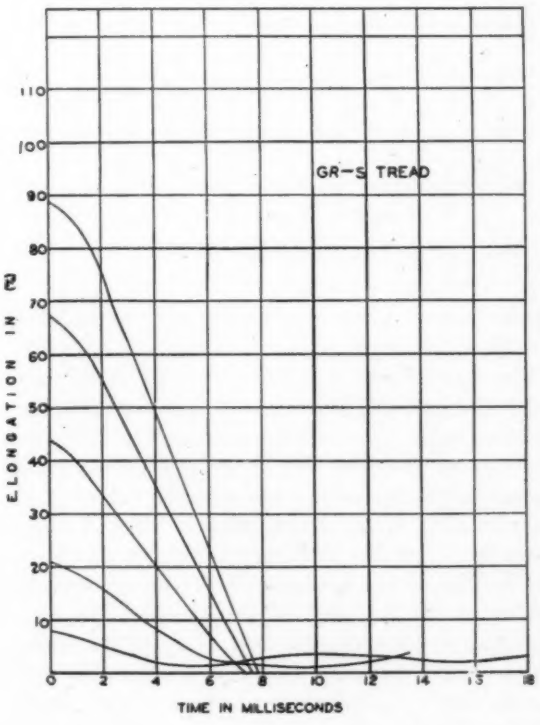

FIG. 10.

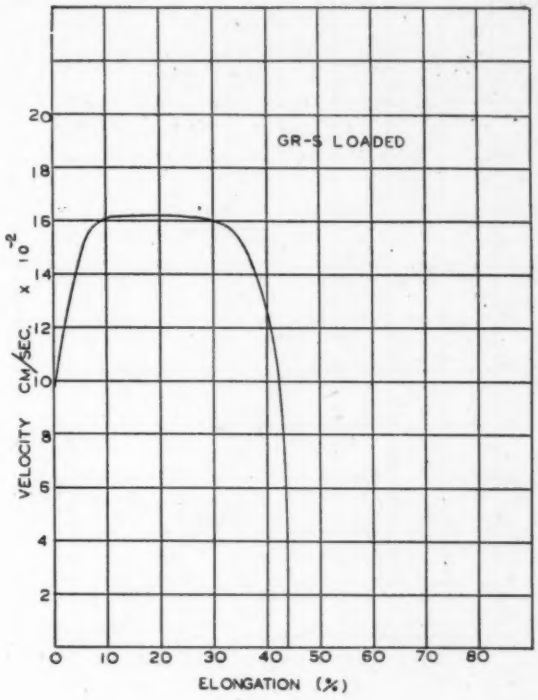

FIG. 11.

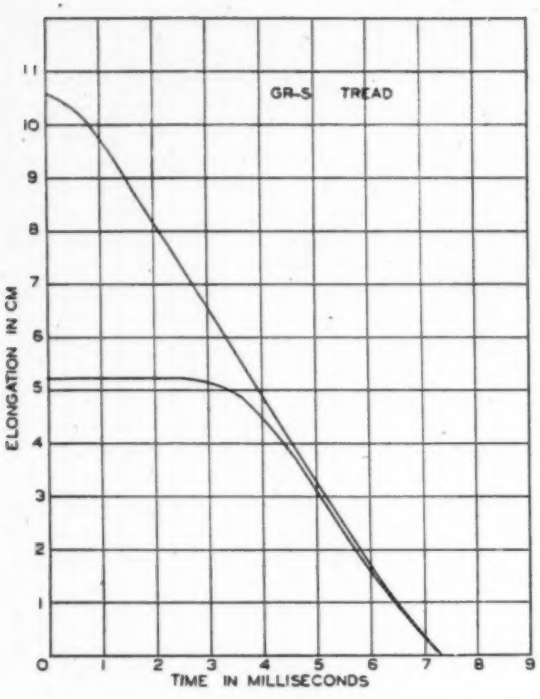

FIG. 12.

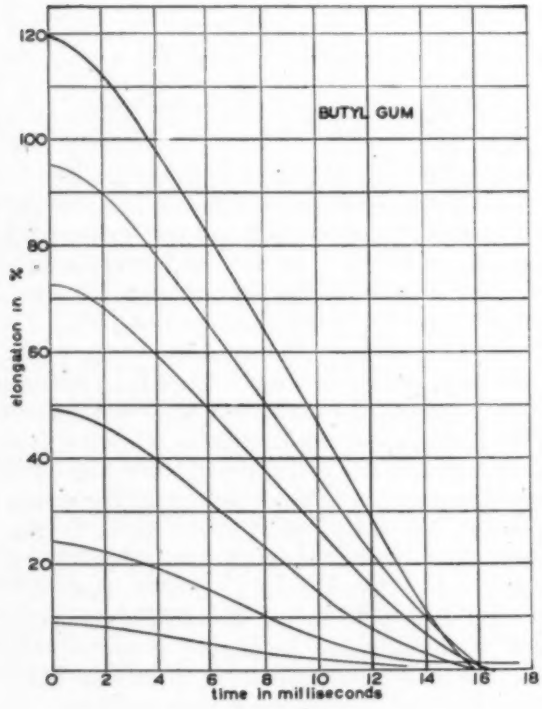

FIG. 13.

retraction. The tip of the sample travels in a straight line from l to l_0. In the same time the wave pulse travels from l to 0, i.e., the entire length of the sample. Any point on the sample between 0 and l, such as $l/2$ or $l/4$, does not change position until the wave pulse arrives at that point. Then it acquires the same velocity as the tip and travels with this velocity until the sample has completely retracted. After the sample has completely retracted it, of course, buckles, beginning at the fixed end.

If we plot this same motion, using the displacement or extension instead of the actual length, we get the graph seen in Fig. 24, for the tip and for any point behind the tip. From Fig. 24 it

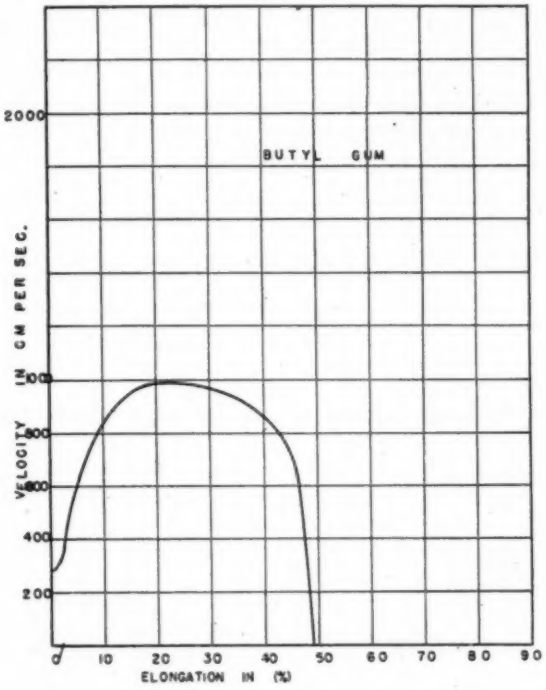

FIG. 14.

follows that the velocity-extension curve is simply a rectangle.

The first element has zero mass. Applying a finite tension, an infinite acceleration results—the final velocity is attained instantly. This is in contrast to the free vibration of a concentrated mass, which always starts with zero velocity. For the actual stylus experiments (cf. Figs. 2 and 3) the velocity starts with zero. This is caused by the weight of the stylus and of the unstretched rubber at the free end of the sample. Since it is not the actual lengths but the displacements which are measured experimentally, we have chosen this type of curve to present our data.

Going back to Eq. (1) let us consider the case

involving large internal friction. Here the inertial term can be neglected and the solution becomes

$$u(x, t) \cong \epsilon x e^{-(E/f)t}. \qquad (4)$$

In this case we neglect the wave pulse and hence this equation holds only after the wave pulse has passed down the sample. A schematic drawing of this case is seen in Fig. 25. Here we see that at any given time the displacement (and also the velocity) of any point on the sample is proportional to its distance from the fixed end. Also, of course, the sample approaches the unstretched state exponentially with time.

The intermediate case may be treated by the Fourier method. However, since most experiments are not extremes it is of interest to treat this case graphically. Figure 26 shows the wave pulse arriving at the fixed end before the sample has completely retracted. Of course, a point on the sample cannot move until the wave pulse arrives there, but after that its velocity depends somewhat on its position. The lower portions of the curves of Fig. 26 are not accurate because of the fact that buckling sets in as soon as the wave pulse is reflected.

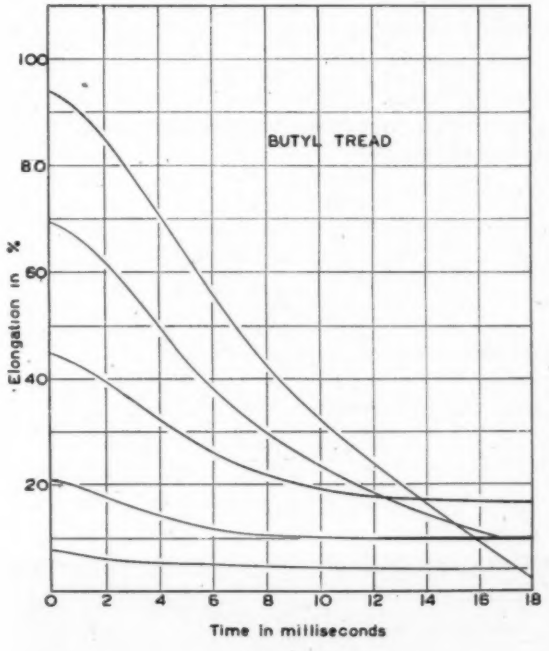

FIG. 15.

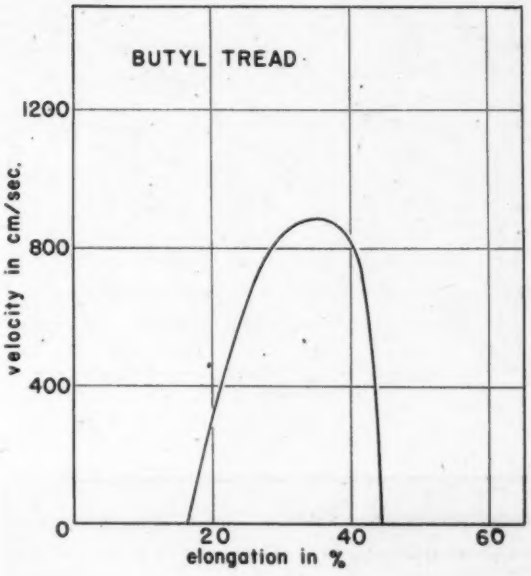

FIG. 16.

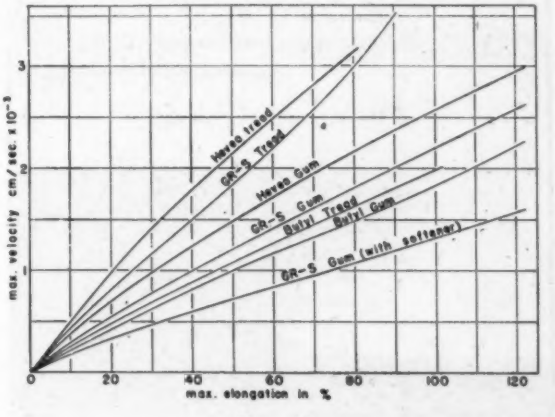

FIG. 17.

In the above considerations we have neglected the weight of the stylus and unstretched rubber at the tip (in the clamp). The effect of this would be to round off any sharp corners in Figs. 22 to 26, especially the beginning of the curves. This accounts for the S-shape of some of the curves.

In our high speed photos, Figs. 19–21 (Hevea tread to Butyl tread) the reflection of the wave pulse at the fixed end will start the buckling.

So far our considerations have been of a very general nature and will hold for rubberlike materials as well as for steel. In order to find the difference between rubber and steel we have to correlate quantitatively the propagation of stress waves with the elastic constants of these materials. Obviously, the big factor (10^4 dynes/cm^2) between Young's modulus for steel ($E=2\times10^{11}$) and rubber ($E=2\times10^7$) will cause quite a quantitative difference in the velocity of stress propagation.

First, we define precisely the velocity of stress

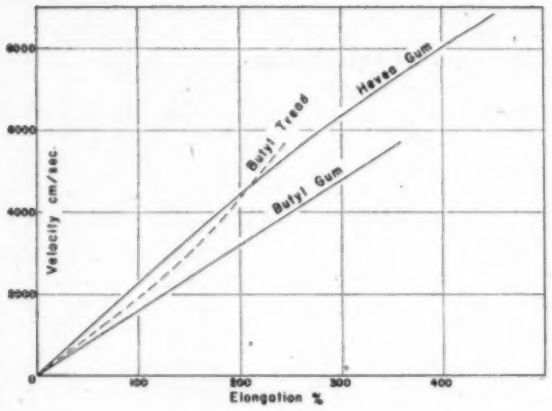

FIG. 18.

FIG. 19.

propagation. Referring to Fig. 23, we see that the velocity of the tip v_t is related to the velocity of the wave pulse v_p by the simple relation

$$\frac{v_p}{v_t}=\frac{L}{L-1}=\frac{\epsilon+1}{\epsilon};\quad \epsilon=L-1:\ \text{Extension}, \tag{5}$$

where L is the relative length; $L=l/l_0$: l being the extended length and l_0 the original length. The pulse travels from the stretched end down to the fixed end, while the tip moves only from the stretched end to the end in the unstretched state.

Next, we write the theoretical expression for v_p as obtained in the theory of James and Guth.

$$v_p=L(E/\rho)^{\frac{1}{2}}=(\epsilon+1)(E/\rho)^{\frac{1}{2}}, \tag{6}$$

where E is Young's modulus, and ρ is the density.

For the velocity of the tip, Eqs. (1) and (2) yield;

$$v_t=(L-1)(E/\rho)^{\frac{1}{2}}=\epsilon(E/\rho)^{\frac{1}{2}}. \tag{7}$$

We see that v_t goes to zero with the extension ϵ, whereas v_p approaches the value $(E/\rho)^{\frac{1}{2}}$.

The validity of Hooke's law is assumed in deriving (6). In addition internal friction was neglected. Therefore it should hold for the initial slope of the velocity *versus* elongation curves for stocks like Hevea gum, where internal friction is comparatively small. The values of E and ρ were determined in this laboratory for the stock in question.

The duration of the retraction follows from (6). Since the pulse travels the distance l with the uniform velocity v_p

$$\tau=l/v_p=l_0/(E/\rho)^{\frac{1}{2}}. \tag{8}$$

For $l_0=10$ cm and the above values of E and ρ we obtain

$$t=10 \text{ milliseconds},$$

$$v_p=3.7\times10^3(\epsilon+1),$$

$$v_t=3.7\times10^3(\epsilon).$$

The corresponding values for steel are;

$$t=0.1 \text{ millisecond},$$

$$v_p=1.6\times10^5(\epsilon+1),$$

$$v_t=1.6\times10^5(\epsilon).$$

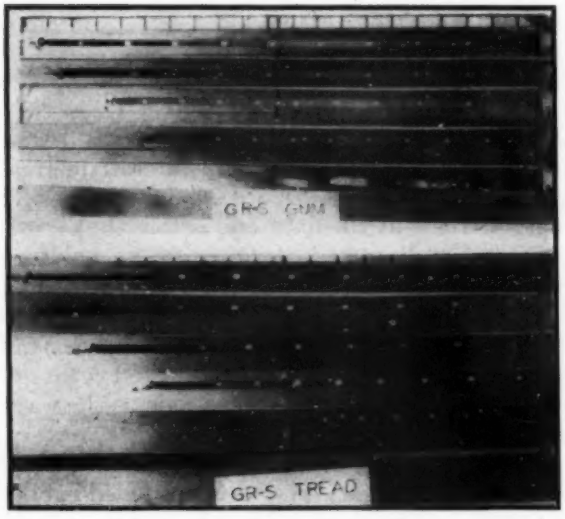

FIG. 20.

This comparison shows that the snapback of steel takes place on a time scale one hundred times smaller than that for rubberlike materials.

For the differential extension (cf. Fig. 22) this simple theory gives the result indicated in Fig. 27, corresponding to instants indicated by dotted lines in Fig. 24.

It was pointed out by James and Guth[2] that deviations from Hooke's law cause broadening of the contraction pulse. Consideration of momentum and energy transfer makes it evident at once that an acceleration pulse of fixed form and limited extent cannot occur except for a Hooke's law bar. Nevertheless, it is instructive to assume approximately the existence of an acceleration pulse of fixed form and limited extent, to apply the energy law and neglect its contradiction to the momentum theorem. According to the theory of James and Guth all sections of the freely retracting sample move with the same constant velocity as the tip. The expression (7) for v_t may be written in the form:

$$\sigma_0 \cdot \tfrac{1}{2} M v_t^2 = \int_{l_0}^{l} Z \sigma_0 dl; \tag{9}$$

$$M = l_0 \sigma_0 \rho = \text{mass of the sample}$$

with

$$Z = E \cdot \epsilon. \tag{9a}$$

For the special problem of computing the velocity of the tip one may consider, therefore, the whole mass M of the sample as "effective." Equation (9) represents the energy theorem for a free

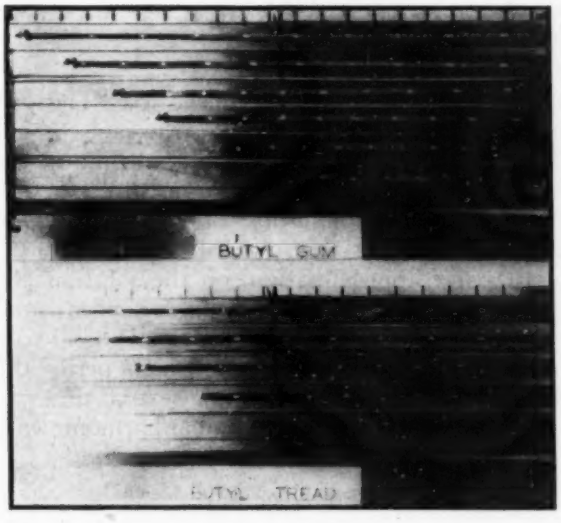

FIG. 21.

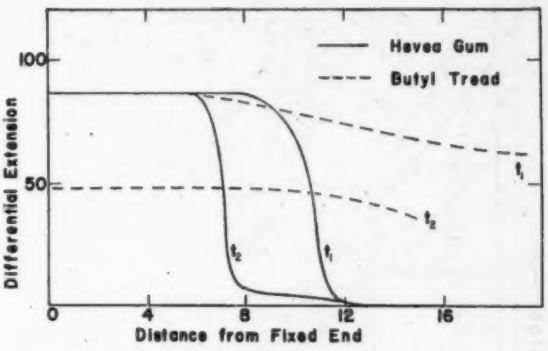

FIG. 22.

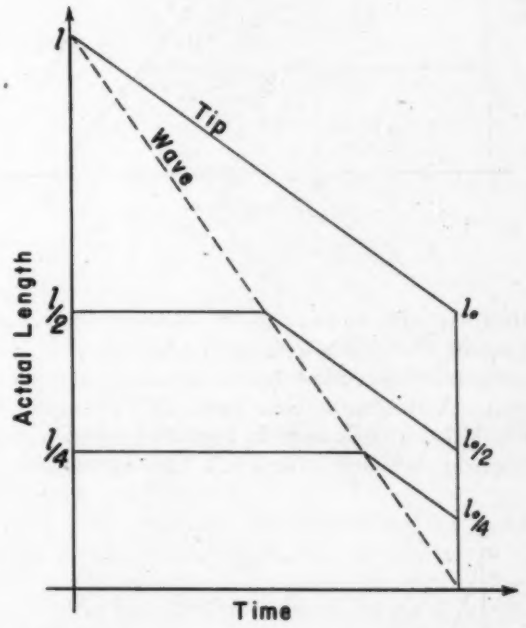

FIG. 23.

vibration. An obvious generalization of (9) is to replace Z by the theoretical stress-strain curve of the theory of James and Guth, instead of its Hookean approximation as in (9a). Then one obtains the following equation with $M/M^* = 1$.

$$v = \left[\frac{E}{3\rho} \times \frac{M}{M^*}\right]^{\frac{1}{2}} \left[L^2 + \frac{2}{L} - 3\right]^{\frac{1}{2}}. \tag{10}$$

The actual experiments show that all sections of the freely retracting sample do not move with exactly the same velocity. A $v(x)$ *versus* $v(l) = v_t$ curve may be derived from our two stylus experiments. $v(x)$ denotes here the velocity at any point at a distance x from the fixed end of the sample. From this curve the kinetic energy may be com-

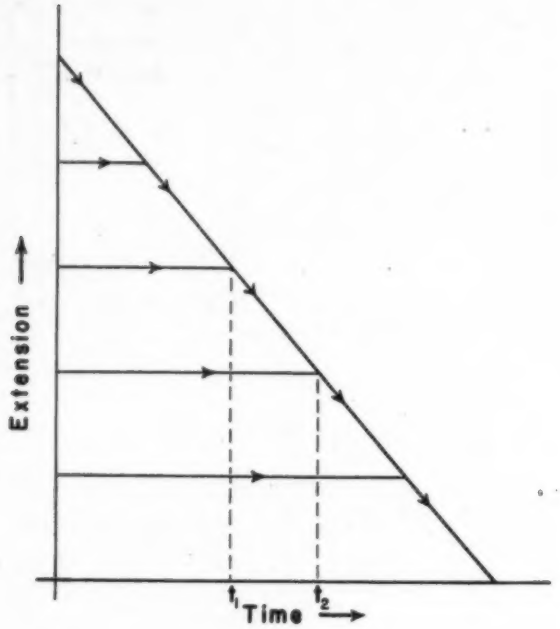

FIG. 24.

puted by the approximate Rayleigh method. Equating the result to $\frac{1}{2}Mv_t^2$ one obtains M/M^*. It depends somewhat upon the particular elongation. A determination gave M/M^* equal to 0.85. This value is used in Fig. 28 for computing the curve labelled "theory." The agreement is

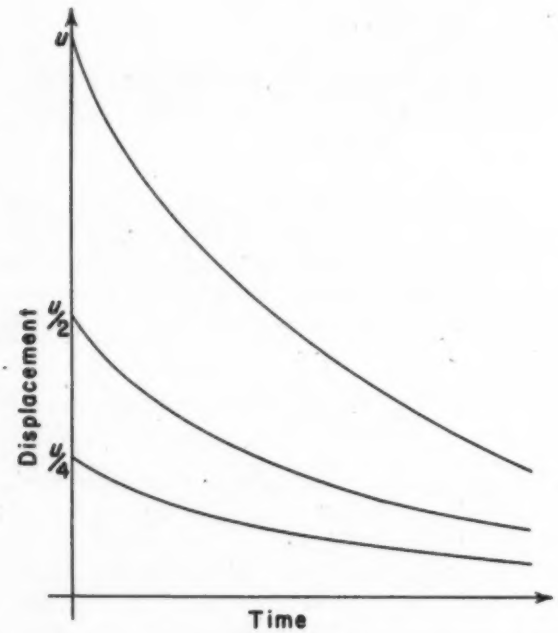

FIG. 25.

rather good for low extensions as would be expected.

Using $M/M^*=3$ is equivalent to assuming the relation

$$v(x)=\frac{x}{l}v(l). \tag{11}$$

Equation (11) does not hold at all according to our experiments for Hevea nor for GR-S. For Butyl tread, however, (11) is a rough approximation. The dotted lines in Fig. 27 refer to Eq. (11) and should be compared with the dotted lines in Fig. 22. It should be stressed that a horizontal line in a plot of the differential ex-

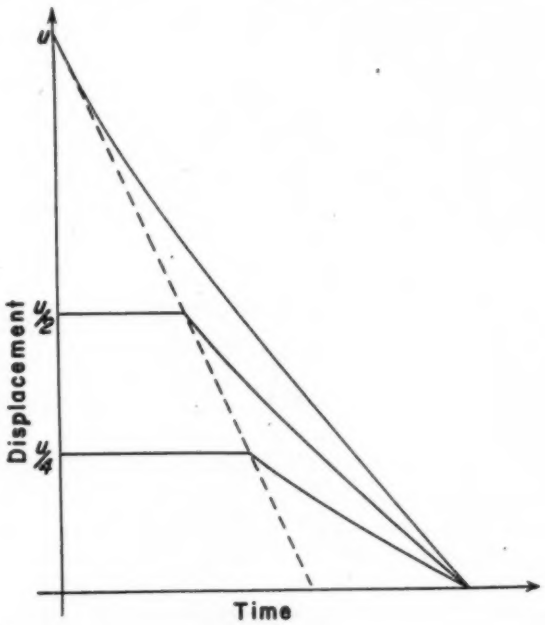

FIG. 26.

tension *versus* distance from the fixed end can mean either that the sections of the same do not move at all or that they move according to the relation (11).

The correct explanation of the behavior of Butyl tread rests, of course, on the equation (1) or to a fair approximation, on the solution (4).

In general the introduction of a concentrated mass, i.e., the passing from an elastic solid to a point mass, is justified only if during a period the wave pulse traverses the sample several times.

The correct treatment of the anharmonic case rests, of course, on the wave equation

$$\rho\frac{\partial^2 u}{\partial t^2}=\frac{dZ}{dL}\cdot\frac{\partial^2 u}{\partial x^2}. \tag{12}$$

Here $L=\partial u/\partial x$, and $dZ/dL=dZ/d\epsilon$, the differential Young's modulus because of the linear connection between L and ϵ. For $Z=Z(L)$ we may substitute the experimentally obtained stress-strain curve of a particular stock, or the theoretical equation by James and Guth.

$$Z=K(L-1/L^2), \tag{13}$$

where K is 3 times Young's modulus best taken

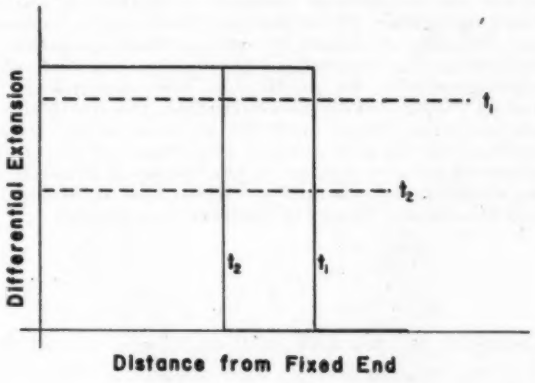

FIG. 27.

from experiment (slope of the stress-strain curve at small extensions).

From (12) one obtains

$$v_t=\left(\frac{1}{\rho}\cdot\frac{dZ}{dL}\right)^{\frac{1}{2}}. \tag{14}$$

This expression checks with experiment much better than (10) and yields a v_t *vs.* ϵ curve of similar shape as the corresponding stress-strain curve.

In 1874 Exner, using an ingenious method, devised by Stefan[4] measured the time (τ) needed by the wave pulse to arrive from the free to the fixed end. His value for unstretched rubber $v_p=3740$ cm/sec. is in fair agreement with the value obtained by us for another compound by extrapolation ($v_p=3800$ cm/sec.). The method of Exner-Stefan is sound in principle. However, the interpretation of v_p for stretched rubber is left open by his work. Exner's aim was to obtain the dependence of E upon temperature. For the case of stretched rubber, however, relaxation effects mask the true dependence. This fact was not known at that time. It is not clear why Exner did

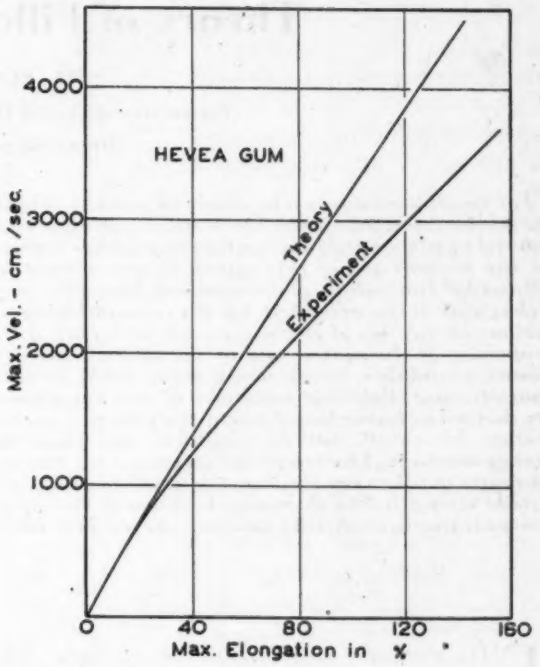

FIG. 28.

not obtain the correct dependence for the unstretched state. Recent work at Notre Dame and at the Bureau of Standards shows conclusively that E increases with rising temperature. This was checked in our work for both extension and compression.

Irons[5] obtained $v_p=15{,}600$ cm/sec. for ebonite using another method also owing to Stefan.

The velocity of a wave pulse, i.e., the velocity of a sound in a rod-like sample, is about 50 times smaller than the usually so-called "velocity of sound" in an infinite medium. In a rod, extension is accompanied by lateral contraction, which is not true for an infinite medium. Only for a substance with a very small Poisson's constant (a substance like cork) will the two velocities be comparable.

REFERENCES

(1) B. A. Mrowca, S. L. Dart, and E. Guth, Phys. Rev. **66**, 30 (1944). Cf. also R. B. Stambaugh, Phys. Rev. **65**, 250 (1944). A comparison of the Goodyear and Notre Dame work will be given in a later issue of this journal.
(2) B. A. Mrowca, S. L. Dart, and E. Guth, Phys. Rev. **66**, 32 (1944).
(3) H. M. James and E. Guth, Phys. Rev. **66**, 33 (1944).
(4) Cf. G. S. Whitby, *Plantation Rubber and the Testing of Rubber* (Longmans and Green, London, 1920), p. 461.
(5) E. J. Irons, J. Sci. Inst. **7**, 323 (1930).

Theory of Filler Reinforcement*

BY EUGENE GUTH

University of Notre Dame, Notre Dame, Indiana

(Received September 4, 1944)

For small loadings (up to about 10 percent volume parts) the colloidal carbon black spheres may be considered as suspended in a continuous rubber matrix. In the present paper this model is generalized for ellipsoidal (including plate- and rod-like) filler particles and it is extended to the computation of various properties of the suspension in terms of the properties of the matrix and of the fillers. Viscosity, Young's modulus, stress-strain curve below crystallization, and dielectric constant of the suspension are derived as linear functions of the volume concentration for small, and as quadratic functions for higher loadings. The stress-strain curves for varying amounts of fillers are similar. For small loadings the tensile strength first decreases because of the stress concentrations occurring around the carbon black spheres when the samples are stretched. The increase of the tensile strength observed for greater loadings is caused by the tendency of the carbon black spheres to form chains and finally, a type of network. The stiffness increases with loading, up to the point where the suspension becomes a dilution of carbon black by rubber. There the tensile strength decreases too. Binding of rubber by carbon black is similar to solvation. The theoretical conclusions were checked experimentally, in particular, the dependence of Young's modulus on concentration, the similarity of stress-strain curves, and the decrease of the tensile strength for small loadings. The theory of the elastic properties is very similar to the theory of Einstein on the viscosity of colloidal solutions and to Maxwell's and Rayleigh's theory of dielectric properties.

THE viscosity of colloidal suspensions and emulsions may be understood by a hydrodynamic analysis, initiated by Einstein[1] in 1906 and embellished by the author[2] and his associates. In this hydrodynamic theory the solvent is considered as a continuum. The suspended colloidal particles perturb the flow in the viscometer. This perturbation leads to an *increase* in the energy dissipated, which corresponds to an *increase* in the viscosity of the solvent. For rigid spheres suspended in a liquid Einstein obtained the now well-known viscosity law,

$$\eta^* = \eta[1+2.5c], \qquad (1)$$

where η^* and η are the viscosity of the emulsion and solvent, and c is the *volume concentration*. η^* thus does not depend explicitly upon the radius of the suspended spheres; Eq. (1) holds both for mono- and polydisperse suspensions of rigid spherical particles. Solvation may be described as a process by which the particles bind solvent and in effect "grow," causing an apparent increase in c.

Einstein's theory of viscosity gives a pattern for similar theories of other physical properties of suspensions of colloidal particles in a continuous medium, whether this medium be fluid or solid. For instance, properties which may be discussed in this way include Young's modulus, thermal conductivity, and dielectric constant. Characteristic of such theories is the appearance of a property p^* of the suspension as a linear function of c for small concentrations and a power series in c for larger concentrations;

$$p^* = p[1+\alpha_1 c+\alpha_2 c^2+\alpha_3 c^3+\cdots], \qquad (2)$$

where p designates the property of the "solvent" corresponding to p. The coefficients $\alpha_1, \alpha_2, \alpha_3, \cdots$, cannot, in general, be obtained in an elementary manner; in most cases a somewhat intricate analysis is necessary for their determination. The α's are just numerical factors for spherical filler particles, but depend upon the shape for asymmetric fillers. The term involving $\alpha_1 c$, is owing to independent action of the filler particles, the term in $\alpha_2 c^2$, to the mutual interaction

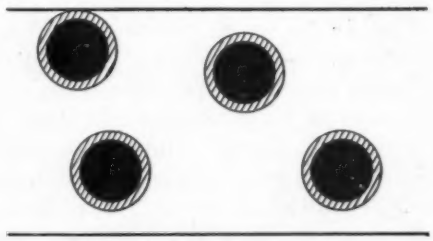

FIG. 1. Model for the rubber-carbon black system in the first range of concentration. The white area between the black spheres represents the continuous rubber matrix. The shaded areas around the black spheres indicate the binding of rubber by the carbon black spheres.

* Presented on June 24, 1944 before the Inaugural Meeting of the Division of High-Polymer Physics of the American Physical Society at Rochester, New York.

of pairs of particles, the term in $\alpha_3 c^3$, to the mutual interaction of triplets of particles, and so on.

Here we wish to outline our theoretical treatment of viscosity, Young's modulus, and dielectric constant. For the sake of definiteness, we shall consider the reinforcement of rubber with carbon black. Our general theory will hold, however, for other systems also.

1. MODELS FOR THE RUBBER-CARBON BLACK SYSTEM

Electron microscope studies, first carried out by Columbian Carbon Company,[3] revealed the *spherical* shape of the *colloidal* carbon black particles.

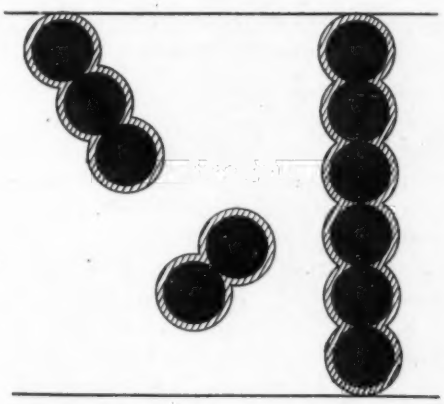

FIG. 2. Model for the rubber-carbon black system in the second range of concentration. Chain formation may lead to a continuous conducting bridge between the boundaries of the rubber-black system. Actually, the chains will not be straight, of course.

For the system rubber-black, three ranges of concentration of the carbon black may be distinguished.

More precisely, we define first the range within which there is no appreciable electrical conductivity (c up to about 10 percent). In this range the colloidal carbon black spheres may be considered as suspended in a continuous rubber matrix. Figure 1 shows the model for this range. The shaded ring around the black particles indicates the possibility of "solvation," i.e., the binding of rubber by the black particles.

In the second range (up to about 30 percent) carbon black *chains* develop, finally leading to a carbon black *network* interpenetrating the rubber network (Goldfinger and Smith[4]). Figure 2 indicates the gradual development of such a conducting network. In general, the chains will not be straight. The rapid rise of the conductivity with concentration shows directly that there must be chains forming continuous paths between the boundaries of the rubber matrix. Then, possibly, the chain, as a whole (rather than the individual spheres), will bind the rubber. As a model for such chains one may consider either a rod (as limiting case of a prolate ellipsoid) or the set of individual spheres directly. The treatment of both models involves certain approximations, and the choice of the model will depend upon the nature of the problem.

The third range ($c > 30$ percent) may be considered as one in which carbon black is diluted by the rubber. Figure 3 illustrates the cubic (most open) packing of the spheres. The rhombohedral (closest packing) corresponds to a higher concentration.

The present paper deals chiefly with the first region. It is hoped that clarification here will lead also to a better understanding of the second and third ranges. Clearly the second range is of greatest technical importance.

The binding of rubber by pigments was apparently first pointed out by le Blanc, Kröger, and Kloz and by Menadue. This idea was put on a firmer basis by Fielding,[5] and has been emphasized lately by Wiegand and his associates. The present experimental methods for the investigation of the rubber-pigment binding seem to be rather difficult and not too accurate. A somewhat simpler method will be indicated in Sections 2 and 3.

Wiegand and associates[6] have advanced the idea of *discrete* rubber spheres surrounded by the colloidal carbon spheres. Obviously, the consequences of such an idea would be of greater importance for the second and third range of concentration than for the first range which is the range of prime interest of the present paper. For this reason consideration of the discrete rubber theory will be deferred to a later paper. Literally taken, this theory implies in the first region a *mixture* of rubber and black spheres rather than a *suspension* of black spheres in a continuous rubber matrix. Actually, both the discrete and continuous rubber models are but different approximations for the complicated real case.

2. VISCOSITY OF THE RUBBER-CARBON BLACK SYSTEM

We have to define first what we mean by the "viscosity" of a rubber-black system. Experiment shows that a post-milled batch of the

rubber-black system exhibits electrical conductivity. Thus curing is not a necessary requirement for the development of continuous paths of black spheres throughout the rubber matrix. This fact, called to the attention of the author by W. W. Vogt and J. H. Fielding, makes plausible the definition of the viscosity of the rubber by the Mooney viscosity of the milled rubber and of the viscosity of the rubber-black system by the Mooney viscosity of the post-milled rubber-black batch.

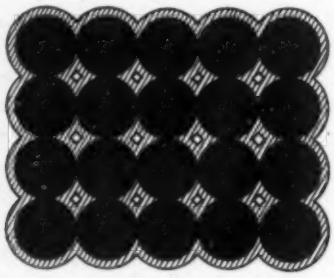

FIG. 3. Model for the rubber-carbon black system in the third range of concentration. Cubic (most open) packing of carbon black spheres.

Guth and Gold[7] have generalized Einstein's theory and computed the coefficient α_2 in Eq. (2). Methods of calculating the interaction of a pair of spheres embedded in a moving fluid were developed by Lorentz and Smoluchowski. These methods resemble the method of images used in electrostatics. Extension of these methods leads to the viscosity law

$$\eta^*=\eta[1+2.5c+14.1c^2]. \tag{3}$$

Introducing the specific viscosity $\eta_{sp}=\eta^*/\eta-1$ the relation (3) may be written

$$\eta_{sp}=2.5c+14.1c^2. \tag{4}$$

The viscosity law, (3) or (4), not only generalizes Einstein's law (1) for larger concentrations, but permits also a determination of the degree of solvation. Dividing Eq. (4) by c, one obtains

$$\eta_{sp}/c=2.5+14.1c. \tag{5}$$

Thus if one plots from experiment η_{sp}/c as a function of c one should obtain a straight line, at least in the range of concentrations from 0 to about 10 percent. The deviation from 2.5 of the intercept of this line on the η_{sp}/c axis measures then the degree of solvation.

Equation (4) assumes that the viscosity of the black η' is very large compared to the viscosity of rubber. For filler systems for which this assumption is invalid, a generalization of Einstein's theory by G. I. Taylor[8] leads to the relation

$$\eta^*=\eta\left[1+2.5c\left(\frac{\eta'+\frac{1}{2.5}\eta}{\eta'+\eta}\right)\right]. \tag{6}$$

For $\eta'\gg\eta$, Eq. (6) reduces to Eq. (1).

For $\eta'\ll\eta$, as is the case with a cavity, Eq. (6) reduces to

$$\eta^*=\eta[1+c]. \tag{7}$$

The problem of the viscosity of a suspension with rod-shaped filler particles is deferred to a later paper, because of its complexity.

3. ELASTIC PROPERTIES OF THE RUBBER-CARBON BLACK SYSTEM

The model in the first range of concentration, black spheres embedded in a continuous matrix of rubber, was first applied by Rehner[9] to a computation of certain elastic properties. In particular he called attention to the stresses in and around the filler particles.

The computation of the change in the elastic constants of rubber by the embedded black spheres is entirely analogous to the procedure in the theory of viscosity. If a rubber-black suspension is stretched, the suspended particles perturb the stresses and strains set up in the body. This perturbation leads to an *increase* in the elastic energy. This in turn gives an *increase* in the elastic constants, i.e., a stiffening of the stock. The detailed calculations are closely similar to those in the treatment of viscosity, and the final result is the same[10] with the Young's modulus E replacing the viscosity η

$$E^*=E[1+2.5c+14.1c^2]. \tag{8}$$

The same relation holds also for the shear modulus G, because of the relation

$$G=E/3. \tag{9}$$

Just as in the derivation of Eq. (4), it is assumed here that Young's modulus E' for the black spheres is large compared to the modulus of rubber, an assumption which holds quite well.

According to the kinetic theory of rubber elasticity, the stress-strain relation for moderate (up to 2–300 percent) extensions contains E only as a parameter:

$$Z=K[L-(1/L^2)]; \quad K=E/3. \tag{10}$$

Here Z is the stress per unit original cross section and L is the relative length. In view of the elasticity law (8) it is plausible to write

$$Z^*=K^*[L-(1/L^2)];$$
$$K^*=K[1+2.5c+14.1c^2]. \qquad (11)$$

According to this formula the embedded black spheres make the whole stress-strain curve steeper, by a factor K^*/K depending only upon the concentration. Thus stress-strain curves for varying amounts of fillers should be *similar* to each other. Binding can then be investigated as in the case of viscosity. Deviations from similarity may be caused by a variety of causes (in general interdependent), such as the beginning of the network formation, change of volume on stretching, crystallization, and time effects. On the other hand, the similarity may hold at concentrations well above the range of validity of the particular K^* in (11). The similarity is not bound to the theoretical stress-strain relation (10); it holds for any one-parameter family of stress-strain curves.

If the concentration increases above 10 percent, the stiffness of the stocks increases much more rapidly than (8) or (11) would predict. The reason for this is the formation of chains by the spheres. One can study this "accelerated stiffening" more quantitatively by considering rod-like filler particles embedded in a continuous matrix. For this model we obtain as an analog of (8)

$$E^*=E[1+0.67f\cdot c+1.62f^2\cdot c^2]. \qquad (12)$$

Here f is the shape factor (=length/breadth) of the rod, and we have assumed $f\gg 1$. For $f\leqq 1$, one comes back to (8). Equation (12) exhibits clearly the rapid increase of E^* with increasing concentration, this being, for large f, more nearly quadratic than in the case of spheres. This is in keeping with the rapid increase with concentration in the viscosity of suspensions of rod-like particles, in contrast to the slower increase for spherical particles.

It is noteworthy that stress-strain curves for varying amounts of fillers should be still similar even in the range of validity of Eq. (12).

Another consequence of elasticity theory for the rubber-black or for any other system is the influence on the tensile strength of the stress concentrations around the filler particles. J. Rehner, Jr., has called to the attention of the author a paper by Goodier[11] in which this effect is treated explicitly for metals. Goodier's solution of the equations of elasticity for static equilibrium is equivalent to the solution of the corresponding viscosity problem by G. I. Taylor, and checks with independent calculations by the author. Therefore, we simply quote his result for rigid spheres, inserting for Poisson's ratio the value 0.5 valid for rubber. In unilateral stress, a rigid sphere intensifies the stress at the poles, A, A' from Z to $2Z$ (cf. Fig. 4) in the same direction as the applied stress (stress concentration factor=2). The stress at the "equator" in the same direction is reduced to a *compressive* stress $(-)(1/2)Z$. It is interesting to remark that in shear there is *no* intensification of the stress by rigid spheres.

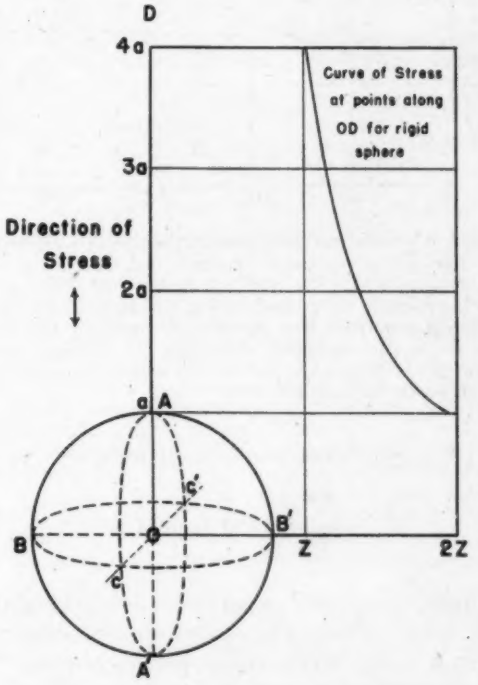

FIG. 4. Illustration of stress concentration around a rigid sphere. OD is the continuation of the radius OA ($=a$). The stress concentration is restricted to the immediate neighborhood of the sphere. Poisson's ratio $\mu=0.3$ was used in this figure, but the value $\mu=0.5$ instead, does not make much change [after Goodier (reference 11)].

An experimental check of all these theoretical conclusions has been undertaken by S. L. Dart at the Notre Dame Rubber Research Laboratory. We present here a few results. Figure 5 shows the effect of Continental S.R.F. in GR-S. The drawn line represents the theoretical equa-

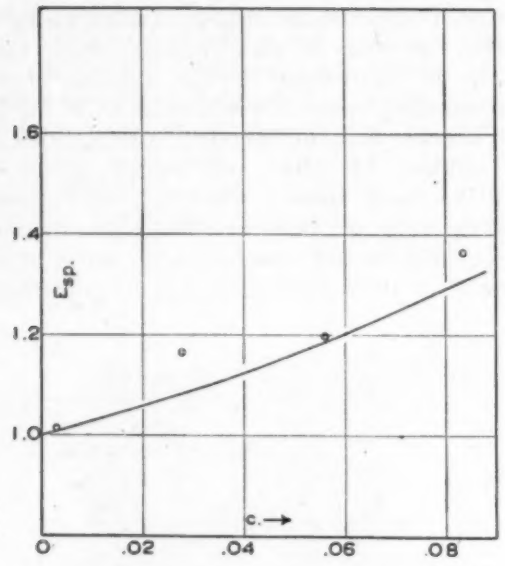

FIG. 5. The solid curve represents the theoretical equation (13). The circles represent experimental data for a GR-S black system, which was not "masterbatched." The second circle is probably misplaced, owing to experimental error. The deviation from the theoretical curve of the fourth circle is in the expected direction. Note that volume concentration is roughly half of the weight concentration, used generally in the literature.

tion (8) in the more convenient form

$$E_{sp}=\frac{E^*}{E}-1=2.5c+14.1c^2. \qquad (13)$$

The agreement with experiment is unexpectedly good, even without the assumption of solvation. Figure 6 shows stress-strain curves obtained by an automatic stress-strain machine. The lower curve represents a GR-S gum stock, the upper curve a stock with 15 percent loading. The crosses were obtained by multiplication of the lower curve by the constant factor 1.32. The deviations, 1.3 percent of the mean, are within the experimental error.

The data of Figs. 5 and 6 were measured on stocks which were not "masterbatched;" i.e., they were not obtained from a masterbatch by dilution. Masterbatched stocks are being investigated. For the stocks and their physical testing we are indebted to Dr. C. S. Yoran of Witco Chemical Company.

The expected decrease of tensile strength owing to stress concentration around the black particles checks roughly with observations on the same rubber-black [and rubber-calcium carbonate (Witcarb *R*)] systems, which were used to check the dependence of stiffness upon concentration. W. W. Vogt has pointed out to the author that he also found a dip in the tensile strength *vs.* concentration curve. The fact that this curve passes through a minimum before it starts rising is not noticed in the literature. Most of these curves reported start at 20 percent *weight* concentration or higher, so that the minimum escaped attention.

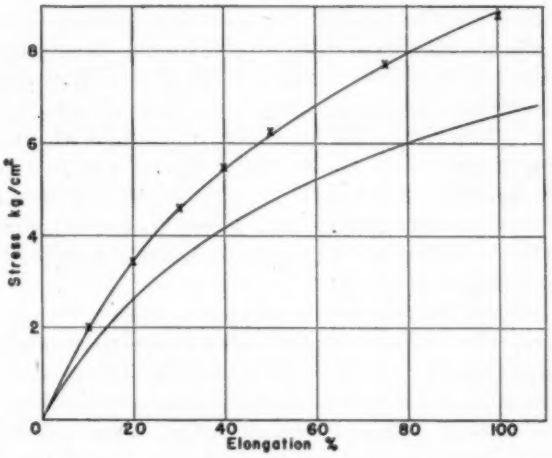

FIG. 6. Lower curve is the stress-strain curve (for unit original cross section) of a GR-S gum stock. The upper curve is the stress-strain curve for the same GR-S stock loaded with 15 percent by weight Continental S.R.F. The crosses were obtained by multiplication of the lower curve with the constant factor 1.32, thus proving the similarity of the lower and of the upper curve.

4. DIELECTRIC PROPERTIES OF THE RUBBER-FILLER SYSTEM

A discussion of the dielectric properties of the rubber-filler system may be based on the work of Rayleigh.[12] Rayleigh considered spheres of dielectric constant ϵ', arranged regularly in a cubic lattice, embedded in a matrix of the dielectric constant ϵ. He derived for the dielectric constant ϵ^* of this system the formula

$$\epsilon^*=\epsilon\left[1-\frac{3c}{\dfrac{2\epsilon+\epsilon'}{\epsilon-\epsilon'}+c-\dfrac{32\cdot(3.11)^2}{5}\cdot\dfrac{\epsilon-\epsilon'}{(4/3)\epsilon+\epsilon'}(3/4\pi)^{10/3}\cdot e^{10/3}}\right]. \qquad (14)$$

For small c this somewhat unwieldy formula simplifies to the relation

$$\epsilon^*=\epsilon\left[1-\frac{\epsilon-\epsilon'}{2\epsilon+\epsilon'}\cdot 3c\right]. \tag{15}$$

Equation (15) may be transformed into the form

$$\frac{\epsilon^*-\epsilon}{\epsilon^*+2\epsilon}=\frac{\epsilon'-\epsilon}{\epsilon'+2\epsilon}\cdot c, \tag{16}$$

if terms of higher order than c are neglected. It is clear that (16) holds only in the same (linear) range of concentration in which (15) is valid. The use of (16) as an exact formula as is done sometimes in the literature has no theoretical significance. The relation (15) or its equivalent was obtained by Maxwell, before Rayleigh's work. For $\epsilon=1$, the Maxwell relation (15) reduces to the well-known Lorentz-Lorenz formula

$$\frac{\epsilon^*-1}{\epsilon^*+2}=\frac{\epsilon'-1}{\epsilon'+2}\cdot c. \tag{17}$$

For asymmetric filler particles a formula of the type of Eq. (16) but with a shape factor s (which reduces to $s=2$ for a sphere)

$$\frac{\epsilon^*-\epsilon}{\epsilon^*+s\epsilon}=\frac{\epsilon'-\epsilon}{\epsilon'+s\epsilon}\cdot c \tag{18}$$

is ascribed to O. Wiener, and used also for the non-linear range of concentrations. It is clear, however, that (18) can have theoretical significance in the linear range only.

Measurements were made by Scott and McPherson[13] on the system rubber-calcium carbonate and (18) was used for the representation of the data with $s=2.7$ (obtained from the non-linear range). Though no electron microscope work was reported on the calcium carbonate used by Scott and McPherson, the electron microscope work on Witcarb *R* makes it plausible that their calcium carbonate particles were also spherical. In fact Scott and McPherson's data give s values closer to 2 in the linear range and thus check roughly Eq. (15).

A full treatment of the theory of filler reinforcement with detailed derivations and more material on experimental verification will follow shortly.

It is a pleasure to thank my friend Professor Hubert M. James for looking over the manuscript of this paper, and for constructive suggestions. It was planned to publish this paper jointly with him. Unfortunately, war exigencies prevented this.

REFERENCES

(1) A. Einstein, Ann. d. Physik **19**, 289 (1906); **34**, 591 (1911).
(2) E. Guth, *Proceedings of the Fifth International Congress of Applied Mechanics* (Cambridge, 1938), p. 448.
(3) Columbian Carbon Company, Rubber Chem. Tech. **14**, 52 (1941); W. B. Wiegand and W. T. Ladd, Rubber Age **50**, 431 (1942); cf. also C. E. Hall, E. A. Hauser, D. S. le Beau, F. O. Schmitt, and P. Talalay, Ind. Eng. Chem. **36**, 834 (1944).
(4) G. Goldfinger and W. R. Smith, paper presented at 1944 New York meeting of Rubber Division, American Chemical Society. The author is indebted to G. Goldfinger for interesting discussions.
(5) J. H. Fielding, Ind. Eng. Chem. **29**, 880 (1937). The author is indebted to J. H. Fielding and W. W. Vogt for interesting discussions.
(6) W. B. Wiegand, Canad. Chem. Process Ind. **28**, 151 (1944). The author is indebted to W. B. Wiegand and his associates for calling his attention to their discrete rubber theory.
(7) E. Guth and O. Gold, Phys. Rev. **53**, 322 (1938); cf. also reference 2, Fig. 1 for the experimental verification of Eq. (3) on a suspension of glass spheres.
(8) G. I. Taylor. Proc. Roy. Soc. London **A138**, 41 (1932).
(9) J. Rehner, Jr., J. App. Phys. **14**, 638 (1943). The author is indebted to J. Rehner, Jr., for interesting discussions on reinforcement.
(10) The definition of E^* leading to Eq. (8) is in agreement with the calculations of Dr. H. M. Smallwood, who independently obtained Eq. (8) in the approximation of Einstein, i.e., without the quadratic term $14.1c^2$. He also undertook an experimental verification of that relation, cf. J. App. Phys. **15**, 758 (1944). The author has considered also another, simpler definition of E^* which yields the relation $E^*=E[1+3c]$ instead of $E^*=E[1+2.5c]$, as given by (8). The approximations involved in the two definitions will be discussed in the detailed treatment of the reinforcement problem. In the discussion of the present paper at the Rochester meeting, Dr. Smallwood mentioned his attempt to check Einstein's viscosity law [see equation (1) of this paper] for the rubber-black system, employing Mooney viscosities in the same way as proposed by the author in Section 2 of this paper.
(11) J. N. Goodier, Trans. A. S. M. E. **55**, 39 (1933).
(12) Lord Rayleigh, Phil. Mag. [5] **34**, 481 (1892).
(13) A. H. Scott and A. T. McPherson, J. Research Nat. Bur. Stand. **28**, 279 (1942).

Kinematic Errors in Bobbin Drives on Roving Frames*

BY S. L. GERHARD

Textile Division, U. S. Rubber Company, Hogansville, Georgia

(Received August 28, 1944)

OWING to practical limitations of one kind or another the machines employed by industries to make their products are not always built according to the theoretically perfect design for a desired motion. It may accordingly be important to know in some instances how much the actual motions deviate from the desired or theoretically perfect ones. This information coupled with a knowledge of the physical properties of the material being processed may be valuable in quality control studies, especially those concerned with uniformity, or in explaining otherwise mysterious phenomena associated with the operation of particular machines.

Examples of the methods and detailed calculations involved in typical kinematic analyses may be of interest to physicists because the kinematics of machinery is usually studied in detail only by engineers. The example chosen is from the textile industry, but the general method of attack described here can be applied to kinematic problems found in any industry. The purpose in making the original investigation was purely economic. Salesmen from time to time made claims for one type of bobbin drive over another type, and we wished to know whether their claims were valid. The purpose in publishing this paper is to illustrate by this example the methods and the usefulness of kinematic analysis in manufacturing problems.

DESCRIPTION OF MACHINE

The essential features of the mechanism to be analyzed are shown in Fig. 1. Roving is delivered from the front rolls R through the flyers F to the bobbins B; only one bobbin is shown, but there are 104 in two rows on one machine, each row driven by one shaft. The bobbins are carried by a carriage C which moves up and down to wind the roving on the bobbins as it comes from the flyers, which remain at a fixed height relative to the frame of the machine. The over-all purpose of the roving operation is to draft or stretch the material and insert a little twist.

The bobbins are driven by the carriage shafts through off-center bevel gears, as indicated in the cut-away part of Fig. 1. The two carriage shafts, only one of which is shown, are in turn driven by the jack shaft J through intervening gears or chains. The problem is to determine the nonuniformity of the bobbin speed as the carriage rises and falls. In certain types of mechanisms for transmitting this motion the vertical displacement of the carriage produces rotation of the shaft C independently of the rotation of J. Other facts about the machine necessary for understanding the analysis are as follows. The front rolls R deliver roving at 26.7 yd./min. and the flyer F turns at about 800 r.p.m. to insert twist. In order for the roving to wind up on the bobbin the latter must turn faster than the flyer, the difference in surface speeds being the surface speed of the front rolls. The differential gears and specially shaped cones coupling the jack shaft to the main drive shaft, flyers, and traversing mechanism are, for the sake of simplicity, not shown. It is assumed that these parts are properly

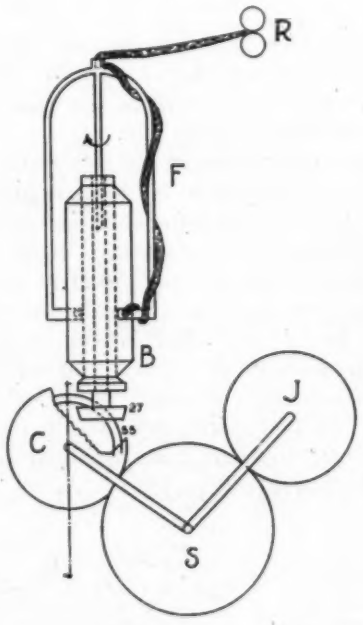

FIG. 1. Swing gear drive and related parts of roving frame.

* Presented on June 24, 1944 before the Inaugural Meeting of the Division of High-Polymer Physics of the American Physical Society at Rochester, New York.

designed to keep constant the surface speed of the package and the lay as the package diameter increases. This assumption may be open to question, but is not relevant to the immediate problem.

MECHANISMS EMPLOYED FOR DRIVING BOBBINS

A kinematically perfect drive is the "angle shaft" drive, so-called because of a shaft going obliquely from J to the base of the machine beneath the carriage. This angle shaft drives a vertical shaft which carries a sliding gear meshing with another gear on the carriage. In this drive the traverse has no influence on the bobbin speed. This mechanism is not used extensively, however, because wear on the gears and sliding keyways on the vertical shafts necessitates frequent repairs.

The swing gear drive shown in Fig. 1 is probably the most popular one. A large "swing gear" S is mounted to mesh with gears C and J at all positions of the carriage. In this instance the kinematic error arises from epicyclic motion of S around J and of C around S as the carriage traverses.

In the simple chain drive shown in Fig. 2 the error comes from the change in length of the driving segment of chain between J and C. In this and Fig. 3 only the driving or tight side of the chain circuit is shown, the other part consisting merely of an idler under spring tension to take up the slack as the carriage traverses. In the improved chain drive in Fig. 3 the change in chain length between J and S is the principal source of error.

ANALYSIS

As these mechanisms are designed to approximate closely the desired motions it requires considerable accuracy to obtain reliable estimates of their errors. But the accuracy of the calculations is limited by the 3 or 4 significant figures obtainable from measurements on the machines themselves.

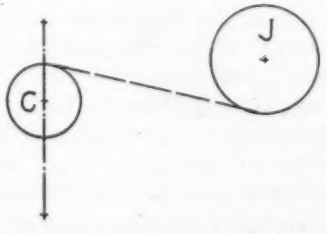

FIG. 2. Simple chain drive.

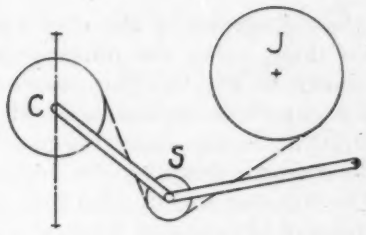

FIG. 3. Improved chain drive.

The (rotational) displacements of the bobbins are first calculated and then the (rotational) speeds are derived therefrom, as will be described below.

In these two steps of the analysis the gear J is assumed to be stationary, because this condition allows the calculation of the erroneous speeds to be made without interference from the much greater speeds present when operating normally.

Displacements: The analysis for the swing gear will be described in some detail. The epicyclic features of this drive are shown in Fig. 4. The first two steps are to apply to S and C in succession the well-known formula for epicyclic gear trains:

$$n = me + \Delta\theta - e\Delta\theta \qquad (1)$$

where

n = turns of last gear,

m = turns of first gear,

e = train value,

$\Delta\theta$ = turns of arm,

and all rotations are with reference to a fixed direction in space. Applied to the motion of S when J is locked and arm a (Fig. 5) rotates $\Delta\theta$ radians counterclockwise this formula gives for the rotation of S

$$n_S = 0 + \Delta\theta - (-50/63)\Delta\theta = 113\Delta\theta/63. \qquad (2)$$

This rotation of S coupled with the rotation $\Delta\phi$ of arm b produces the following rotation of C

$$n_C = (113\Delta\theta/63)(-63/46) + \Delta\phi - (-63/46)\Delta\phi. \qquad (3)$$

Inserting the train value of 55/27 between C and B the rotation of B is found to be

$$n_B = 4.827(\Delta\phi - 1.037\Delta\theta). \qquad (4)$$

This is the strictly kinematic part of the analysis and shows that the object of the next few steps

must be the calculation of the angles ϕ and θ.*

This was done, using the dimensions of the machine shown in Fig. 5. The position of the carriage was chosen as the independent variable with the origin at the top of the traverse, in which position the roving is wound on the bottom of the bobbin. The traverse was divided into $\frac{1}{2}''$ steps, making a total of 13 positions. From this point on the calculations may be made either analytically

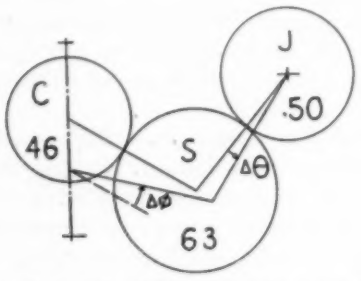

FIG. 4. Epicyclic relations in swing gear drive.

or graphically, and both these methods will be described.

The analytic method may involve conic sections and other plane curves, but it usually consists in the solution of a connected series of triangles, in this instance the triangles *JOC* and *JCS* for each $\frac{1}{2}''$ step. The following equations were employed:

$$k=h-2.25,$$

$$\tan\alpha=k/13.82,$$

$$x=13.82/\cos\alpha,$$

$$s=(a+b+x)/2,$$

$$r=((s-a)(s-b)(s-x)/s)^{\frac{1}{2}},$$

$$\tan A/2=r/(s-a), \text{ etc.}$$

$$A/2+B/2+C/2=90°,$$

checked to within one second.

$$\theta=90°-\alpha-B,$$

$$\phi=90°-\alpha+A,$$

$$\left.\begin{aligned}\Delta\theta&=\theta-\theta_0\\ \Delta\phi&=\phi-\phi_0\end{aligned}\right\}\text{where the zero subscripts indicate the values when } h=0.$$

$$n_B=4.827(\Delta\phi-1.037\Delta\theta). \qquad (4)$$

The work was laid out in tabular form, a column for each $\frac{1}{2}''$ step and lines for each operation indicated by the above equations. Seven-place log tables and a calculating machine were used.

The graphic method, which will now be described, may in many problems be the only practicable one, because of excessive complications in the analytic method. The lines in Fig. 5 were laid out accurately to half-size and the positions of the arms drawn in for each $\frac{1}{2}''$ step along h at the left of the figure. Lengths were measured on the graph to obtain from their ratios the sines or tangents of ϕ and θ. These angles were then used as in the last equation to get the displacement of the bobbin. The displacements obtained by the two methods agree very well.

The values thus obtained for bobbin displacement are shown by the small circles and smooth curve in Fig. 6, where they are compared with curves actually traced on a bobbin while the carriage was racked up and down by hand, the jack shaft being locked. The directions in which these curves were traced are indicated by arrows. It is seen that agreement is very good, taking into consideration the lost motion during the upper part of the traverse and at the ends of the traverse. The longer curves below are for the full 12" traverse, and the shorter ones above for the 7" traverse used when the bobbin is full.

The displacements produced by the two chain drives were determined in a similar fashion. The length of the driving segment was calculated for

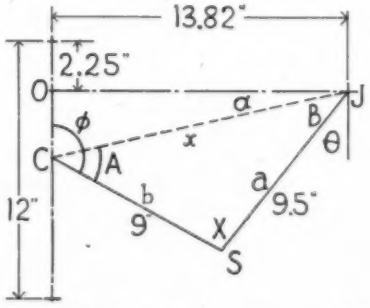

FIG. 5. Dimensions of swing gear drive.

each $\frac{1}{2}''$ step from the lengths of the tangents and the arcs of contact on the sprockets, between fixed (vertical) directions on J and C. The differences between the length at $h=0$ and the lengths for other positions were converted into bobbin displacements, ΔL taking the place of $\Delta\phi$ and $\Delta\theta$ in a simpler formula to get n_B. This required the solution of triangles as in the swing gear problem, and need not be described in more detail. No

* Another derivation using the angle X instead of ϕ in Fig. 5 and transforming to and from the rotating coordinates associated with the arm a produces exactly the same numerical results.

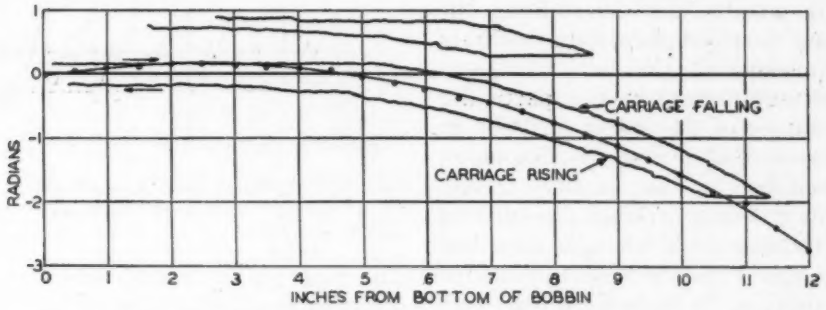

FIG. 6. Observed and calculated displacements of bobbin on swing gear drive.

frames with chain drives were available for observing and recording the actual bobbin displacements.

Speeds: Having the erroneous displacements, the next step is to determine the speeds resulting therefrom, because the relative speeds of bobbin and front rolls govern the amount of deformation of the material, as will be explained later. From here on the arguments and procedures are the same for both kinds of drives. As the displacement is a function of the carriage position the speed of the latter will determine the erroneous speed of the bobbin. If dh/dt is the carriage speed during the traverse, the erroneous bobbin speed will be

$$dB/dt = (dh/dt)\Delta B/\Delta h,$$

where $\Delta B/\Delta h$ is the average slope of the displacement curve between each $\frac{1}{2}''$ step, as calculated above. The carriage speed at the beginning of the doff is 0.77 yd./min., which produces $1.54\Delta B$ yd./min. error in the surface speed of the bobbin. The jack shaft and traversing speeds are automatically adjusted at the ends of each traverse to decrease in proportion to the increase in package diameter, hence the error speed of the package surface at a given height is the same throughout the doff.

These small erroneous speeds are superposed on the constant speed transmitted by the rotation of the jack shaft J. They are in the nature of speed variations and will be so designated from here on. They are shown in Fig. 7 for all three drives as a percentage of the front roll speed.

In contrast to the fairly smooth displacement curves in Fig. 6 the calculated points for the speed variation curves in Fig. 7 are somewhat scattered along the general direction of straight lines. This demonstrates the necessity for using a large number of significant figures in the calculations, because the speed variations come from the differences between successive displacements, and these differences are small compared to the numbers themselves. From the greater scatter of the points obtained in the graphic solution, indicated by solid circles for the swing gear, it is evident that the trigonometric method is somewhat more accurate.

The speed variations of the chain drives are linear over the entire height of the bobbin, and for the improved one are slightly less than for the simple drive. The swing gear variations are linear in all but the upper third of the bobbin, where they change more rapidly; and they are about as bad as those for the simple chain drive.

A better estimate of the speed variation could be obtained by differentiating the equation of the

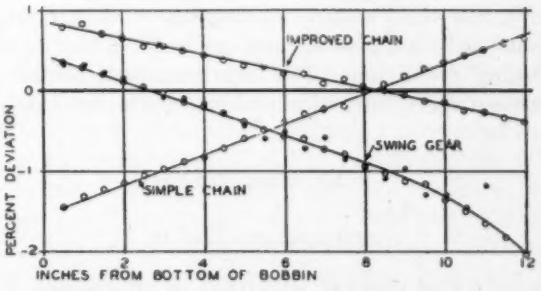

FIG. 7. Percent deviation in speed and size for the three drives.

displacement curve, if the equation were available. The numerous steps in the calculations indicate that it would be impracticable to attempt to find it analytically in all but the simplest mechanisms. But the empirical equation can in general be found by plotting the displacements on log paper or some other more suitable rulings to give a straight line, from which graph the proper constants can be determined. Probably the most practicable over-all procedure would be to employ the graphic method with great care, using as

large a scale as possible for determining the displacements and then plot these data to obtain the empirical equation.

Another important feature in this particular problem is the nature of the speed variation in successive traverses. Up to now the discussion has been confined to the case of the carriage falling. When the carriage reverses direction at the end of the traverse dh/dt changes sign, but $\Delta B/\Delta h$ does not; hence there is an abrupt change in the speed variation, as shown for two successive traverses in Fig. 8. The speed variation changes from a positive to an equally great negative value, or vice versa, at each end of the traverse. This satisfies the necessary condition that the total displacement over a complete cycle shall be zero.

EFFECT ON MATERIAL

The influence of these speed variations is estimated by noting the physical properties of the material. The roving at this stage has little power of recovering elongations produced by slight tensions. The front rolls deliver roving at a constant speed while the bobbin winds it up. If both speeds were constant and the bobbin turned one percent faster the roving would be irreversibly stretched by this amount and would weigh one percent less per unit length. However, if the bobbin ran slower than the front rolls the roving being non-rigid would not increase in weight but would only hang loose and probably make poor running conditions. The mathematical relation between speed variation and size variation would thus be

$$\Delta Y \begin{cases} = \Delta S & \text{when } \Delta S > 0, \\ = 0 & \text{when } \Delta S \leqslant 0, \end{cases}$$

where ΔY is percent variation of the roving in yd./lb. and ΔS is the percent speed variation.

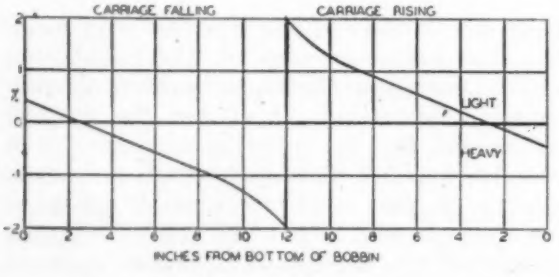

FIG. 8. Percent variation for swing gear frame in successive traverses.

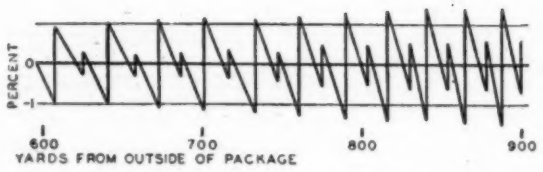

FIG. 9. Calculated variations produced by bobbin drive along roving as unwound from the bobbin.

The twist in the roving will vary by equal but negative percentage amounts.

Actually the bobbin runs at a slightly varying speed, sometimes faster and sometimes slower than the front rolls. This should produce roving with variations as shown by the curves above the zero line in the graphs, i.e., the roving responds only to those variations in bobbin speed that tend to make it lighter, but not to those that tend to make it heavier. The total range in size should be from 0 to about one percent light. It is possible that the variations may at times be different from the values shown here, which were based on the ordinary running conditions existing at the time the measurements of traverse speed were made on this particular frame. If other machine constants obtain at other times the methods and principles applied here will still be the same, only the magnitudes of the results being altered.

The variations along the roving as unwound from the bobbin were next calculated, taking into account the changing diameter and changing traverse. Part of this curve is shown in Fig. 9. It is seen that the variations are quasi-periodic, with increasing amplitude and frequency as the barrel of the bobbin is approached. From this curve it is apparent that the most favorable place to find the predicted variations is near the barrel, where they have the greatest amplitude.

The results of this calculation demonstrate another important fact pertaining to subsequent operations. Except in the "one-process roving" machine organization two of these strands are fed side-by-side into the next roving frame. Consequently the variations in the material going through the rolls are the sum of two curves like those shown in Fig. 9. As the two packages in the creel are not started together the two curves are staggered somewhat, thereby producing another quasi-periodic curve which contains "beats." To complicate matters further this machine has similar errors in the bobbin drive, and superposes on this beat curve another set of variations like those in Fig. 9. The complexity of the resulting curve is left to the reader's imagination. It is thus

evident that the likelihood of finding the variations predicted for roving size as a function of height on the slubber bobbin is exceedingly small after any subsequent operation. It may be profitable to bear this in mind when studying other kinematic errors, and these results emphasize the importance of looking for and measuring the effects of a certain operation or machine immediately after introduced into the material rather than in the finished product where it may be obliterated by intermediate causes.

Short length variations in yarn size, which presumably result from even shorter variations in roving size, are important factors in determining yarn and cord strength. Experimental investigations have shown that breaks occur at the thinnest segments in test specimens, and these thin segments may be only an inch long. It is therefore important to eliminate as far as possible variations in the processes prior to spinning.

The influence of variations like these on size control is briefly as follows. If the lengths weighed for size control are shorter than the yards per layer at the customary place for sampling in a package, then erroneous conclusions might be drawn about the average size, and may also result in unwarranted gear changes, the more so the shorter the length weighed. The importance of this relation in any particular instance can be judged from the fact that the yards per layer range approximately from 10 to 25 on slubber and intermediate frames.

The results of similar analyses of other mechanical causes of variations might shed some welcome light upon the statistical problem of deciding how many yards of material should be weighed in analyzing or comparing the variations produced by different machines. Here again the relative magnitudes of the length weighed and the wave-length of the variations from yard to yard will be an important factor.

This concludes the mathematical part of the analysis, and supplies part of the answer to the original question, namely, that the chain drives produce the same kind and approximately the same amount of speed variations as the swing gear. The remainder of the problem is to determine by measurements on the roving itself whether the resulting size variations are detectable, and if so whether they are great enough to warrant improvements in the bobbin drive.

MEASUREMENTS ON ROVING

About a dozen packages were picked at random and tested for size variation as a function of height on the bobbin and direction of traverse by weighing individual one-yard lengths. When the data were analyzed it was found that there was as much variation within bobbins and between bobbins as there was between heights on the bobbin. And there was no perceptible difference between successive layers, that is, between carriage rising and carriage falling. From this particular experiment it may thus be concluded that the errors in existing bobbin drives may produce variations in roving size but that these variations are imperceptible among those originating in other causes. However, the errors in these drives can only make matters worse, so far as variations are concerned.

SUMMARY

A method of determining the kinematic characteristics of a machine has been described, and it is shown how the results may be used to predict variations in the material being processed. As the material normally handled by the textile industry is noted for its non-uniformity statistical analysis must be used to interpret most of the data obtained. One of the major objectives of the industry is to study the sources of non-uniformity in an attempt to eliminate them. Therefore any clue toward a physically predictable pattern of variation is of value, for around this nucleus can be assembled a rational statistical analysis. Such an analysis can evaluate directly the seriousness of any such physical cause; this is in contrast to the necessarily empirical analysis that is the only recourse in the absence of physical theories. It is hoped that the procedures outlined in this paper may suggest other applications of kinematic analysis and may aid in a more direct and fruitful attack on manufacturing problems.

The author wishes to thank Mr. A. C. Link and other members of the Stark Mills organization for their cooperation in the initial phases of this work, and Mr. S. H. Sherman and Mr. J. J. Mills for their interest and suggestions while it was in progress. The author is indebted to Mr. E. C. Lamon for assistance in making the calculations. The permission of the U. S. Rubber Company to publish this work is gratefully acknowledged.

Control of Elongation in Highly Stretched Cotton Tire Cord*

BY HOWARD J. PHILIPP AND CARL M. CONRAD

*Southern Regional Research Laboratory,** New Orleans, Louisiana*

(Received August 14, 1944)

INTRODUCTION

THE useful life of a pneumatic tire is known to depend to a large degree on the quality of the cord used in its manufacture. Quality is not a simple function of any one measurable property, but rather a combination of a multitude of properties. Just what the contribution of some of the individual properties is, or what constitutes the best combination of properties, is not completely understood. This study is primarily concerned with only two properties, (1) the breaking strength and (2) the elongation† at a load of ten pounds, and with methods for their improvement and control.

Many efforts have been directed toward the improvement of cord strength because, other things being equal, the stronger cord will make the better tire. Most of the methods that have been described for the improvement of cord strength are stretching treatments. F. L. Sessions,[1] as early as 1930, described a treatment by which the dry tire cord was stretched with or without the application of heat and pressure during the stretching. The use of a rubberizing bath during stretching was contemplated, but no water was employed. C. R. Brownell[2] improved the strength of very highly twisted tire cord by applying a stretching treatment to the plied yarns as well as to the whole cord. The stretching was carried out with or without previous wetting of the cord, but no heat was applied during or after the stretching. He stated that a cord which was passed through a liquid before the stretching had a greater strength and lower elongation than one merely stretched in the dry state. Gwaltney, Graybill, and Newton[3] patented a process for the manufacture of heat-resistant tire cord in which the plied yarns were saturated with a liquid and then either wet-twisted under a tension just short of the breaking point, or wet-twisted in the usual manner, after which the finished wet cord was stretched under a tension short of the breaking point. They, too, did not contemplate the use of heat during the stretching, but reported an even greater strength and lower elongation when the wet cord was compressed by passing it through a nipper after the stretching.

A treatment used to improve the strength of sewing thread by wetting and stretching without heat is reported by A. Burgeni.[4] The process is similar to the tire cord treatment of Brownell, as well as that of Gwaltney, Graybill, and Newton.

R. F. Nickerson obtained an Australian patent[5] for a method of improving the strength of tire cord by wetting it, then stretching and while under tension heating it by means of moist or dry heat. He obtained improvements in bone-dry strength of about 45 percent with elongations at 10 pounds as low as 2 to 3 percent. Nickerson observed that the strength was directly, and the elongation inversely, proportional to the tension used. He stated that no additional benefits were gained by giving cord repeated stretching treatments under identical conditions.

Most tire manufacturers agree that cord having too much stretch will permit an undesirable permanent enlargement of the tires during use, known as "tire growth." Too little stretch in the cord will impair the impact strength of tires; i.e., they will not be able to withstand the sudden shocks caused by stones and irregularities of the road. There is no general agreement as to what the optimum elongation is, but some tire manufacturers consider an elongation of around 6 percent at 10 pounds, measured under bone-dry conditions, as most desirable for cotton cord. In this investigation, the range of 6 to 6.5 percent was considered to be the optimum. Of course, the stretch characteristics of tire cord are fully represented only by a load-elongation curve; but as long as the general shape of this curve remains

---

* Presented on June 24, 1944 before the Inaugural Meeting of the Division of High-Polymer Physics of the American Physical Society in Rochester, New York.

** This is one of the laboratories of the Bureau of Agricultural and Industrial Chemistry, Agricultural Research Administration, U. S. Department of Agriculture.

† Elongation is to be understood as the deformation in the direction of load caused by a tensile force, in accordance with the definition under D123-42 of A.S.T.M. Committee D-13 on Textile Materials (reference 6). It is expressed as a percentage of the original length.

the same, the elongation at a particular load is a fair measure of the stretch properties of the cord.

The elongation of tire cords which have been treated by any of the known stretching methods is always much lower than that of untreated cords. When cord is stretched to such a degree as to give it the greatest possible strength, its elongation at 10 pounds is usually well below the optimum range. There is a definite reciprocal relationship between the strength and elongation of stretched tire cords. As a result, one has the choice of producing either very strong cords, of very low elongation, or cords of optimum elongation, with comparatively slight improvement in strength. The two properties, strength and elongation, are thus linked together in such a manner that it has seemed impossible to take full advantage of any of the stretching treatments. Part of the potential strength obtainable by stretching had to be sacrificed in order to keep the elongation at 10 pounds within an acceptable range. Strength and elongation could not be controlled independently.

Recently, however, our efforts to produce a tire cord that would combine almost maximum strength with optimum elongation have led to the development of a dual-stretching treatment which permits a control of the elongation to be realized almost independently of the improvement in the strength of the cord.

MATERIALS AND METHODS

All the tire cords used in this investigation were made on conventional machines in the experimental cotton mill at the Southern Regional Research Laboratory. Several different cotton varieties and cord constructions were used in the experiments to make sure that the observed effects were not restricted to any one cotton or construction. The cottons used, together with their staple lengths, were as follows:

Stoneville 2*B*	$1\frac{3}{32}$ inches
Delfos 651	$1\frac{1}{8}$ inches
Acala 1517	$1\frac{5}{32}$ inches
Wilds 13	$1\frac{11}{32}$ inches
S×*P*	$1\frac{1}{2}$ inches.

Treated and untreated cords were tested for tensile strength and for elongation at 10 pounds on a Scott tire-cord tester equipped with ink recording device, in conformity with specifications for testing tire cord of the American Society for Testing Materials, Committee D-13 on Textile Materials,[6] with the exception that ten breaks only were made for most samples and that the tests were made under "bone-dry" conditions instead of standard conditions of temperature and humidity. Bone-dry conditions were selected so that the results could be more readily compared with those obtained by other laboratories which maintain different atmospheric conditions. In order to have the samples bone-dry, a bundle of cords, consisting of a few more than ten pieces cut to a suitable length and held together loosely by a cord bearing an identification tag, was placed with one end slightly protruding in an open wide-mouthed bottle. The bottle was placed in an electric, forced-draft oven, thermostatically controlled at 225°F. After two and one-half hours the bottle was removed from the oven and a wad of cotton was pushed into the top in such a way that one end of the bundle of test pieces remained outside, permitting the pieces to be pulled out individually for testing. Ten breaks were finished in about five minutes, so that almost no trend could be observed in the strength and elongation data caused by absorption of moisture from the air during testing. The elongations were read from the autographic load-elongation charts obtained by the Scott tire-cord tester. Where gauge or count measurements are given, they were taken under standard atmospheric conditions of 70°F and 65 percent R. H.

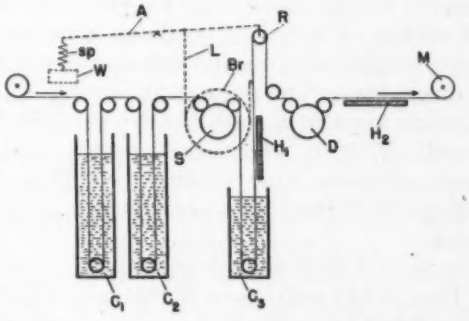

FIG. 1. Laboratory-scale stretching apparatus. C_1, C_2, C_3, liquid containers; *S*, snub rolls; *D*, driving rolls; *Br*, brake roll; *M*, winding spool; *R*, small roll; *A*, lever arm; *L*, leather belt; *sp*, spring; *W*, weight; H_1, H_2, electric hot plates

The various stretching treatments were carried out on a small, laboratory-scale stretching apparatus, similar to that used by Nickerson,[5] which was especially adapted for the purpose at hand.

Figure 1 shows a schematic drawing of this apparatus.

The cord was allowed to pass through the two containers C_1 and C_2, which were filled with a swelling agent for cellulose. As such, plain water was used, or water containing a wetting agent which accelerated penetration of the cord and thereby hastened the swelling action. The cord was then stretched under constant tension between the snub rolls S and the driving rolls D by a mechanism indicated by the dotted lines in Fig. 1. This tensioning device consisted of a small roll R over which the cord had to pass on its way from the snub rolls to the driving rolls and which was attached to the lever arm A. The lever arm carried a weight W suspended by means of a spring sp on the other end and could act upon the snub rolls S by way of the leather belt L laid around the brake roll Br which, in turn, was mounted on the same shaft as the snub roll S. The spring sp acted as a shock absorber and greatly improved the smoothness of operation of the mechanism. The only motor-driven parts in the whole apparatus were the driving roll D and the roll M onto which the treated cord was wound. Between the driving rolls D and the winding roll M the cord was under only negligible tension.

The snub rolls S were driven by the cord itself but they could only turn if the grip which the leather belt had on the brake roll was released by a downward movement of the small roll R thus creating a tension in the cord which could be controlled by the size of the weight W. If, because of irregularities, some parts of the cord stretched more than preceding parts, then the small roll R moved upwards, thereby slowing up the snub rolls until the predetermined tension was set up in the cord again. If a part of the cord did not stretch sufficiently, then the roll R was pulled down to such an extent as to speed up the snub rolls until equilibrium was re-established. It was thus possible to stretch cord at any predetermined constant load. While under tension, the cord could be wetted again by a liquid contained in C_3.

If it was desired to apply heat during or after the stretching an electric hot plate, twelve inches long, could be placed either at H_1 or at H_2. In the position H_1 heat was applied to the cord under tension. In the position H_2 the heater merely served as a drier, since the rolls M and D moved at about the same surface speed and consequently the cord was under no tension at H_2. The temperature of the hot plate could be regulated by means of a variable transformer. The surface temperature was selected so that it would completely dry the cord without damaging it; this depended on the gauge of the cord and the speed at which it passed over the heater. At the slow speed at which this particular stretching apparatus was operated (about 143 yards per hour) the surface temperature of the hot plate was between 320 and 360°F.

It appeared from experiments, using several variations of the machine described, that the particular type of stretching mechanism used does not affect the results in general, although it may have an influence on the uniformity of the product. Thus, two sets of rolls driven at different speed, or two sets of rolls of different diameter driven at the same speed, or a pair of capstans were also found satisfactory for stretching the cord. In place of the electric heater, infra-red radiation proved adequate.

EXPERIMENTS AND RESULTS

Stretching Under Various Conditions of Moisture and Heat

In order to find the best combination of factors known to improve the strength of tire cord, various treatments involving one stretching under various conditions of moisture, heat, and tension were investigated. The following are representative of the results obtained. In one experiment a tire cord, made from $S \times P$ cotton and having a 21/5/3 construction, was simply stretched in the apparatus after the manner of the Sessions method,[1] without any liquid being in the three containers, in the absence of any heat, and with the greatest tension possible without breakage. In this instance the applied tension could not exceed 15 pounds. As will be seen from Table I, rows 1 and 2, the strength of this "dry-stretched" cord was increased by about 28 percent as the result of this treatment, while the cord's gauge and its elongation at 10 pounds were reduced, the latter well below the optimum range. When lower tensions were used for stretching, the elongation could be brought up to 6 to 6.5 percent but the strength increase was very small.

In another single-stretching experiment, employing 21/5/3 tire cord made from Acala cotton, the three containers C_1, C_2, and C_3, through which the cord had to pass before being stretched at a tension just short of the breaking point (13 pounds), were filled with ordinary water. Again no heat was applied to the cord under tension, but the cord was dried over the electric hot plate

TABLE I. Influence of various stretching treatments on strength, and on elongation at 10 pounds of 21/5/3 tire cords made from different cottons.

Cotton variety	Treatment	Cord gauge in.	Bone-dry strength lb.	Strength based on control percent	Bone-dry elongation at 10 lb. percent
(1) $S \times P$	Control	0.034	20.0	100.0	8.2
(2) $S \times P$	Dry-stretching	.031	25.6	128.0	4.4
(3) Acala	Control	.033	15.7	100.0	9.4
(4) Acala	Cold-wet-stretching	.030	20.0	127.4	6.8
(5) Stoneville 2*B*	Control	.034	16.2	100.0	9.4
(6) Stoneville 2*B*	Steam-stretching	.030	20.7	127.8	5.7
(7) Acala	Control	.033	15.7	100.0	9.4
(8) Acala	Hot-wet-stretching	.029	23.3	148.4	4.6

at H_2, when it was no longer under tension. The only difference between this and the preceding experiment is that in this one the cord was stretched in a wet condition, as contemplated in the Brownell patent.[2] Since no heat was employed while the cord was under tension, this treatment will be referred to as "cold-wet-stretching." The results of the tests, given in Table I, rows 3 and 4, show that this treatment gave about the same relative increase in strength and decrease in gauge, but that the elongation was not reduced to below the optimum range. A further reduction in elongation was impossible because the cord broke if greater tension was used. Almost identical results (not shown) were obtained by this treatment omitting use of the hot plate in position H_2.

Next, the effect of a "steam-stretching" treatment on a 21/5/3 tire cord made from Stoneville 2*B* cotton was tried. Before being stretched at maximum tension (14 pounds), the cord passed through a glass tube, 10 inches long and of $\frac{1}{4}$-inch inside diameter, which was placed between the container C_2 and the snub rolls S (see Fig. 1). Saturated steam was blown through the tube, entering through a sidearm located midway between the ends. The three containers were empty. Again no heat was applied while the cord was being stretched, but at times a heater was placed at H_2 without having any influence on the results obtained. The testing results given in Table I, rows 5 and 6, show that the effects of this treatment on gauge, strength, and elongation were about the same as those of the two single-stretching treatments previously described. The elongation was reduced to a value below the optimum and could only be increased by use of a lower tension which greatly reduced the strength of the treated cord.

Finally, a single-stretching treatment, which consisted of the combined application of water, tension, and heat according to the method described by Nickerson,[5] was applied to the same 21/5/3 cord as was employed for the cold-wet-stretching experiment (Acala cotton). In this experiment the experimental conditions were almost the same as for the cold-wet-stretching treatment reported in row 4 of Table I, the only exception being that the heater was placed at H_1 instead of H_2 so that heat was applied to the moistened and stretched cord while under tension. The cord was wetted by passing through the two containers, C_1 and C_2, filled with water; was stretched just short of the breaking point (11 pounds) between the snub rolls S and the driving rolls D; and was exposed to heat, while under tension, at H_1. This treatment, which will be referred to as "hot-wet-stretching," gave the results shown in Table I, rows 7 and 8. The relative strength increase amounted to about 48 percent, while gauge and elongation again showed a pronounced decrease. This same treatment, applied to the 21/5/3 cords made from the $S \times P$ and Stoneville 2*B* cottons, gave strength increases of 53 percent and 40 percent, respectively.

The greatest strength increase was thus obtained by the "hot-wet-stretching" treatment. It is important to point out the difference between this and the "cold-wet-stretching" treatment. Heat was employed in both processes. However, while it served merely as a means of drying in the cold-wet-stretching treatment, it was an essential part of the process in the hot-wet-stretching treatment. This is evidenced by the facts that the strength and elongation at 10 pounds of a cold-wet-stretched tire cord were not influenced by use or non-use of heat after the stretching, whereas, when heat was omitted during the hot-wet-stretching treatment, only a little more than half as much strength increase was obtained. Fundamentally, hot-wet-stretching consists of the simultaneous application of moisture, heat, and tension, while cold-wet-stretching employs moisture and tension only.

Influence of Amount of Tension During Hot-Wet-Stretching

In order to determine the influence of amount of tension employed during hot-wet-stretching, a tire cord of 29/5/3 construction, made from Wilds 13 cotton, was passed through water and then, while under different tensions, over the

heater placed at position H_1 in Fig. 1. Thus, all the cords in this series were treated alike—i.e., they were moistened, stretched, and heated while in the stretched condition—except for the amount of tension used for the stretching. The results, presented in Table II, clearly demonstrate a

TABLE II. Influence of tension during hot-wet-stretching on strength and elongation of a 29/5/3 tire cord made from wilds 13 cotton.

Treatment	Tension lb.	Bone-dry strength lb.	Strength based on control percent	Bone-dry elongation at 10 lb. percent
Untreated	—	15.5	100.0	8.8
Hot-wet-stretched	1.5	16.8	108.4	5.6
Hot-wet-stretched	2.5	17.4	112.3	5.1
Hot-wet-stretched	4.5	17.8	114.8	4.8
Hot-wet-stretched	8.5	20.7	133.5	4.2
Hot-wet-stretched	10.5	20.8	134.2	3.9

reciprocal relationship between strength and elongation of cords subjected to the hot-wet-stretching treatment. As the tension employed during the stretching was increased, the treated

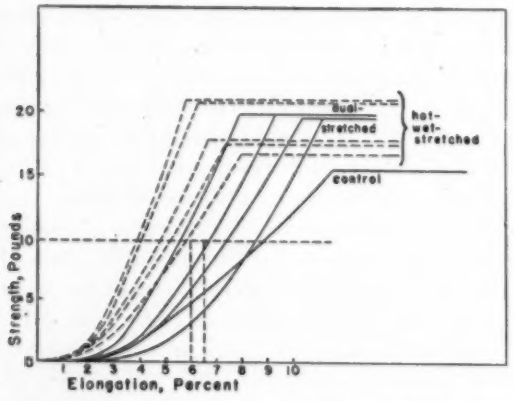

FIG. 2. Load-elongation curves of variously treated 29/5/3 tire cords made from Wilds 13 cotton. Broken lines for cords hot-wet-stretched with tension, reading from left to right, of 10.5, 8.5, 4.5, 2.5, and 1.5 pounds. Continuous lines (except control) for cords dual-stretched with 10.5 pounds tension during the first phase and, reading from left to right, with 6.5, 3.5, 0.5, and 0 pounds tension during second phase.

cord became stronger, but its subsequent elongation at 10 pounds became smaller. The load-elongation curves, obtained on the Scott tire-cord tester, and from which the data of Table II were taken, are shown as broken lines in Fig. 2. In general, the observations recorded in Table II and Fig. 2 apply to the other single-stretching treatments as well.

Influence of Time of Swelling Before Hot-Wet-Stretching

Another factor found to have an influence, mainly on the elongation at 10 pounds, is the degree of swelling of the cotton cord before being exposed to tension and heat. This is shown by an experiment with samples of a 29/5/3 tire cord, made from Acala cotton, which were all stretched and heated under the same tension (9½ pounds) by the heater in position H_1 but, before the stretching, were swollen to varying degrees by adjusting the level of water in C_1 and C_2. The time during which the cords were exposed to water varied from 2 to 60 seconds and was used as a measure of their degree of swelling. From the results of this experiment, given in Table III, the

TABLE III. Influence of time of swelling before hot-wet-stretching on strength and elongation of a 29/5/3 tire cord made from Acala cotton.

Time of swelling seconds	Bone-dry strength lb.	Bone-dry elongation at 10 lb. percent
2	17.3	4.1
14	17.6	4.2
36	17.5	4.5
60	18.2	4.7

time of swelling had an inconsequential influence on the strength of the treated cord but there was a tendency toward higher elongation with increasing degree of swelling. This effect was also observed when a wetting agent was added to the water instead of increasing the time of swelling. Thus, variation of the degree of swelling permits a very limited control of elongation independently of the strength; however, in most cases this control is insufficient to bring the elongation up into the optimum range.

Influence of Water of Various Temperatures on Hot-Wet-Stretched Cord

When a 29/5/3 tire cord (made from Wilds 13 cotton), which had been strengthened about 38 percent by hot-wet-stretching, was cut into 10-yard pieces and immersed in water of selected temperatures for 3 minutes, and then air dried, these pieces were found to have increased elongation, regardless of the temperature of the water used (see Table IV), and in some cases the elongation exceeded that of the untreated control cord. The strength, however, remained about 26 percent greater than it was before the application

TABLE IV. Influence of water of various temperatures on strength and elongation of hot-wet-stretched 29/5/3 tire cord, made from Wilds 13 cotton.

Treatment	Temperature of water degrees C	Bone-dry strength lb.	Strength based on control percent	Bone-dry elongation at 10 lb. percent
Untreated control	—	15.5	100.0	8.8
Hot-wet-stretched	—	21.4	138.1	4.0
As above, then water 3 min.	15	19.8	127.7	8.0
As above, then water 3 min.	25	19.6	126.5	8.4
As above, then water 30 min.	25	19.0	122.5	9.8
As above, then water 3 min.	35	19.3	124.5	9.8
As above, then water 3 min.	50	19.4	125.2	10.4
As above, then water 3 min.	75	19.2	123.9	10.4
As above, then water 3 min.	100	19.5	125.8	8.7

TABLE V. Influence of tension during second phase of dual stretching on strength and elongation of a 29/5/3 tire cord made from Wilds 13 cotton.

Treatment	Tension during 1st stretching lb.	Tension during 2nd stretching lb.	Bone-dry strength lb.	Strength based on control percent	Bone-dry elongation at 10 lb. percent
Untreated Control	—	—	15.5	100.0	8.8
Hot-wet-stretched	10.5	—	20.8	134.2	3.9
Dual stretched	10.5	6.5	19.8	127.7	5.7
Dual stretched	10.5	3.5	19.8	127.7	6.8
Dual stretched	10.5	0.5	19.4	125.2	7.5
Dual stretched	10.5	0	19.6	126.5	8.4

of the stretching treatment, which means that in this particular case almost 70 percent of the improvement was retained even after 3 minutes' exposure to boiling water. The cord was almost as strong after 30 minutes' exposure to water of room temperature. Stretching the cord in the presence of water and heat and subsequently exposing it to water thus produced a cord which had about the same elongation at 10 pounds but considerably more strength, when compared to the untreated cord.

Control of Elongation by Dual Stretching

The observation on the effect of water on hot-wet-stretched cord suggested a method which for the first time permits improvement in the strength of tire cord without reducing its elongation at 10 pounds below the optimum value. Obviously, it was only necessary to decrease the elongation of an already strengthened and relaxed cord. For this purpose, a second wet-stretching treatment was considered to be logical. Therefore, a 29/5/3 tire cord (made from Wilds 13 cotton) was first hot-wet-stretched in the stretching apparatus with the heater position at H_1 (see Fig. 1). The cord was then allowed to travel a second time through the two water-filled containers, C_1 and C_2, after which it was stretched between S and D in the absence of heat and dried over a hot plate at position H_2. This treatment will be referred to as the "dual stretching" process. Four samples were prepared, each under a different tension during the second stretching, as shown in Table V. (In the treatment at zero tension the hot-wet-stretched cord was immersed in water for 3 minutes and then allowed to air-dry.)

It will be seen from Table V that when a single hot-wet-stretching treatment was employed, using a tension of 10.5 pounds and the heater at H_1, an increase of some 34 percent in strength over the control was obtained but the elongation at 10 pounds was reduced to 3.9 percent. When this treatment was followed by a second hot-wet-stretching, the elongation remained unchanged. When parts of the once hot-wet-stretched cord were stretched a second time with the heater at H_2 and with tensions ranging from 6.5 to 0.5 pounds, elongations at 10 pounds of 5.7 to 7.5 percent were obtained. With tensions greater than 6.5 pounds elongations down to 3.9 percent could be produced in this cord and with smaller tensions than 0.5 pound up to 8.4 percent. At the same time Table V shows that the strength retained in the dual-stretched cord is independent of the tension applied during the second stretching treatment and about 27 percent higher than that of the control. These conditions are also demonstrated by Fig. 2 in which the load-elongation curves of these dual-stretched cords, as obtained on the Scott tire-cord tester, are shown as continuous. This means that the second stretching treatment maintained almost 80 percent of the increase in strength achieved by the first stretching treatment, while it permitted adjustment of elongation at 10 pounds to any value between that of the control and that of the hot-wet-stretched cord. In many cases it has been possible to maintain an even higher percentage of the maximum potential strength of the cord, as will be seen later (Table VII).

Influence of Swelling Time Before Second Phase of Dual Stretching

A 23/4/3 tire cord, made from Stoneville 2*B* cotton, was first hot-wet-stretched at a tension of 8.5 pounds, with the heater at H_1. This pre-stretched cord was then cut into several lengths, each of which was cold-wet-stretched at a tension of 10.5 pounds, with the heater at H_2 for drying after release of tension. The only variable during

the second stretching was the time of swelling, which was again controlled by the proper adjustment of the water level in containers C_1 and C_2, the speed of the machine being constant. The results of strength and elongation measurements given in Table VI, when compared with those in Table III, show that the influence of the time of swelling before the second stretching is considerably more pronounced than before the first stretching. The strength, however, does not appear to be affected by the time of swelling.

TABLE VI. Influence of time of swelling before second part of dual stretching on strength and elongation of a 23/4/3 tire cord made from Stoneville 2*B* cotton.

Time of swelling seconds	Bone-dry strength lb.	Bone-dry elongation at 10 lb. percent
2	17.7	4.7
12	16.9	5.3
60	17.1	6.3

Application of Dual-Stretching Treatment

With proper selection and control of tension and degree of swelling during the second stretching, the dual-stretching treatment was applied to a number of cotton cords of different construction, gauge, and cotton variety. The procedure employed for the preparation of these cords consisted in passing them through water containing a wetting agent (Aerosol *OT*), applying the highest tension that could be used without breaking them, and heating them while under this tension. The maximum tension that could be applied safely was, roughly, about 68 percent of the average bone-dry strength of the untreated cord. Small portions of each hot-wet-stretched cord were then restretched under various conditions of swelling and tension in order to determine the proper conditions for optimum elongation. Guided by these preliminary trials, the remaining portion of each cord was stretched, and the properties of the dual-stretched cord were measured. The results are presented in Table VII, the unstretched controls being identified by *c*, the hot-wet-stretched cords by *h*, and the dual-stretched by *d*. Some of the cords listed in Table VII represent lots of 1000 yards; most of them represent only 200 yards.

According to Table VII the strength increase for the hot-wet-stretching treatment ranged from about 39 to 63 percent, while the other single-stretching treatments did not improve the strength by more than 28 percent (Table I). The improvement in strength was accompanied by a reduction in gauge and an increase in yarn number or count. If the strength is expressed as count-strength product or in grams per denier, either of which takes account of the simultaneous change in yarn number and strength, the hot-wet-stretching treatment gave increases ranging from 48 to 83 percent for the thirteen cords listed in Table VII. The strengths of the dual-stretched cords were from 25 to 48 percent higher than those of the untreated samples (Table VII); or, expressed as count-strength product or in grams per denier, the increase varied from 34 to 68 percent for different cords. On the average, 93 percent of the count-strength product obtained

TABLE VII. Properties of unstretched, hot-wet-stretched and dual-stretched tire cords made from different cottons.

Cotton variety	Construction	Treatment*	Gauge in.	Yarn No.	Bone-dry strength lb.	Strength based on control percent	Bone-dry elongation at 10 lb. percent
Stoneville 2*B*	29/5/3	*c*	0.029	1.56	12.0	100.0	9.9
Stoneville 2*B*	29/5/3	*h*	0.025	1.78	17.0	141.7	4.1
Stoneville 2*B*	29/5/3	*d*	0.026	1.72	15.8	131.7	6.0
Acala	29/5/3	*c*	0.028	1.64	12.4	100.0	10.2
Acala	29/5/3	*h*	0.025	1.81	16.6	133.9	5.6
Acala	29/5/3	*d*	0.025	1.79	16.4	132.2	6.0
Delfos	29/5/3	*c*	0.028	1.60	12.3	100.0	10.2
Delfos	29/5/3	*h*	0.025	1.77	17.4	141.5	5.1
Delfos	29/5/3	*d*	0.025	1.71	16.7	135.8	6.4
Wilds 13	29/5/3	*c*	0.028	1.54	15.5	100.0	10.0
Wilds 13	29/5/3	*h*	0.026	1.75	21.6	139.4	4.4
Wilds 13	29/5/3	*d*	0.026	1.65	19.4	125.2	6.6
S×*P*	29/5/3	*c*	0.029	1.59	15.0	100.0	10.3
S×*P*	29/5/3	*h*	0.025	1.81	20.5	136.7	5.7
S×*P*	29/5/3	*d*	0.025	1.80	19.6	130.7	6.7
Stoneville 2*B*	23/4/3	*c*	0.030	1.52	12.6	100.0	9.2
Stoneville 2*B*	23/4/3	*h*	0.026	1.69	17.5	138.9	5.2
Stoneville 2*B*	23/4/3	*d*	0.027	1.67	17.1	135.7	6.2
Acala	23/4/3	*c*	0.029	1.52	12.0	100.0	10.6
Acala	23/4/3	*h*	0.026	1.67	16.8	140.0	5.2
Acala	23/4/3	*d*	0.026	1.69	16.0	133.3	6.3
Delfos	23/4/3	*c*	0.029	1.49	13.4	100.0	10.2
Delfos	23/4/3	*h*	0.026	1.68	19.4	144.8	5.0
Delfos	23/4/3	*d*	0.026	1.66	17.7	132.1	6.0
Wilds 13	23/4/3	*c*	0.029	1.50	14.4	100.0	9.9
Wilds 13	23/4/3	*h*	0.026	1.69	20.8	144.4	4.8
Wilds 13	23/4/3	*d*	0.026	1.68	20.2	140.3	5.9
S×*P*	23/4/3	*c*	0.029	1.53	14.8	100.0	9.9
S×*P*	23/4/3	*h*	0.026	1.71	21.7	146.6	4.7
S×*P*	23/4/3	*d*	0.025	1.68	21.4	144.6	6.2
Wilds 13	17/4/3	*c*	0.033	1.12	19.2	100.0	10.2
Wilds 13	17/4/3	*h*	0.029	1.27	29.2	152.1	4.4
Wilds 13	17/4/3	*d*	0.030	1.27	27.1	141.1	6.4
Stoneville 2*B*	21/5/3	*c*	0.034	1.15	15.8	100.0	9.2
Stoneville 2*B*	21/5/3	*h*	0.029	1.29	25.8	163.3	4.3
Stoneville 2*B*	21/5/3	*d*	0.030	1.31	23.3	147.5	6.2
Acala	20/5/3	*c*	0.035	1.05	17.3	100.0	11.6
Acala	20/5/3	*h*	0.030	1.27	26.0	150.3	4.3
Acala	20/5/3	*d*	0.031	1.21	23.6	136.4	6.7

* *c* = untreated control; *h* = hot-wet-stretched; *d* = dual-stretched.

by the hot-wet-stretching treatment was retained after the second stretching.

DISCUSSION OF RESULTS

The hot-wet-stretching treatment, involving the combined application of tension and heat to the swollen cord, gave considerably greater strength than other single-stretching treatments employing various combinations of tension, moisture, and steam. However, the main difficulty involved in this as well as in the other single-stretching treatments is the reciprocal relationship between strength and elongation, as illustrated by Table II. In the case of the 29/5/3 cord reported in this table, a tension of 10.5 pounds produced a cord having a strength 34 percent greater than that of the control but an elongation of only 3.9 percent at 10 pounds which is definitely too low for tire cord. The elongation could be maintained at 5.6 percent or above by using a tension of 1.5 pounds or less, but such a low tension yielded a cord only 8.4 percent stronger than the control. This reciprocal relationship prevents the full utilization of the potential strength of the cord and thus limits the practical usefulness of this and similar single stretching treatments.

The cold-wet-stretching treatment recorded in Table I, rows 3 and 4, had the advantage of not reducing the elongation as much as did the other single-stretching treatments, but it too did not permit independent control of the elongation. With any of these treatments a compromise between optimum elongation and maximum strength would have to be accepted.

In this respect, the advantage of the dual-stretching treatment over the single-stretching treatment is at once evident. This is demonstrated by Fig. 2 which shows the influence of tension on strength and elongation of both hot-wet-stretched and dual-stretched cords, and also by comparison of Tables II and V. When the tension used in the preparation of hot-wet-stretched 29/5/3 cord from Wilds 13 cotton was decreased (Table II), the elongation became greater but at the same time the strength declined until, at a tension of 1.5 pounds, the strength was only 8.4 percent greater than that of the control and the elongation was 5.6 percent, which was still short of the optimum. When, however, the tension during the second phase of the dual-stretching treatment was lowered (Table V) the elongation at 10 pounds was increased, up to that of the control, while the strength remained independent of the elongation. The proper tension for yielding optimum elongation can easily be determined, and the strength of the dual-stretched cord will be about 27 percent greater than that of the control, regardless of the choice of elongation. By single stretching a strength increase of about 27 percent could be obtained for this cord only if an elongation at 10 lb. of between 4.2 and 4.6 percent were accepted.

The dual-stretching treatment thus permits the production of a tire cord having greatly improved strength, and a predetermined, independently controlled elongation at 10 pounds between that obtainable by the hot-wet-stretching treatment and that of the untreated cord, or even a little higher than the latter. In the case of the thirteen cords for which data are given in Table VII, the average count-strength product of the dual-stretched cords was only about 7 percent lower than the maximum obtainable by hot-wet-stretching, and the elongation at 10 pounds of each of the dual-stretched cords was either within or very close to the optimum range of 6 to 6.5 percent.

Different cords showed different response to the single as well as to the double-stretching treatment. It can be expected that the twist and the construction of the cord will be important factors in determining how much improvement in strength is obtainable by any stretching treatment. Most important of all, however, appeared to be the uniformity of the cord. Cords of high uniformity could be subjected to relatively higher tensions during stretching and consequently their relative increase of strength, after stretching under maximum tension, was greater. Cords with weak spots or "riders" (cork-screw) showed the least benefit from the treatment; the 29/5/3 Acala cord in Table VII is an example of such a non-uniform cord.

The dual-stretching treatment does not seem to offer any difficulties that would impede commercial application, although the experiments thus far have been restricted to small, laboratory-scale production. The treatment consists of two phases which, however, can easily be combined into one continuous process by proper design of the stretching machine. During the first phase the cord is given possibly the greatest strength that can be attained, without regard to elongation. This is accomplished by wetting the cord, stretching it under a tension just short of the breaking point, and heating it while under tension. During the second phase, the cord is wetted again and stretched at a predetermined tension

in the absence of heat, but is dried without tension just before it is wound on a spool. This phase gives the cord the desired elongation at 10 pounds while retaining approximately 93 percent of the maximum count-strength product obtained during the first phase. The proper tension for the second stretching is determined by a few preliminary trials on short pieces of cord. If the desired elongation should lie outside of the range of elongations obtainable by variation of tension, a further adjustment is possible by varying the degree of swelling. This can be done by adding a wetting agent to the water through which the cord travels or by changing the time during which the cord is exposed to the swelling action of water in the second phase. Thus, in the dual-stretching treatment a method has been found to control effectively the elongation of highly stretched and strengthened tire cord.

SUMMARY

1. Cotton tire cords, differing with regard to gauge, construction, and variety of cotton, were subjected to stretching treatments involving various combinations of tension, heat, and moisture. It was found that all these treatments increased the strength of the cords but reduced their gauge and elongation at 10 pounds. The greatest increase in strength was obtained when tire cord was stretched in a swollen condition and in the presence of heat. Increases in count-strength product from 48 to 83 percent were observed.

2. Experiments showed a reciprocal relationship between the strength and the elongation at 10 pounds obtainable by single-stretching treatments of tire cord, which makes impossible the control of elongation, independently of strength. Bone-dry elongations of about 6 percent at 10 pounds could be obtained only with negligible increase in strength.

3. The original elongation was restored by treating highly stretched tire cord with water at room temperature for 30 minutes or with boiling water for 3 minutes, while most of the increase in strength resulting from stretching was retained. A hot-wet-stretched tire cord after treating with water had equal elongation but greater strength as compared with the untreated cord.

4. A dual-stretching method was devised which permits the control of elongation at 10 pounds independently of strength. The treatment consists of two phases: the first imparts to the cord the maximum potential breaking strength and the second serves to adjust the elongation at 10 pounds to a predetermined controlled value while maintaining over 90 percent of the maximum count-strength product. Control of the elongation is achieved by proper selection of tension and degree of swelling during the second phase of the dual-stretching treatment.

ACKNOWLEDGMENT

The writers wish to express their indebtedness to W. James Lyons, who designed and built the stretching apparatus with the assistance of Leon Segal, and to Rita C. Council, Mary L. Nelson, and Leon Segal, who performed much of the experimental work.

REFERENCES

(1) F. L. Sessions, U. S. Patent 1,747,533 (1930).
(2) C. R. Brownell, U. S. Patent 2,075,777 (1937).
(3) E. C. Gwaltney, L. A. Graybill, and R. B. Newton, U. S. Patent 2,103,218 (1937).
(4) A. Burgeni, U. S Patent 2,173,997 (1939).
(5) R. F. Nickerson, Australian Patent 114,376 (1941).
(6) American Society for Testing Materials, Committee D-13 on Textile Materials, A.S.T.M. Standards on Textile Materials, 1942.

Ultraviolet Spectra of Biologically Important Molecules*

BY GLADYS A. ANSLOW

Department of Physics, Smith College, Northampton, Massachusetts

(Received July 17, 1944)

INTRODUCTION

THE extensive utilization of spectrophotometric studies in the ultraviolet region during the last two decades by organic and biochemists has proven an extremely valuable tool in the solution of structure problems leading to the identification of newly discovered or synthesized molecules, as well as for the quantitative measurement of compounds containing constituents with well-known absorption spectra. They have also been used to identify spectral regions to be employed in the study of chemical and biological effects of radiation, and for such studies as the effects of digestion of these molecules by animals and plants. The methods employed and the nature of the spectra obtained from various types of molecules have been the subjects of numerous articles and even of books,** so no attempt should be made, nor would time permit, to review the entire scope of the work accomplished. Yet many physicists have only a meager knowledge of this fertile field of research. Hence the justification of the present discussion, which will be confined to a review of the comprehensive studies which have dealt with two well-known groups of biologically important molecules, the vitamins and the proteins, and to a summary of our present knowledge of the nature of the irradiation effects produced in simple organic molecules and in these large molecules. These are selected because the vitamins include molecules with a wide variety of structures embodying many of the features typical of simple organic molecules and because two conflicting theories for the structure of proteins have been proposed, and the facts revealed by ultraviolet absorption spectra should be used in the solution of this problem. In the course of the discussion evidence will be given for a fresh interpretation of the short wave-length absorption occurring in certain simple molecules, which is confirmed by the structure of the vitamins and should be utilized in the discussion of the protein structure problem. The analyses described with respect to these two types of molecules have frequently been utilized in similar discussions dealing with other molecules of biological and industrial importance, such as the hormones, enzymes, and many drugs.

THE ABSORPTION MEASUREMENTS

But first of all a few remarks must be made concerning the usual graphical representation of the absorption measured at the wave-lengths concerned, though time will not be taken to describe the instruments employed. All permit measurements of the molecular extinction coefficient of a solution of the substance being studied with respect to its solvent, this coefficient being defined by the equation

$$\epsilon cd = \log I_0/I,$$

where ϵ is the mass absorption coefficient, c the concentration, d the length of the light path through the solution, and I_0 and I are incident and transmitted intensities of the beam passing through the solution. As Beer's law states, if the solvent does not act upon the molecule in the solution, this equation should hold rigorously with changes in concentration. Deviations must indicate such interactions as salt formation in alkaline solutions, interchange of molecular groups, or the breaking down of polymers. The instruments employed permit the measurement of $\log_{10} I_0/I$ at various wave-lengths and the

* Presented on June 24, 1944 before the Inaugural Meeting of the Division of High-Polymer Physics of the American Physical Society at Rochester, New York.

** Excellent discussions of the construction and operation of spectrophotometric instruments and of the spectral characteristics of different chromophoric groups, of typical simple organic molecules in various solvents, and of many biologically important molecules will be found in the following books and articles: F. Twyman and C. B. Alsopp, *The Practice of Absorption Spectrophotometry* (Adam Hilger, Ltd., London, 1934); W. R. Brode, *Chemical Spectroscopy* (John Wiley & Sons, Inc., New York, 1929); *Recent Applications of Absorption Spectrophotometry* (Adam Hilger, Ltd., London, 1939); V. Henri, *Table Annuelles de Constantes et Données Numeriques* (McGraw-Hill Book Company, Inc., New York, 1910–1936); E. P. Carr, M. L. Sherrill, and V. Henri, *International Critical Tables* (McGraw-Hill Book Company, Inc., New York, 1929), Vol. 5; E. S. Miller, *Quantitative Biological Spectroscopy* (Burgess Publishing Company, Minneapolis, 1939); R. A. Morton, *The Application of Absorption Spectra to the Study of Vitamins and Hormones* (Adam Hilger, Ltd., London, 1942), second edition; J. R. Loofbourow, Rev. Mod. Phys. **12**, 267 (1940); H. Sponer and E. Teller, Rev. Mod. Phys. **13**, 76 (1941).

resulting value of ϵ, or sometimes of ϵc, is plotted either against the wave-length as is common with chemists, who are concerned with identifying the nature of the absorption band, or against the wave number or the frequency in Fresnel numbers, as is common with physicists who are primarily concerned with the photon energies absorbed and the resulting molecular energy transitions.

SPECTRAL CHARACTERISTICS OF TYPICAL ORGANIC MOLECULES

Origin and Character of Bands

To accomplish the discussion of the spectra obtained with biologically important molecules it is first necessary to review the nature of the spectra produced by simple organic molecules of various types, energy having been absorbed in their respective chromophoric groups. It is well known that in ultraviolet spectra many discontinuous bands consisting of series of narrow bands appear, resulting from electronic excitations accompanied by vibrational energy transitions. If dissociation occurs as a secondary effect of this energy absorption these bands are usually quite diffuse. In the vapor state, but not in the liquid state, these may be observed as composed of large numbers of fine bands, caused by simultaneous changes in vibration and rotation energy. If the absorption band is entirely structureless, i.e., truly continuous, molecular dissociation must have been a primary process. The latter type of bands are not very strong in the near ultraviolet, but do occur in the vacuum ultraviolet, as do Rydberg series lines corresponding to electronic excitations of the undissociated molecule. In this region, beyond the scope of the quartz spectrophotometer, lie the spectra of saturated molecules, such as methane, ethane, and the other alkanes, for which the methyl group is chromophoric. But the spectra of unsaturated molecules, those with one or more double bonds, produced by excitation of the non-bonding electron, lie for the most part in the 2000–3000A region, the province of the quartz instrument. The chromophoric groups in these molecules are mainly,

$$\diagdown\!\diagup C{=}C \diagup\!\diagdown \quad , \quad C{=}O, \quad C{=}N-, \text{ and } -N{=}N-$$

both in chain and in cyclic formations.

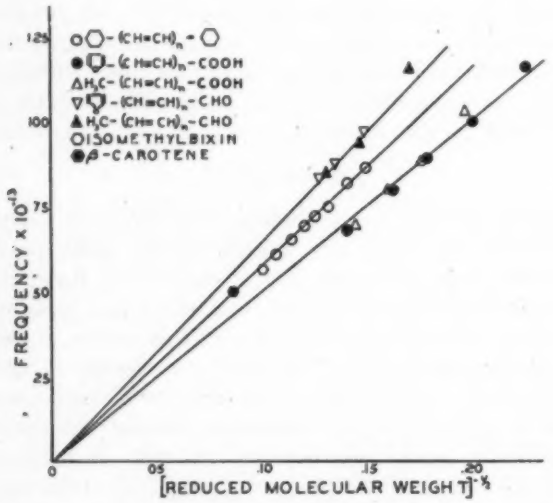

FIG. 1. Dependence of frequency of absorption center on reduced mass of molecule vibrating about central ethylene group.

Effects of Substitutions and Conjugations

In the following discussion the outstanding spectral characteristics typical of the chromophoric groups as they occur in various molecular configurations will be briefly stated, without referring to the specific researches except in those cases where a new emphasis is being given the results. All molecules containing the ethylene linkage, $\diagdown\!\diagup C{=}C \diagup\!\diagdown$, exhibit a band with four principal components, which occur in the spectrum of ethylene near 1770A and in butadiene near 2200A. Substitutions of methyl, hydroxyl, or other single-bonded groups produce slight shifts toward the long wave-length regions, accompanied by some increase in the absorption coefficient ϵ. Greater shifts and increases in ϵ are produced by an increase in the degree of unsaturation, provided the chromophoric groups are conjugated. Typical of this effect are the spectra of ethylene, butadiene, and their derivatives, studied by Carr, Price,[1] and others, as shown in Table I. In the spectra of the substituted mole-

TABLE I. Relative effects of substitutions and conjugations on ethylene linkage.

Molecule	Maximum λ of band	max ε	Molecule	Maximum of band	max ε
ethylene	1740A	10,000	butadiene	2162A	21,000
propylene	1885		isoprene	2231	24,000
butene-*cis*	2072		dimethyl butadiene	2283	20,000
trimethyl ethylene	2181	10,000			
tetramethyl ethylene	2318				

cules two new regions of general absorption appear, in trimethyl ethylene at 3000 and 2420A, in tetramethyl ethylene at 3300 and 2500A, respectively. These must have their origin in the CH_3 chromophores and in the C—C bonds effecting the substitutions. A break in the conjugation through the introduction of two or more single bonds between the double bonds causes independent absorption by the unsaturated components.

A comprehensive study of the effect of the length of the conjugated chain in the polyenes has been conducted by Hausser, Smakula, Kuhn[2] and their associates, who found the intensity of the absorption to be a linear function of the number of ethylenic groups in the molecule, ϵ varying from 10^4 to 10^5, and observed a regular shift in the wave-length with increase in the number of ethylenic linkages in the molecule. It has been found by this author[3] and one of her associates that the frequencies and hence the absorbed energies are such functions of the molecular masses as to indicate that the main energy absorption is of a vibrational nature and accumulates in the central ethylenic group. This is shown in Fig. 1 for diphenyl, and for methyl and furyl, acid and aldehyde polyenes.

Introduction of a carbonyl group, $\diagdown C{=}O$, in $\diagup$ a conjugated position produces a small displacement of the ethylene absorption. It is itself responsible for a very weak absorption band, $\epsilon \sim 20$, in the 2900 region. This band occurs in the spectra of all aldehydes and ketones.

Introduction of a hydroxyl group has only a slight effect on the ethylene absorption: —OH itself is usually considered to be transparent, though all molecules containing the group, such as the phenols, alcohols, starches, and the carboxylic acids show a continuous band in the 2400–2300A region, as is apparent in Fig. 2, which summarizes the nature of the absorption obtained with fatty acids, alcohols, and starches. The curves plotted have been obtained in the Smith College laboratory, with the exception of the dotted portions for the fatty acids, and agree with those published for similar molecules by their respective observers, Ramart-Lucas,[4] Marchlewski and others,[5] and Henri.[6] The band shifts to lower energy regions in alkaline solutions, resulting from salt formation, and probably has its origin, not in —OH itself, but in the adjacent C—O bond, or possibly in the larger $\diagdown \; | \; | \; \diagup$ —C—C—OH group. The dotted portion of the fatty acid curves, indicating very weak diffuse absorption, was obtained for pure liquids by Hartleb[7] and appears in the spectra of the starches and the heavier alcohols, in which there are at least two CH_2 groups, and consequently two single C—C bonds. Apparently, long saturated chains are not transparent to 2400A but absorb slightly, possibly because of dissociation, in the 2700–2800A region, the intensity increasing with the length of the chain. This is apparent for some of the heavier alcohols in Brode's[8] study on the transparency of solvents, and in the spectra of the starches in alkaline solutions.[5] In addition, starches under these conditions exhibit a band near 3150A, the location of a weak band in the heavy alcohols and of the band owing to the CH_3 group in the substituted ethylenes.

Cyclized Molecules

Cyclization of the molecules shifts the spectrum slightly to the lower wave-length region and reduces the intensity. Aromatization, as in benzene, further increases the intensity, but brings out the fine structure of the band. Substitutions in the ring as those of phenol, pyridine, and indole cause a shift toward the visible with some loss of definition. Related aromatic compounds, such as the aromatic amino acids, exhibit slightly increased shifts. Those resulting from —OH substitutions

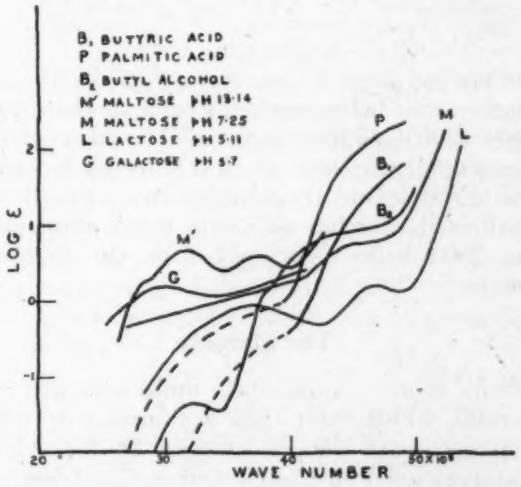

FIG. 2. The 240 mμ ($\sim 42 \times 10^3$ cm^{-1}) band associated with the $\diagdown \; | \; | \; \diagup$ —C—C—OH group in alcohols, starches, and fatty acids.

TABLE II. Principal photolysis products of organic vapors.

Molecule	Formula	Wave-length range	Principal products after recombinations	Bonds ruptured
methane[a]	CH_4	1550–1350A	H_2, C_2H_4, C_2H_2	two (C—H)'s
ethane[a]	C_2H_6	same	H_2, C_2H_2	same
higher alkanes[b]	C_nH_{2n-2}	1800	H_2, unsaturated hydrocarbons	same
ethylene[c,d]	$CH_2{=}CH_2$	1860	H_2, C_2H_2	same
acetylene[e]	$CH{\equiv}CH$	2350	C_6H_6, cuprene	C≡C
benzene[f,g]	C_6H_6	2537 2200	H_2, CH_4 unidentified products	all bonds
formaldehyde[h]	HCHO	3650 1600	H, CO, H_2 same increased	C—H two (C—H)'s
acetaldehyde[i]	CH_3CHO	2750	CH_4, H, C_2H_6	C—C, C—H
acrolein[j]	$CH_2{=}CHCHO$	3630–2537	CO, alkanes, H	same
crotonaldehyde	$CH_3CH{=}CHCHO$	3100–2300	CH_4 and above	same
glyoxal[k]	CHOCHO	3660	CO, H_2	same
other aldehydes[l]	RCHO	3630–2537	RH, CHO, H, CO, alkanes	same
acetone[m,n,o]	CH_3COCH_3	3200–2500 1900 1700	$CH_2COCOCH_3$, C_2H_6 C_2H_4, CO H_2	same two (C—C)'s two (C—H)'s
higher ketones[p]	$RCOCH_3$	3100	CO, acetone, alkanes	same and C—H
alcohols normal[q]	RCH_2OH	2000	RCHO, H, CO, OH	C—H, C—C, O—H, C—O
isopropyl	$(CH_3)_2CH_2OH$	same	$(CH_3)_2CO$	O—H, C—H

[a] See reference 9a. [b] See reference 9b. [c] See reference 9c. [d] See reference 9d. [e] See reference 9e. [f] See reference 9f. [g] See reference 9g. [h] See reference 9h. [i] See reference 9i. [j] See reference 9j. [k] See reference 9k. [l] See reference 9l. [m] See reference 9m. [n] See reference 9n. [o] See reference 9o. [p] See reference 9p. [q] See reference 9q.

are shifted most in alkaline solutions, the frequency shift being much the same as that of the 2400–2200 band just discussed. The other groups, containing nitrogen, are less affected by alkalinity, indole and tryptophane being practically unaffected. Nor has alkalinity much effect upon the 2900 band associated with the carbonyl group.

The Steroids

Still more complicated molecules are the steroids, which make their appearance in industrial chemistry and in vitamin D, formed by juxtaposition of three six-membered and one five-membered ring attached to a long saturated or unsaturated chain. Those which are saturated hydrocarbons or hydroxy-bodies, or unsaturated alcohols with only one double bond, show negligible absorption above 2000A. But selective absorption occurs when at least two conjugated double bonds occur. If they are in the first ring, called the *A* ring, the absorption is similar to that of cyclohexadiene, with two maxima near 2700 of similar intensity. If the two bonds are in the second or *B* ring, the bands are shifted slightly to longer wave-lengths, but if the two double bonds are not in the same ring, the position of the maximum is at shorter wave-lengths, approximately 2400A. If the conjugation is broken, selective absorption in this region disappears.

PHOTOCHEMICAL DECOMPOSITIONS PRODUCED IN SIMPLE ORGANIC MOLECULES

Dissociation Products

During the last decade some chemists have conducted systematic investigations of the photolytic

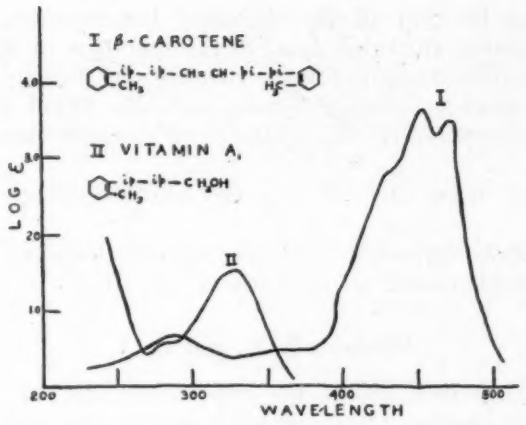

FIG. 3. Absorption bands of β-carotene (reference 11) and vitamin A (reference 12). The longest wave-length absorption in both occurs in isoprene chains, and the 270-mμ absorption in the rings.

effects produced by monochromatic radiations on simple organic molecules, and have identified some of the products which have resulted either from the primary or secondary reactions. These lead to the conclusion that in many of these reactions dissociation must have resulted after irradiation by light with wave-lengths those of absorption bands. Although the investigations are in some instances fairly complete, yet in many inadequate attention has been paid to narrowing down the wave-length region in which particular reactions occur. Yet the results for the simpler molecules listed in Table II[9] are very impressive. They indicate the frequent rupture of C—C and C—H single bonds, one or two at a time.

The Dissociation Process

At present it is assumed that the molecule first becomes electronically excited and that the energy absorbed is utilized in consequent dissociation processes. But it is also reasonable to assume that the photon energy is absorbed simultaneously in several adjacent bonds, exciting some into discrete vibration levels and dissociating others. A liquid drop theory of molecular energy configurations could probably be developed to describe the phenomena. Neilsen's[10] theory of vibration-rotation bands in polyatomic molecules can be extended to predict the dissociation energies. It should be possible to test this assumption with a mass spectroscopic examination of products produced when irradiated with monochromatic light while the organic gas is suffering electron bombardment. The electron energy necessary to ionize should indicate the state of the molecule and its fragments, if they are produced by the irradiation. The magnetic field would measure their masses. This investigation is being undertaken in the Smith College physics laboratory.

THE SPECTRA OF THE VITAMINS

These facts are adequate to explain the spectra of the vitamins. For some of these the structure was known before the spectrum analysis. For others the nature of the spectrum suggested a probable structure, and synthesis of various molecules with this structure but different substitutions eventually produced one with an identical spectrum and identical biological effect.

Vitamin A

The relation between vitamin A, the vitamin which restores visual purple in the retina, and carotene is a matter of common knowledge. About twenty carotenoids occur in nature, all with similar spectra, three or more strong bands in the visible with similar relative intensities, a less strong band near 2700 or 2800A, and generally weak absorption near 3300A. All have similar structure, a long chain with two pairs of isoprene units, facing each other, and a six-membered ring at either end with two methyl groups in the 1 position on the ring. Their specificities are determined by the position of the double bond in the ring and by hydroxyl or carbonyl substitutions. Four of these are unsubstituted and have the formula $C_{40}H_{56}$, α-, β-, and γ-carotenes and lycopene. Vitamin A is derived from the β-form, in which the double bond is in the 5, 6 position in both rings. α- and γ-carotenes have asymmetrical rings. Lycopene's are symmetrical but are open. In vitro the carotene is split into two equal parts between the 15–15′ atoms of the isoprene chain and becomes two vitamin A molecules by the addition of water to each portion. For example, the liver of an animal which has been fed β-carotene, when ashed, gives an absorption spectrum for which the non-protein component is that of vitamin A.

Figure 3[11,12] shows the spectra of β-carotene and vitamin A. The visible bands of the carotene are undoubtedly caused by ethylene absorption in the isoprene units, for the diphenyl-polyene line in Fig. 1 predicts that long conjugated chain molecules with their molecular weight should have bands of their character and frequency. Similarly molecules with the mass of vitamin A

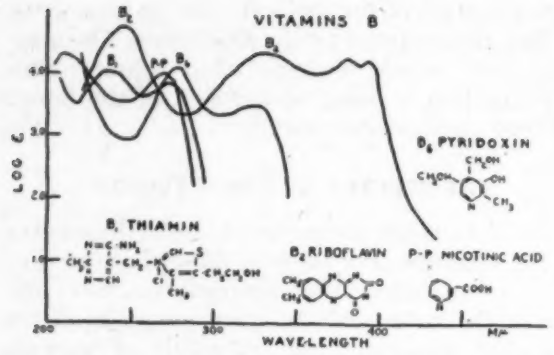

FIG. 4. Spectra of vitamins B_1 (reference 13), B_2 (reference 14), B_6 (reference 15), and the $P-P$ complex (reference 16). Energy absorption in the substituted pyridine and pyrimidine rings results in 270–280-mμ bands of $P-P$, B_1 and B_6, and in 330-mμ band in B_2; in the thiozole ring of B_1 in a band at 245 mμ; in the carbonyl substituted ring of B_6 in the 380-mμ absorption. The short wave-length absorption for B_1, B_6, and $P-P$ occurs in the —C—C—OH group.

should show absorption with a maximum near 3250A. The 2700 band must arise from the double bond chromophore in the ring, which is conjugated to an isoprene unit. Undoubtedly the slight general absorption in the carotene spectrum near the vitamin band arises from photochemical formation of the vitamin. Vitamin A, itself, is decomposed by 3250A photons. As Matlack[13] has found, carotenes are partially oxidized after standing in the dark, and a few seconds of irradiation produce as much decomposition as forty-eight hours of dark oxidation.

The Vitamin B Complex

The B vitamins are diverse in their biological effects and show a corresponding diversity in their structure except that pyridine or pyrimidine rings with various substitutions are, apparently, characteristic of all these vitamins B. At least those whose spectra and structure have been thoroughly analyzed may be so classified. Their spectra are shown in Fig. 4.[14–17] All have a band near 2800A, appearing furthest in the ultraviolet for the $P-P$ complex, since its ring has only the carboxylic substitution, shifted very little in B_1, but more in B_6 with its hydroxyl and alcoholic substitutions. The maximum shift occurs, however, in the spectrum of B_2, which has two nitrogen containing rings responsible for the two bands in the 3000–4000A region, the nearest to the visible being produced by the ring with carbonyl substitutions. The third B_2 band near 2450A must be that of the dimethyl benzene ring. Similarly, the other band in the spectrum of B_1 has to be attributed to the thiozole ring. Finally, the short wave-length absorptions near 2300A in the spectra of B_1, B_2 and the $P-P$ complex must result from the —C—C—OH chromophore in alcohols, carboxylic acid, and hydroxyl substitutions identified earlier in this paper.

Vitamins E, K, and D

Vitamins E and K, the antisterility and anti-blood clotting vitamins, have similar structure, both with saturated long chains which can absorb only weakly in the 2700 region and cannot be responsible for the strong absorption shown in Fig. 5.[18–20] The aromatic ring in vitamin E with its hydroxyl and three methyl substitutions must produce the strong 2900 band; the narrow band at 2260 may be that arising in the hydroxyl substitution. In vitamin K the short wave-length band with structure in the 2300–2750 region must be partly owing to the benzene ring. Possibly the short wave-length portion results from the ethylene group in the chain. The 3250 band has the location of the CH_3 absorption recognized earlier in this paper.

Vitamin D, the antiricketic vitamin, is a steroid known as calciferol, which is produced by the irradiation of ergosterol, and itself becomes toxisterol upon irradiation. Since its absorption band has a maximum at 2650A, conjugated double bonds must occur in the open *B* ring of the sterol.

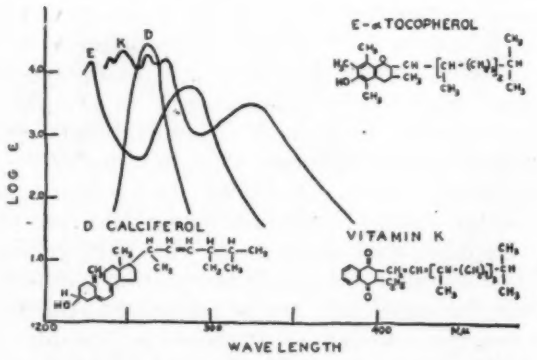

FIG. 5. Spectra of vitamins E, K (references 17, 18), and D_2 (reference 19). Absorption in the aromatic rings gives rise to the 290-mμ band in vitamin E and to the 230–275-mμ band in vitamin K. The 325-mμ band in the latter is probably —CH_3 absorption. Absorption at 265 mμ by the steroid vitamin D_2 indicates an open *B* ring.

Vitamins C and P

There remains the discussion of vitamins obtained from citric fruits, vitamins C and P, ascorbic acid and citrin, the antiscurvy and antihemmorrhage vitamins. The spectra of both, Fig. 6,[21,22] show the short wave-length absorption typical of the —C—C—OH group, while ascorbic acid has a band near 2700A typical of its five-membered ring, and citrin shows two bands, one of which may be the resultant of absorption in the two outside rings with their OH substitutions and the other of the inner ring, which contains oxygen and a carbonyl group. The identity of the R substitutions indicated in the formula will be eventually disclosed by obtaining syntheses whose spectra are identical under similar conditions of *p*H and temperature.

THE PROTEIN PROBLEM

Fabric Absorption

Proteins are very large molecules composed of units containing 288, or a multiple of 288, amino acids, three of which show selective absorption, phenylalanine, tyrosine, and tryptophane, whose spectra have already been shown. It is generally assumed that the selective absorption between 2900 and 2700A occurring in proteins is entirely caused by absorption in the aromatic rings of tyrosine and tryptophane, and that the end absorption is that of the amino acids. The spectra

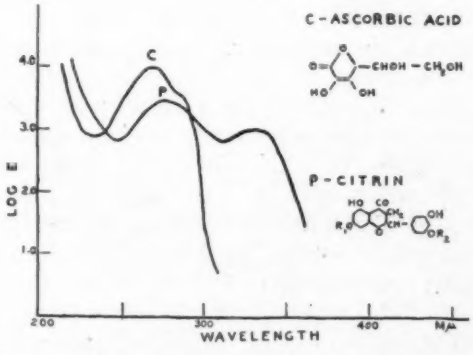

FIG. 6. Absorption bands of vitamins C (reference 20) and P (reference 21). —C—C—OH absorption produces the short wave-length band in both vitamins; absorption in the cyclized portion of vitamin C causes the 270-mμ band, the 285-mμ band of vitamin P must be owing to the two outside rings with their —OH substitutions, and the longer wave-length band to the inner ring containing a carbonyl group.

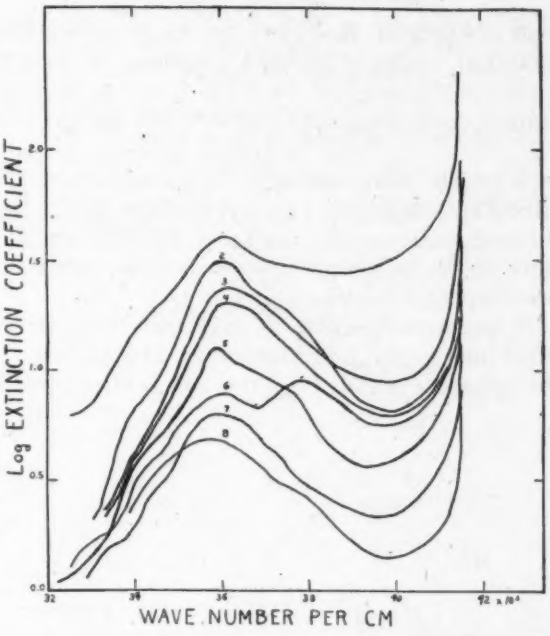

FIG. 7. Absorption spectra of the proteins: 1. Horse liver catalase. 2. Human epidermis. 3. Papain. 4. Serum albumin. 5. Tobacco mosaic virus. 6. Prolactin *p*H 7.4. 7. Crystalline prolactin. 8. Pepsin.

of a few of these proteins and related substances, such as hormones and enzymes, are shown in Fig. 7, which is based mainly on spectra obtained in the laboratories of the Rockefeller Foundation by Lavin and others.[23–25] In fact Holiday[26] and others have used the spectra to determine quantitatively the tyrosine and tryptophane content of certain proteins, though the results have seldom checked the chemical analyses within experimental error. Consequently a general pigment absorption has been assumed by Goodwin and Morton,[27] its origin unstated, but assumedly produced by the protein fabric, be it a long polypeptide chain[28] as generally assumed or cyclol as proposed by Wrinch.[29] Assuming that the chemical analyses are nearly correct it has been shown by the author and one of her colleagues[25] that gelatin which contains no tyrosine or tryptophane and the albumins containing these two amino acids both have a fabric absorption which is selective, has an appearance somewhat similar to that of tryptophane, but is shifted in position by alkaline solvent, Fig. 8, as is tyrosine, but not tryptophane. Hence it is probable that a ring is responsible for the shift, a ring which possesses —OH, as does tyrosine, and contains nitrogen as does tryptophane.

Moreover, the end absorption, which begins

near 2400 and has not yet been completely analyzed, shifts in alkaline solutions as do substances containing the 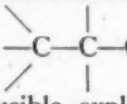 group. This is a much more plausible explanation of the strong end absorption than is the statement that it has the same origin as that of the amino acids, since in the proteins the carboxylic groups have been replaced by fabric linkages.

If the structure is long chain the basic structural unit is the peptide group, structure *A*. If the structure is the cyclol the unit is structure *B*.

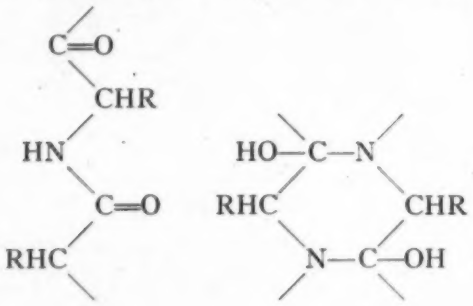

A *B*

Peptide groups absorb in the 2800 region, showing two bands, whose intensity and location are practically unaffected by solvent action. The location is the same as the maximum of the single wide band appearing in the spectra of the aldehydes and ketones, commonly ascribed to the carbonyl group. If the Wrinch pattern is true there should be diffuse absorption such as occurs weakly in methenamine in the 2300 region, shifted to longer wave-lengths by the —OH side groups and the R chains, and because of the —OH groups shifted still further by alkaline solutions. Such are the spectroscopic facts; hence it is obvious that ultraviolet spectroscopic evidence favors the cyclol and not the long-chain structure theory for proteins.

Other Protein Bands

In some of the spectra exhibited in Fig. 7 a band occurs near 2600A, best defined in the spectrum of prolactin, one of the enzymes. This absorption occurs in all the nucleoproteins and results from absorption in the pyrimidine or the purine rings occurring in the protein. Not exhibited in these figures are the bands of cytochrome, in which porphyrin groups are linked to protein structures. Absorption by the porphyrin rings and the linking metallic nucleus

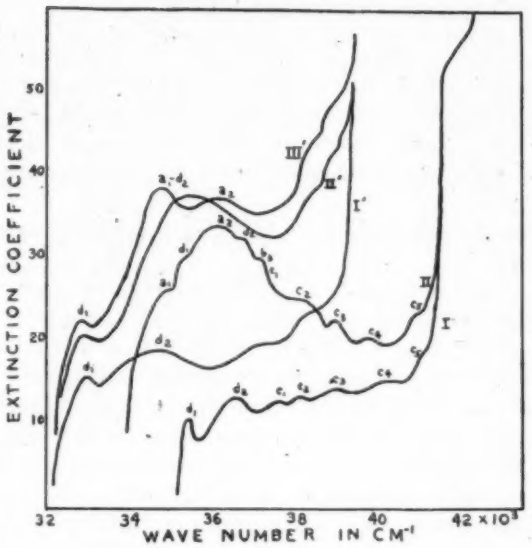

FIG. 8. Absorption curves of aqueous solutions of *I*—gelatin and *II*—egg albumen; of 0.1 *N* NaOH solutions of *I'*—gelatin, *II'*—egg albumen, *III'*—lactalbumin. Max. a_1 and a_2 may be identified as tryptophane bands; b_3 as the short wave-length member of the tyrosine group, the *c*'s as phenylalanine bands, and the *d*'s as protein fabric bands. The alkaline shift of the *d*'s and of the end absorption indicate 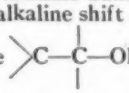 groups in the protein fabric.

produces distinctive bands in the visible, the subject of much study and utility in biochemical investigations.

Effects of Irradiation

It has long been known that the vitamins deteriorate when exposed to light with wave-length that of their absorption band, and that irradiation by photons of wave-length less than 2800 denatures proteins.[30] In egg albumen, for example, denaturation by irradiation occurs at a much lower temperature than required for heat denaturation. It is a unimolecular phenomena, the affected molecules reacting with water to flocculate. This occurs in the crystalline lens of the eye under normal conditions, but since it is normally precipitated only by heat, the lens remains clear under ordinary conditions. But precipitation does occur with high calcium concentration, or when subject to heat. Tubercle bacilli, vaccines, and various virus are rendered non-virulent by 2600A light, but remain immunizers.[31]

As for the spectra concerned, the intensity of the 2800A band changes continuously with irradiation, first becoming stronger and then weaker, indicating photolytic action on the

fabric.[25,32] Is it possible that this band originates in the denatured protein rather than in the native protein and that the denaturation produced by irradiation consists of the transformation of the affected sections of the fabric from a saturated to an unsaturated state containing conjugated groups? Cross links, for example those between the cystine and cysteine side-chains, must be affected. For Gates[33] has shown that the enzyme pepsin which contains cystine, irradiated for 120 hours, has a spectrum showing strong absorption in the 2500 and 3250 regions, which are fairly transparent in fresh pepsin. These are the regions in which absorption has been identified as characteristic of cystine and cysteine, respectively.[34] Apparently irradiation of pepsin releases these amino acids from their side-chain linkages, just as hydrolysis of the enzyme produces detectable —SH and —SS— groups.[35]

These are only a few aspects of the effects of irradiation on biologically important molecules which might be mentioned. They are adequate, however, to indicate the idportance of investigations on the effects of ultraviolet irradiation and of the identification of the absorption bands which indicate the most effective wave-lengths to be utilized.

BIBLIOGRAPHY

(1) E. P. Carr and M. K. Walker, J. Chem. Phys. **4**, 751 (1936); E. P. Carr and G. T. Walter, *ibid.* 756 (1936); W. C. Price and W. T. Tutte, Proc. Roy. Soc. **A174**, 205 (1940); W. C. Price and A. D. Walsh, *ibid.* 220 (1940).

(2) B. W. Hausser, R. Kuhn, A. Smakula, *et al.*, Zeits. f. physik. Chemie **B29**, 363, 371, 378, 384, 391, 417 (1935).

(3) G. A. Anslow and E. Vaughan, Phys. Rev. **62**, 298 (1942).

(4) Mme. Ramart-Lucas *et al.*, Comptes rendus **190**, 1196 (1930).

(5) L. Marchlewski and W. Urbanzyk, Bull. int. Acad. polon. d sc. ed. d. litt., Cl. med. **9**, 409 (1933); Biochem. Zeits. **262**, 248 (1933). J. E. Purvis, J. Chem. Soc. London 2515 (1923).

(6) V. Henri, *Etudes de Photochemie* (Gauthier-Villars, Paris, 1919), p. 54.

(7) O. Hartleb, Strahlentherapie **39**, 442 (1931).

(8) W. R. Brode, J. Am. Chem. Soc. **46**, 581 (1924).

(9) *a* P. A. Leighton and A. B. Steiner, J. Am. Chem. Soc. **58**, 1823 (1936); W. Groh and Laudenklos, Naturwiss. **24**, 796, 828 (1936); W. Groh, Zeits. f. physik. Chemie **B38**, 366 (1937).
b W. Kemula and A. Dyduszynski, Rocznike Chem. **17**, 430 (1937).
c R. B. Mooney and E. B. Ludlum, Trans. Faraday Soc. **25**, 442 (1929).
d A. R. Olson and C. H. Meyers, J. Am. Chem. Soc. **48**, 2438 (1937).
e B. L. Dunicz, J. Am. Chem. Soc. **63**, 2461 (1941).
f J. R. Bates and H. S. Taylor, J. Am. Chem. Soc. **49**, 2438 (1937).
g E. P. Carr and H. Stucklen, J. Chem. Phys. **4**, 751 (1936).
h E. Gorin, J. Chem. Phys. **7**, 256 (1939).
i R. G. W. Norrish and W. A. Noyes, Proc. Roy. Soc. **A163**, 221 (1937); R. G. W. Norrish and F. W. Kirkbride, J. Chem. Soc. 1518 (1932).
j F. E. Blacet and R. W. Moulton, J. Am. Chem. Soc. **63**, 868 (1941).
k F. E. Blacet *et al.*, J. Am. Chem. Soc. **59**, 2375 (1937); **61**, 273 (1939).
l G. K. Rollefson and M. Burton, *Photochemistry and the Mechanism of Chemical Reactions* (Prentice-Hall, Inc., NewYork, 1942).
m R. Spense and W. Wild, Nature **138**, 206 (1937); G. H. Damon and F. Daniels, J. Am. Chem. Soc. **55**, 2363 (1933); D. S. Herr and W. A. Noyes, *ibid.* **62**, 2052 (1940).
n J. P. Howe and W. A. Noyes, J. Am. Chem. Soc. **58**, 1404 (1936).
o W. M. Manning, *ibid.* **56**, 1404 (1936).
p R. G. W. Norrish and M. E. S. Appleyard, J. Chem. Soc. 874 (1934).
q A. Terenin and H. Neujmin, J. Chem. Phys. **3**, 436 (1935).

(10) H. A. Neilsen, Phys. Rev. **60**, 794 (1941).

(11) P. Karrer *et al.*, Helv. Chem. Acta **13**, 1084 (1930).

(12) R. A. Morton, Biochem. J. **26**, 1165 (1932).

(13) M. B. Matlack and Charles E. Sando, J. Biol. Chem. **104**, 407 (1934).

(14) Robert R. Williams *et al.*, J. Am. Chem. Soc. **60**, 2721 (1938); **61**, 454, 1421 (1939).

(15) R. Kuhn *et al.*, Ber. d. D. Chem. Ges. **B67**, 894 (1934).

(16) R. Williams *et al.*, J. Am. Chem. Soc., **57**, 517 (1935).

(17) R. Kuhn and H. Vetter, Ber. d. D. Chem. Ges. **B68**, 2384 (1935).

(18) O. H. Emerson, J. Biol. Chem. **122**, 99 (1937).

(19) D. T. Ewing, J. Biol. Chem. **131**, 345 (1939).

(20) A. L. Bacharach, E. Allchorne, and H. E. Glynn, Biochem. J. **30**, 2004 (1936).

(21) N. Mohler and N. Lohr, Helv. Chem. Acta **21**, 485 (1938).

(22) R. A. Morton, *The Application of Absorption Spectra to the Study of Vitamins and Hormones* (Adam Hilger, Ltd., London, 1942), second edition, p. 137.

(23) G. I. Lavin and J. H. Northrop, J. Am. Chem. Soc. **57**, 874 (1935); G. I. Lavin and W. M. Stanley, J. Biol. Chem. **118**, 269 (1937); G. I. Lavin, H. S. Loring, and W. M. Stanley, *ibid.* **130**, 259 (1939); J. S. Fruton and G. I. Lavin, *ibid.* **130**, 375 (1939); A. White and G. I. Lavin, *ibid.* **132**, 717 (1940); K. G. Stern and G. I. Lavin, Science **88**, 263 (1938).

(24) N. S. Lucas, Biochem. J. **25**, 57 (1931).

(25) G. A. Anslow and S. C. Nassar, J. Opt. Soc. Am. **31**, 118 (1941).

(26) E. R. Holiday, Biochem. J. **24**, 619 (1930); **30**, 1795 (1936); **32**, 1166 (1938).

(27) T. W. Goodwin and R. A. Morton, *The Application of Absorption Spectra to the Study of Vitamins and Hormones* (Adam Hilger, Ltd., London, 1942), second edition, p. 184.

(28) R. B. Corey, Chem. Rev. **26**, 227 (1940).

(29) D. Wrinch, Proc. Roy. Soc. **A160**, 59 (1937); **A161**, 505 (1937); Phil. Mag. [7] **24**, 940 (1937) and others.

(30) J. H. Clark, J. Gen. Physiol. **19**, 199 (1935); Am. J. Physiol. **113**, 538 (1935); Ann. Rev. Physiol. **1**, 21 (1939).

(31) G. I. Lavin *et al.* Am. Rev. Tuber. **39**, 782 (1939); J. Exper. Med. **72**, 729 (1940).

(32) M. Spiegel-Adolf, Archiv. Path. **12**, 533 (1931).

(33) F. L. Gates, J. Gen. Physiol. **18**, 263 (1934).

(34) G. A. Anslow and M. L. Foster, J. Biol. Chem. **97**, 37 (1932); G. A. Anslow and E. R. Lyman, J. Opt. Soc. **31**, 114 (1941).

(35) H. E. Minsky and M. L. Anson, J. Gen. Physiol. **19**, 427 (1936).

The Thermodynamics of Rubber at Small Extensions*

BY D. R. ELLIOTT AND S. A. LIPPMANN

United States Rubber Company, Detroit, Michigan

(Received October 23, 1944)

On analyzing their own data, Meyer and Ferri have concluded that at small extensions, rubber is an ideal elastomer according to the definition that $(\partial E/\partial L)_{P,T}=0$. Further analysis of Meyer and Ferri's data does not sustain their conclusion. If, however, $(\partial E/\partial L)_{V,T}=0$ is taken as a new criterion for an ideal elastomer, Meyer and Ferri's data do indicate that rubber is ideal, at least for extensions up to 166 percent. The new criterion implies that the valence angles do not store an appreciable amount of energy when the rubber is stretched. However, both the molecular orientation and the interatomic displacements do influence the energy required for extension.

DISCUSSION OF MEYER AND FERRI'S[1] CONCLUSIONS

ON the assumption of reversible stretching, Wiegand and Snyder[3] derived the following thermodynamic relationship.

$$\left(\frac{\partial E}{\partial L}\right)_{T,P=0}=F-T\left(\frac{\partial F}{\partial T}\right)_{L,P=0}, \qquad (1)$$

where F is the force keeping the elastomer in a stretched condition. Meyer and Ferri concluded from an equivalent equation that if $(\partial E/\partial L)_{T,P=0}=0$ then F measured at constant extension should vary directly as the absolute temperature. Mathematically,

$$F=GT; \quad P=0, \quad L=\text{const.} \qquad (2)$$

where G is the constant of proportionality. Experimentally, Meyer and Ferri found a linear relationship between the temperature and force, but not proportionality. They were led to the assumption that, since the length of the unstretched rubber changes as a result of thermal expansion, the force requires a temperature correction. For example, the corrected force is

$$F_c=F+M\beta(T-T_0), \qquad (3)$$

where

$$\beta=\frac{1}{L}\left(\frac{\partial L}{\partial T}\right)_{D,P=0}$$

and

$$M=L\left(\frac{\partial F}{\partial L}\right)_{T,P=0}.$$

D is the deformation or the ratio of two perpendicular lengths, one normal to the direction of stress and one parallel to it. They found that this corrected force was proportional to the absolute temperature;

$$F_c=aT \qquad (4)$$

when P and L are constants; and it was concluded that $(\partial E/\partial L)_{T,P=0}=0$.

Equation (1) does not assume that the length of an unstretched rubber sample remains constant during temperature variations. The equation of state from which this equation is derived contains the assumption that the force is a function of the temperature, and therefore, no corrections to include this fact are necessary. Therefore, the conclusion drawn from Eq. (4) is in error; $(\partial E/\partial L)_{T,P=0}\neq 0$.

THE CHANGE IN INTERNAL ENERGY WITH EXTENSION

In order to examine the implications of Meyer and Ferri's data, another variable, the hydrostatic pressure (P), will have to be considered. This variable is introduced so that the volume of the sample may be made independent of the extension and temperature. The entire testing environment, weights, sample, and all will be considered immersed in a non-buoyant fluid that does not penetrate the rubber and whose pressure is variable at will. (See Fig. 1.)

Below the range of extensions in which crystallization takes place, the stretching of rubber is a reversible phenomenon, if sufficient time is allowed for the sample to come to equilibrium. Thus at equilibrium and for small extensions the properties of the rubber are determined by its temperature, length, and the hydrostatic pressure

* Presented on June 24, 1944 before the Inaugural Meeting of the Division of High-Polymer Physics of the American Physical Society at Rochester, New York.

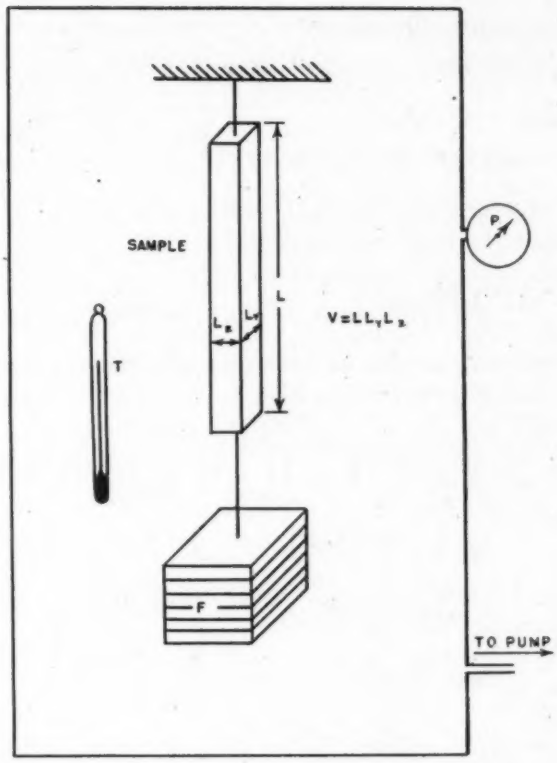

FIG. 1. Schematic diagram of extended sample in its testing environment.

of the fluid in which it is immersed; e.g.,

$$E=E(T, P, L), \tag{5}$$

$$S=S(T, P, L), \tag{6}$$

$$V=V(T, P, L), \tag{7}$$

where S is the entropy, and V is the volume. From the first law of thermodynamics

$$T\delta S-\delta E-P\delta V+F\delta L=0. \tag{8}$$

Therefore, from (5)–(8)

$$F=F(T, P, L). \tag{9}$$

Expanding (5)–(7); and substituting in (8), we obtain

$$\begin{aligned}T[&(\partial S/\partial T)\delta T+(\partial S/\partial P)\delta P\\&+(\partial S/\partial L)\delta L]-[(\partial E/\partial T)\delta T\\&+(\partial E/\partial P)\delta P+(\partial E/\partial L)\delta L]\\&-P[(\partial V/\partial T)\delta T+(\partial V/\partial P)\delta P\\&+(\partial V/\partial L)\delta L]+F\delta L=0.\end{aligned} \tag{10}$$

Since T, P, and L are independent variables; δT, δP, and δL may be chosen independently of each other. Thus from Eq. (10),

if $\delta P=\delta L=0$;

$$T(\partial S/\partial T)-(\partial E/\partial T)-P(\partial V/\partial T)=0, \quad \text{when } \delta T\neq 0;$$

if $\delta T=\delta L=0$;

$$T(\partial S/\partial P)-(\partial E/\partial P)-P(\partial V/\partial P)=0, \quad \text{when } \delta P\neq 0;$$

if $\delta P=\delta T=0$;

$$T(\partial S/\partial L)-(\partial E/\partial L)-P(\partial V/\partial L)+F=0, \quad \text{when } \delta L\neq 0. \tag{11}$$

Solving for the entropy terms in Eqs. (11) we get

$$\partial S/\partial T=1/T[(\partial E/\partial T)+P(\partial V/\partial T)],$$

$$\partial S/\partial P=1/T[(\partial E/\partial P)+P(\partial V/\partial P)],$$

and

$$\partial S/\partial L=1/T[(\partial E/\partial L)+P(\partial V/\partial L)-F]. \tag{12}$$

Since by mathematical identity,

$$\partial^2 S/\partial P\partial T=\partial^2 S/\partial T\partial P;$$

$$\partial^2 S/\partial T\partial L=\partial^2 S/\partial L\partial T;$$

$$\partial^2 S/\partial L\partial P=\partial^2 S/\partial P\partial L$$

it follows from Eqs. (12) that

$$(\partial E/\partial P)_{T, L}=-P(\partial V/\partial P)_{T, L}-T(\partial V/\partial T)_{P, L} \tag{13}$$

$$(\partial E/\partial L)_{T, P}=F-T(\partial F/\partial T)_{P, L}-P(\partial V/\partial L)_{T, P=0} \tag{14}$$

and

$$(\partial V/\partial L)_{T, P}=(\partial F/\partial P)_{L, T}. \tag{15}$$

For zero hydrostatic pressure Eq. (14) reduces to the Wiegand and Snyder equation.

It follows from Eqs. (5) and (7) that $E=E(T, P(V, L, T), L)$. By differentiating E partially with respect to length, we get

$$(\partial E/\partial L)_{V, T}=(\partial E/\partial L)_{P, T}+(\partial E/\partial P)_{T, L}(\partial P/\partial L)_{V, T}. \tag{16}$$

Similarly from Eqs. (7) and (9),

$$(\partial P/\partial V)_{F, T}=(\partial P/\partial V)_{L, T}+(\partial P/\partial L)_{V, T}(\partial L/\partial V)_{F, T}. \tag{17}$$

Equation (16) is an alternative expression of the term $(\partial E/\partial L)_{V, T}$ for which we are solving. The relation does not consist as yet of experimentally observed quantities. The two partial derivatives

of the internal energy, however, are already expressed in familiar experimental terms in Eqs. (13) and (14). Now, we must find such an expression for the partial derivative of the pressure with respect to length.

From Eqs. (7) and (9), $P=P(V, L, T)$. Thus by identity,

$$(\partial P/\partial L)_{V,T}=-(\partial P/\partial V)_{L,T}(\partial V/\partial L)_{P,T}, \quad (18)$$

and therefore

$$(\partial P/\partial V)_{F,T}=(\partial P/\partial V)_{L,T} \times[1-(\partial V/\partial L)_{P,T}(\partial L/\partial V)_{F,T}]. \quad (19)$$

Expanding the right-hand side of Eq. (15), we get

$$(\partial V/\partial L)_{P,T}=-(\partial F/\partial L)_{P,T}(\partial L/\partial P)_{F,T}. \quad (20)$$

Substituting Eqs. (19) and (20) in (18) we are able to evaluate $(\partial P/\partial L)_{V,T}$.

$$(\partial P/\partial L)_{V,T}=(\partial P/\partial V)_{F,T} \times(\partial F/\partial L)_{P,T}(\partial L/\partial P)_{F,T}\Big/ \left[1+\left(\frac{\partial F}{\partial L}\right)_{P,T}\left(\frac{\partial L}{\partial P}\right)_{F,T}\left(\frac{\partial L}{\partial V}\right)_{F,T}\right]. \quad (21)$$

The partial derivatives in Eq. (21) can be replaced in general by more common moduli, e.g.,

$$M=L(\partial F/\partial L)_{P,T}.$$
$$Y=ML/V.$$
$$K=-V(\partial P/\partial V)_{F,T}. \quad (22)$$
$$\beta_1=(\tfrac{1}{3}V)(\partial V/\partial T)_{L,P=0}.$$
$$A=(3V/L)(\partial P/\partial V)_{F,T}(\partial L/\partial P)_{F,T} =(3V/L)(\partial L/\partial V)_{F,T}.$$

M is the stress-strain modulus, Y is Young's modulus, K is a bulk modulus, and β_1 is a thermal coefficient of linear expansion. A is the anisotropy factor which is described in detail in a later section. It is sufficient to mention here that $A=1$ for isotropic rubber.

When YA/k is small compared to 9, β_1 is very nearly equal to the coefficient of expansion measured at constant deformation and zero hydrostatic pressure. This may be proven in the following manner.

Since $D=D(T, P, L)$, it can be shown, in a manner similar to the derivation of Eq. (12), that

$$(\partial V/\partial T)_{D,P}=(\partial V/\partial T)_{L,P} +(\partial V/\partial L)_{P,T}(\partial L/\partial T)_{D,P}. \quad (23)$$

In addition by identity

$$(\partial F/\partial P)_{L,T}=-(\partial F/\partial L)_{P,T}(\partial L/\partial P)_{F,T}, \quad (24)$$

and

$$(\partial L/\partial P)_{F,T}=(\partial L/\partial V)_{F,T}(\partial V/\partial P)_{F,T}. \quad (25)$$

Substituting (15), (24), (25) in Eq. (23) we obtain the following expression.

$$(\partial V/\partial T)_{D,P}=(\partial V/\partial T)_{L,P}-(\partial L/\partial V)_{F,T} \times(\partial F/\partial L)_{P,T}(\partial L/\partial T)_{D,P}(\partial V/\partial P)_{F,T}. \quad (26)$$

In terms of the coefficients and moduli already used, Eq. (26) becomes

$$3V\beta=3V\beta_1+\left(\frac{AL}{3V}\right)\left(\frac{V}{K}\right)\left(\frac{VY}{L^2}\right)(BL), \quad (27)$$

or

$$\beta=\beta_1/(1-AY/9k). \quad (28)$$

If $YA/k\ll 9$, $\beta\doteqdot\beta_1$. Substituting relations (22) into Eq. (21), we obtain

$$(\partial P/\partial L)_{V,T}=(MA/3V)/(1-YA^2/9k), \quad (29)$$

or

$$(\partial P/\partial L)_{V,T}\doteqdot(MA/3V), \text{ when } YA^2/k\ll 9. \quad (30)$$

Substituting Eqs. (13), (14), (22), and (30) in Eq. (16) we obtain the equation

$$(\partial E/\partial L)_{V,T}=F-T(\partial F/\partial T)_{P,L}-M\beta TA. \quad (31)$$

ANISOTROPY FACTOR, A

The term A, defined in Eqs. (22), is measured only with difficulty. Nevertheless, its value for an isotropic elastomer can be predicted. This quantity will be referred to as the anisotropy factor. The significance of A becomes evident, if the effect of a change in hydrostatic pressure on the dimensions of a rectangular rubber strip is examined. Maintaining the force and temperature constant, the three perpendicular dimensions taken along the principal axis of the strain tensor will vary in the following manner.

$$\delta L=L\alpha_L\delta P, \quad \delta L_Y=L_Y\alpha_Y\delta P, \quad \delta L_Z=L_Z\alpha_Z\delta P, \quad (32)$$

where the α's are coefficients of extensibility. That is to say, the change in a dimension in the direction of an axis of the strain tensor is proportional to its length, and to the change in pressure. The corresponding change in volume is

$$\delta V=LL_YL_Z-(L+\delta L) \times(L_Y+\delta L_Y)(L_Z+\delta L_Z). \quad (33)$$

It follows from Eqs. (32) and (33) that if $\delta P \rightarrow 0$,

$$\frac{3V}{L}\left(\frac{\partial L}{\partial V}\right)_{F,T} = \frac{3\alpha_L}{\alpha_L+\alpha_Y+\alpha_Z}, \qquad (34)$$

and from Eqs. (22) and (34)

$$A = 3\alpha_L/(\alpha_L+\alpha_Y+\alpha_Z).$$

Where the material is isotropic, the α's are all equal and A is 1. This condition is met for ordinary rubber at zero extension, and is met approximately at small extensions. For anisotropic conditions the extensibilities in the directions normal to the direction of stress may or may not equal the extensibility in the stress direction. Thus, as the material becomes anisotropic, A may differ from 1. At small extensions when $A \doteq 1$, Eq. (31) becomes:

$$(\partial E/\partial L)_{V,T} = F - T(\partial F/\partial T)_{L,P=0} - M\beta T. \qquad (35)$$

ANALYSIS OF MEYER AND FERRI'S DATA

From Eqs. (3) and (4), which summarize the Meyer and Ferri data, for small extensions

$$F = aT - M\beta(T-T_0). \qquad (36)$$

Differentiating partially with respect to temperature, we obtain

$$(\partial F/\partial T)_{L,P=0} = a - M\beta - \beta(T-T_0)(\partial M/\partial T). \qquad (37)$$

Substituting the values of F and its partial derivative as given by Eqs. (36) and (37) into Eq. (35), the following relation results.

$$(\partial E/\partial L)_{V,T} = M\beta T_0 + \beta T[(T-T_0)(\partial M/\partial T) - M];$$

and letting $T \rightarrow T_0$,

$$(\partial E/\partial L)_{V,T} = 0. \qquad (38)$$

Similarly from Eqs. (36), (37) and (1),

$$(\partial E/\partial L)_{T,P} = M\beta T, \quad P = 0. \qquad (39)$$

Thus, we see from Eqs. (38) and (39) that the Meyer and Ferri data requires that

$$(\partial E/\partial L)_{V,T} = 0$$

and *not* that $(\partial E/\partial L)_{P,T} = 0$.

STRUCTURAL CHANGES IN RUBBER DURING EXTENSION

Relations (38) and (39) are indicative of the major processes that take place in rubber on extension. There are three possible mechanisms for the isothermal absorption of the extension energy in an elastomer. One is the distortion of the valence angles, the second is the separation of adjacent atoms, and a third is the orientation of the molecules.

In rubber the valence angle distortion mechanism is not consistent with the Meyer and Ferri data. The energy absorbed in distorting the valence angles would appear as an increase in the internal energy. It should be noted that a change in valence angles is not necessarily accompanied by a change in volume, since all volume changes that would normally occur on extending rubber can be eliminated by varying the hydrostatic pressure. Thus, a change in valence angle would result in an increase of the internal energy of the rubber even for isothermal stretching at constant volume. This is in direct contradiction to Eq. (38) which states that there is no internal energy change if the volume and temperature are constant.

According to Eqs. (38) and (39), on isothermal extension, the internal energy of rubber increases only when the volume is allowed to grow. Since an increase in volume necessarily means that the average interatomic distance becomes greater, the internal energy stored in the rubber on isothermal stretching must be taken up in pulling the atoms apart.

The change in the average interatomic distances, however, cannot be the sole means by which energy is absorbed on stretching. This is particularly obvious in the case of rubber extended isothermally at constant volume, for there is no internal energy accumulation under these conditions, and yet work is done on the rubber. According to the first law of thermodynamics,

$$-\delta W = \delta E - T\delta S, \quad T\delta S = \delta Q, \qquad (40)$$

where S is the entropy, and W is the work performed by the sample on its surroundings. The quantity $T\delta S$ is the increase of isothermally unavailable energy. In a system undergoing thermal agitation, S is a measure of the amount of molecular or atomic disorder. Therefore, $-T\delta S$ might be referred to as the change in orientation energy. Equation (40) indicates that the work of extension divides itself between the internal energy and the orientation energy. Since the change in orientation energy is equal to the heat given up by the rubber, the portion of the work that causes the orientation appears as

heat, having made an equal amount of the rubber's internal energy isothermally available.

Based on the conclusion that the internal energy change is entirely owing to interatomic displacements, either Eq. (9) or (39) permits the calculation, from experimental data, of how the energy taken up in stretching the rubber is divided between the orientation energy and interatomic displacement energy. Thus, since the differential work input on stretching is

$$-\delta W = F\delta L, \tag{41}$$

and from Eq. (39)

$$\delta E = (\partial E/\partial L)_{T,P=0}\delta L = M\beta T\delta L, \tag{42}$$

therefore, from Eqs. (41) and (42)

$$(\delta E/\delta W)\times 100 = 100M\beta T/F \text{ percent.} \tag{43}$$

Where $(\partial E/\partial L)=0$, Eqs. (9) and (39) yield the following relationship:

$$(\delta E/\delta W)\times 100 = [(1-T/F)(\partial F/\partial T)_{L,P=0}]\times[100] \text{ percent.} \tag{44}$$

In Eq. (43) the ratio is calculated from stress-strain data, while Eq. (44) requires thermal data. It should be noted that both relations hold only when $(\partial E/\partial L)_{V,T}=0$, but that Eq. (43) has the additional requirement that A is approximately 1. Meyer and Ferri's data indicate that the interatomic displacement absorbs the entire energy input at 8 percent extension. For, at this extension $(\partial F/\partial T)_{L,P=0}=0$ and Eq. (44) reduces to $\delta E/\delta W=1$. The terms M and β do not vary much with the strain of the rubber, although they do decrease somewhat. Thus above the 8 percent extension and in the range for which Eq. (43) is true, the relative contribution of the interatomic displacement energy to the total retractive energy decreases with increasing force.

EQUATION OF STATE

The form of the equation of state of rubber at low extensions also follows from the Meyer and Ferri data. If in Eqs. (5)–(8) V, L, and T are used as independent variables instead of P, L, and T; the equation that corresponds to Eq. (31) is

$$(\partial E/\partial L)_{V,T} = F - T(\partial F/\partial T)_{V,L}. \tag{44}$$

Now, according to Eq. (38), $(\partial E/\partial L)_{V,T}=0$ and Eq. (44) becomes,

$$F = T(\partial F/\partial T)_{V,L}. \tag{45}$$

Therefore,

$$F = T\psi(V, L), \tag{46}$$

where ψ is an undetermined function of V and L that must be consistent with Eq. (15). The final relation, Eq. (46), gives the form of the equation of state of rubber at low extensions as required by the Meyer and Ferri data.

TABLE OF SYMBOLS

A Anisotropy factor, $\frac{3V}{L}\left(\frac{\partial L}{\partial V}\right)_{F,T}$.

D Deformation, the ratio of two perpendicular dimensions, one taken in the direction of stress, and one normal to this direction.

E Total internal energy, or intrinsic energy.

F Force acting on a rubber sample keeping it in a stretched condition.

F_c Corrected force of Eq. (3).

G Proportionality constant of Eq. (2).

K Compression modulus at constant load and temperature, $-V(\partial P/\partial V)_{F,T}$.

L Length of the sample in the direction of stress.

L_y Dimension of rectangular sample normal to the direction of stress.

L_z Dimension of rectangular sample perpendicular to both L and L_y.

M Extension modulus of the sample, $L(\partial F/\partial L)_{P,T}$.

P Hydrostatic pressure of the medium in which the test is performed.

Q Heat absorbed by the sample from its surrounding.

S Entropy.

T Absolute temperature.

V Volume of the sample.

W Work performed by the rubber sample on its surroundings.

Y Young's modulus, $\frac{L^2}{V}\left(\frac{\partial F}{\partial L}\right)_{P,T}$.

α Coefficient of extensibility, $\frac{1}{L}\left(\frac{\partial L}{\partial P}\right)_{F,T}$.

β Thermal coefficient of linear expansion at constant deformation and at zero pressure, $\frac{1}{L}\left(\frac{\partial L}{\partial T}\right)_{D,P=0}$.

β_1 $\frac{1}{3}$rd thermal coefficient of volume expansion at constant length and at zero pressure, $\frac{1}{3V}\left(\frac{\partial V}{\partial T}\right)_{L,P=0}$.

BIBLIOGRAPHY

(1) K. H. Meyer and C. Ferri, Helv. Chim. Acta **18**, No. 3, 570–589 (May 2, 1935).

(2) W. W. Vogt, *Chemistry and Technology of Rubber*, edited by Davis and Blake (Reinhold Publishing Corporation, New York, 1937), p. 371. Houwink, *Elasticity, Plasticity, and the Structure of Matter* (Cambridge University Press, 1937), p. 195.

(3) W. B. Wiegand and J. W. Snyder, Trans. Inst. Rubber Ind. **10**, No. 3, 234–262 (Oct. 1934).

Letters to the Editor

Theory of Filler Reinforcement

JANE M. DEWEY
General Laboratories, United States Rubber Company, Passaic, New Jersey
October 20, 1944

IN a recent paper in this Journal, John Rehner, Jr.,[1] discusses the stresses in the neighborhood of a spherical filler particle in rubber. He finds that all the stresses are discontinuous at the surface of the particle. His work is based on formulae derived by Sezawa and Miyazaki[2] on the usual assumption of continuity of displacement and of the surface stresses at the spherical boundary. As the conclusions of Rehner are, therefore, inconsistent with the assumptions on which they are based, the work must contain a mathematical error at some point.

A correct solution of the problem of a spherical inclusion of any rigidity in an elastic medium under simple tension has been given by J. N. Goodier.[3] Goodier's paper gives formulae for the stresses at any point in the medium or inclusion when the medium is under simple tension.

Rehner considers a number of particular cases of filler particles in an elastomer. In each case the imbedded particle is much more rigid than the surrounding medium and Poisson's ratio of the surrounding medium is very close to $\frac{1}{2}$. When these conditions are fulfilled the stresses are the same, to a very high degree of approximation, as if the particle were entirely rigid and the medium incompressible. From Goodier's results it follows that each stress on the surface of the particle is 5/2 the similar stress at a large distance from the particle. Filler particles in elastomers or plastics are always so much more rigid than the surrounding medium that the error introduced by considering them as entirely rigid is much less than the error introduced by the use of Hooke's law.

Sezawa and Miyazaki[2] give a general two-dimensional solution of the equations

$$\nabla^2\nabla\cdot s=0, \tag{1}$$

$$(\lambda_1+\lambda_2)\nabla\nabla\cdot s+\lambda_2\nabla^2 s=0, \tag{2}$$

arising in the theory of equilibrium of elastic media and in the theory of the steady flow of viscous fluids. In the discussion of the elastic or viscous properties of a medium containing a large number of inclusions, the three-dimensional solution is much more convenient.[4] This can be obtained in spherical coordinates by separation of variables.

$$\begin{aligned}s=\sum_m e^{im\varphi}\sum_\gamma\Big(&a_\gamma r^\gamma\Big\{P_{\gamma-1}^{|m|}i_r+\frac{(\gamma+2)\lambda_1+(\gamma+4)\lambda_2}{\gamma[(\gamma-1)\lambda_1+(\gamma-3)\lambda_2]}\\&\times\Big[\frac{\partial P_{\gamma-1}^{|m|}}{\partial\theta}i_\theta+\frac{im}{\sin\theta}P_{\gamma-1}^{|m|}i_\varphi\Big]\Big\}\\&+b_\gamma r^\gamma\Big\{P_{\gamma+1}^{|m|}i_r+\frac{1}{\gamma+1}\Big[\frac{\partial P_{\gamma+1}^{|m|}}{\partial\theta}i_\theta+\frac{im}{\sin\theta}P_{\gamma+1}^{|m|}i_\varphi\Big]\Big\}\\&+a_{-\gamma}r^{-\gamma}\Big\{P_\gamma{}^{|m|}i_r-\frac{(\gamma-2)\lambda_1+(\gamma-4)\lambda_2}{\gamma[(\gamma+1)\lambda_1+(\gamma+3)\lambda_2]}\\&\times\Big[\frac{\partial P_\gamma^{|m|}}{\partial\theta}i_\theta+\frac{im}{\sin\theta}P_\gamma{}^{|m|}i_\varphi\Big]\Big\}+b_{-\gamma}r^{-\gamma}\Big\{P_{\gamma-2}^{|m|}i_r\\&-\frac{1}{\gamma-1}\Big[\frac{\partial P_\gamma{}^{|m|}}{\partial\theta}i_\theta+\frac{im}{\sin\theta}P_\gamma{}^m i_\varphi\Big]\Big\}\Big),\end{aligned} \tag{3}$$

m integral, γ integral >0, $P_\gamma{}^{|m|}=P_\gamma{}^{|m|}(\cos\theta)$ = Legendre polynomial of order γ, $|m|$ and argument $\cos\theta$.

For the usual boundary conditions at infinity,

$$s\underset{r\to\infty}{\longrightarrow}Axi+Byj+Czk \tag{4}$$

and boundary conditions in the finite region independent of angle, the solution becomes

$$\begin{aligned}s_{r>R}=&\Big[\tfrac{1}{2}(A+B+C)(r+b_{-2}r^{-2})\\&+(r+c_{-2}r^{-2}+c_{-4}r^{-4})M(\theta,\varphi)\Big]i_r\\&+\frac{1}{2}\Big(r+\frac{2\lambda_2}{3\lambda_1+5\lambda_2}c_{-2}r^{-2}-\frac{2}{3}c_{-4}r^{-4}\Big)\\&\times\Big(\frac{\partial M}{\partial\theta}(\theta,\varphi)i_\theta+\frac{1}{\sin\theta}\frac{\partial M}{\partial\varphi}(\theta,\varphi)i_\varphi\Big),\\s_{r<R}=&\Big[a_1r+(c_1r+c_3r^3)M(\theta,\varphi)\Big]i_r\\&+\frac{1}{2}\Big(c_1r+\frac{5\lambda_1+7\lambda_2}{3\lambda_1}c_3r^3\Big)\\&\times\Big(\frac{\partial M}{\partial\theta}i_\theta+\frac{1}{\sin\theta}\frac{\partial M}{\partial\varphi}i_\varphi\Big),\\M=&\tfrac{1}{2}(A+B-2C)P_2(\cos\theta)\\&+(1/12)(A-B)P_2{}^2(\cos\theta)(e^{2i\varphi}+e^{-2i\varphi})\\=&A\sin^2\theta\cos^2\varphi+B\sin^2\theta\sin^2\varphi\\&+C\cos^2\theta-\tfrac{1}{2}(A+B+C).\end{aligned} \tag{5}$$

The undetermined constants are fixed by the boundary conditions in the finite region.

In an elastic medium of bulk modulus λ_1, modulus of rigidity λ_2, in which there is a spherical particle of radius R, with Lame's constants λ_1' and λ_2', at the origin of coordinates, the constants have the values, on the usual assumption of single-valued displacements and single-valued stresses on the surface of the particle,

$$\begin{aligned}b_{-2}&=(3\lambda_1+2\lambda_2-3\lambda_2'-2\lambda_2')(4\lambda_2+3\lambda_1'+2\lambda_2')^{-1}R^{-1},\\c_{-2}&=-5(3\lambda_1+5\lambda_2)DR^{-1},\\c_{-4}&=+9(\lambda_1+\lambda_2)DR^{-3},\\a_1&=(A+B+C)(\lambda_1+\lambda_2)(4\lambda_2+3\lambda_1'+2\lambda_2')^{-1},\\c_1&=15\lambda_2(\lambda_1+2\lambda_2)D(\lambda_2'-\lambda_2)^{-1},\\c_3&=0,\\D&=[2\lambda_2'(3\lambda_1+8\lambda_2)+\lambda_2(9\lambda_1+14\lambda_2)]^{-1}(\lambda_2'-\lambda_2).\end{aligned} \tag{6}$$

When $A=B=-\sigma C$, σ = Poisson's ratio $=\lambda_1/2(\lambda_1+\lambda_2)$, the stresses calculated from these solutions are those given by Goodier. When $\lambda_1'\to\infty$, $\lambda_2=\mu$, the coefficient of viscosity, λ_1' and $\lambda_2'\to\infty$, these solutions reduce to those given by Einstein[4] in Cartesian coordinates. Einstein's method of averaging over the particles can be used to determine approximately the elastic properties of a filled medium in which the filler particles are widely separated.

[1] John Rehner, Jr., J. App. Phys. **14**, 638 (1944).
[2] K. Sezawa and B. Miyazaki, J. Soc. Mech. Eng. Tokyo **31**, 625 (1928).
[3] J. N. Goodier, J. App. Mech. **1**, 39 (1933). This paper was brought to the writer's attention by Dr. Rehner. When his paper on the subject was published, Dr. Rehner was unaware of Goodier's work.
[4] Cf. A. Einstein, Ann. d. Physik **19**, 289 (1906), and **34**, 591 (1911).

Etymology of the Word Microradiograph

L. V. CHILTON
The Royal Photographic Society of Great Britain, London, England
October 27, 1944

IN a letter in the August issue of *Journal of Applied Physics*,[1] under the above title, S. E. Maddigan claims that since records of the type to which the above name has been applied by himself and others show the body structure rather than the surface structure of the sample tested, there is a case for describing them by a different term from that proposed—radiomicrograph or, better, x-ray micrograph—

by Miss E. L. Garvin[2] and independently by me.[3] To support this claim, Maddigan refers to "general usage in the field of metal investigations" whereby "micrograph or photomicrograph is understood to mean an enlarged reproduction of the metal *surface*" (Maddigan's italics). He goes on to support the corresponding use of the term electron micrograph.

Surely, however, we ought to recognize that the accepted term photomicrograph is used equally of reflection and transmission records; so, too, is electron micrograph—in fact, in the latter case the bulk of the records obtained with current electron microscopes is transmission records, rather than records of a surface.

The essential point concerning the use of the prefix micro- in connection with records on photographic materials is that when the record is an enlargement of a "microscopically" small object, the prefix micro- follows a second prefix indicating the type of radiation used and immediately precedes the term -graph, e.g., photomicrograph: The converse order, microphotograph, is used wheer the record is very small (and the object usually much larger). Contrary to Maddigan's statement, this convention is now universal among English-speaking users (as regards the particular example just quoted), although it is true that there has been confusion in the past. Maddigan's examples from *Webster* reveal such confusion, but it ought to be stated that none of his examples is from the photographic field. The *Shorter Oxford Dictionary* also shows apparent synonymity between microphotograph and photomicrograph, but the date quoted for this is 1858; and already in 1867 we find the terms being distinguished[4] in accordance with the modern convention.

Thus there seems a strong case for using the term radiomicrograph or x-ray micrograph for the enlarged record at all events. The actual x-ray record in this application might be described, when a special term is needed, as a "contact microradiograph." The type of record obtained by Trillat's technique,[5] to which Maddigan refers, would be a reflection radiomicrograph.

In conclusion, I should like to repeat a plea made elsewhere[3] that the actual photographic record should be designated by the suffix -gram (as in spectrogram, electron microgram, etc.), and that -graph be reserved for the recording instrument.

[1] S. E. Maddigan, J. App. Phys. 15, 626 (1944).
[2] E. L. Garvin, J. App. Phys. 15, 455 (1944).
[3] L. V. Chilton, J. Sci. Inst. 21, 33 (1944).
[4] E. T. Wilson, Pop. Sci. Rev. 6, 54 (1867).
[5] J. J. Trillat, Comptes rendus (Dec. 1941); *ibid.* (Jan. 1942).

Here and There

Diesel Engine Manufacturers Association

Manufacturers of Diesel engines met in Chicago, October 7 with 23 deans and professors from engineering schools to discuss the need for better facilities for turning out competent Diesel engine operators—and pledged support from the manufacturers. The occasion was the luncheon get-together of the educational committee of the Diesel Engine Manufacturers Association, with the engineering instructors, at the LaSalle Hotel.

New Appointment

The University of Pittsburgh has announced the establishment of a Westinghouse Graduate Professorship in Engineering and the appointment of Dr. Alexander J. Allen as Westinghouse Graduate Professor of Engineering. Dr. Allen, formerly an Associate Professor of Physics at the University of Pittsburgh, returned as Westinghouse Graduate Professor after having served in important research at the Massachusetts Institute of Technology and as Assistant Director of the Biochemical Research Foundation of the Franklin Institute. The University of Pittsburgh and Westinghouse in 1927 inaugurated a graduate study program to provide advanced training in the fields of engineering, science, and business. The purpose of the professorship is to enlarge this program.

Textile Research Institute Fellowships

A cooperative program of graduate training of the Textile Research Institute went into effect at Princeton, New Jersey, commencing November 1, 1944. Through this program, the Institute will offer a number of research fellowships. The fellows will have an opportunity to work toward their Doctor's degree at Princeton University, and also to do research work in the laboratories of the Textile Research Institute at Princeton. Those accepted as fellows will receive $700 per year, and the Institute will also pay the graduate tuition fees. Prospective fellows are invited to send inquiries concerning the program to Dr. Henry Eyring, acting Director of Fundamental Research, Textile Research Institute Laboratories, Princeton, New Jersey.

Optical Society of America

The Spring meeting of the Optical Society of America will be held at the Hotel Statler, in Cleveland, Ohio, on April 12, 13, and 14, 1945.

Honors and Awards

The Legion of Merit has been awarded in Paris to Colonel David Sarnoff, of New York, President of the Radio Corporation of America, "for ingenuity and resourcefulness in restoring cables severed by the enemy," and for his work with the U. S. Signal Corps of the Supreme Allied Expeditionary Force in preparing news communications for the invasion and later.

The Oersted Medal for 1943 of the American Association of Physics Teachers has been conferred on Dr. Roland R. Tileston, of Pomona College, Claremont, California, since 1943 Director of the Pre-Meteorological Program for the Air Forces, U. S. Army.

Staff Change

Dr. Lyle Winston Phillips, of the Department of Physics of the University of Illinois, has joined the staff of the research laboratories of the Armstrong Cork Company.

American Society of Metals

Dr. Kent R. Van Horn, of Cleveland, Research Metallurgist of the Aluminum Company of America, was elected at the Cleveland meeting on October 18 President of the American Society for Metals, and Dr. Charles H. Herty, Jr., Research Engineer and Assistant to the Vice President of the Bethlehem Steel Company, was made Vice President.

Contributed Original Research

The Magnetic Permeability of Iron Wires at Radiofrequencies

ALVA W. SMITH, F. P. DICKEY,* AND S. W. FOOR**
Mendenhall Laboratory of Physics, The Ohio State University, Columbus, Ohio
(Received August 16, 1944)

The magnetic permeability of iron wires of selected diameters is measured at fields of low intensity and at frequencies corresponding to wave-lengths from 54 to 1150 meters. The observed permeabilities decrease with increase in frequency and increase of wire size. The results do not confirm the existence of an anomalous dispersion of permeability previously reported by some investigators.

I. INTRODUCTION

A KNOWLEDGE of the dependence of the magnetic permeability of iron upon frequency or wave-length has long been recognized as significant in the theories of magnetism, and its value in the design of iron-core coils is obvious. Measurements of permeability at high frequencies have usually been made on iron wires, since from the simple geometry of the wire the complex effects of eddy current phenomena in the sample are more easily evaluated. In some of the methods that have been used, the iron sample is longitudinally magnetized by placing it in a coil carrying the high frequency current; in other methods, the specimen is circularly magnetized by passing the current through the specimen. Investigations in which logitudinal magnetization has been used depend upon the change in inductance of the magnetizing coil resulting from the introduction of the specimen. This effect has been utilized by Wwedensky and Theodortschik,[1] Wait,[2] Wait, Brickwedde, and Hall,[3] and Woods.[4] In investigations employing circular magnetization of the specimen, measurements have usually been made of the wave-length of the electromagnetic waves on parallel iron wires, the familiar Lecher system; on the other hand, some have depended upon the change in radiofrequency resistance of the specimen, determined by resonance or bridge methods. For wave-lengths not exceeding a few meters, the Lecher system has been used; for longer wave-lengths, resonance and bridge methods are more suitable. Results obtained by Lecher wire measurements have been reported by Hoag and Jones,[5] Glatthart;[6] by resonance methods, Wwedensky and Theodortschik;[1] by the bridge method, Kreielsheimer.[7]

In view of the inherent complexity of the magnetic phenomena and the difference in methods of magnetizing the samples, it is not surprising that one finds three high frequency permeabilities recognized in the literature. From the change in resistance of the sample with frequency, the resistance permeability μ_R is obtained by means of a skin-effect formula owing to Zenneck. A second permeability μ_L, calculated from the inner self-inductance of the specimen, was determined for circular magnetization by Kreielsheimer,[7] and for longitudinal magnetization by Woods.[4] Both employed formulas to correct for lack of uniformity of radial distribution of flux in the specimen. A third permeability, used by Wait[2] and his associates, is referred to as the apparent permeability μ. The apparent permeability μ differs from μ_L only because the latter has been obtained from the former by the application of formulas to correct for eddy-current effects in the specimen. The values of μ_R and μ_L are ideal values of permeability that are assumed to exist in an eddy-current-free sample. However, measured values of μ_R and μ_L obtained on the same specimen differ widely from each other, as shown by Kreielsheimer.[7] Correct values of μ_R and μ_L should throw light on our understanding of the phenomenon of magnetization.

* Now with the U. S. Navy.
** Now with the Eastman Kodak Company.
[1] B. Wwedensky and K. Theodortschik, Ann. d. Physik **68**, 463 (1922); Physik. Zeits. **24**, 216 (1923).
[2] G. R. Wait, Phys. Rev. **29**, 566 (1927).
[3] Wait, Brickwedde, and Hall, Phys. Rev. **32**, 967 (1928).
[4] R. W. Woods, J. App. Phys. **13**, 314 (1942).
[5] J. B. Hoag and H. Jones, Phys. Rev. **42**, 571 (1932).
[6] J. L. Glatthart, Phys. Rev. **55**, 833 (1939).
[7] K. Kreielsheimer, Ann. d. Physik **17**, 293 (1933).

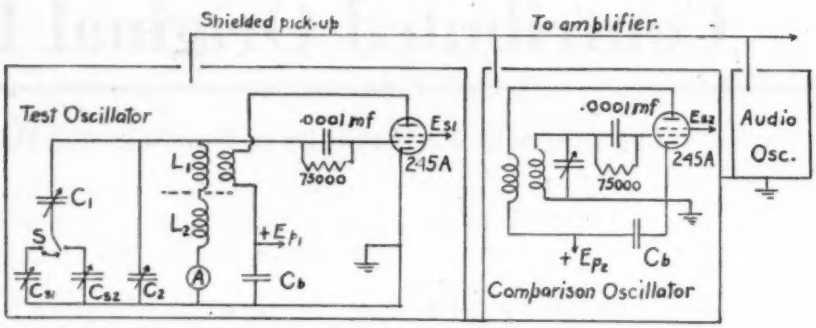

FIG. 1. Plan of the three-oscillator assembly.

On the other hand, μ appears to be of major interest in technical applications.

Wwedensky and Theodortschik[1] plotted values of μ_L against the wave-length λ and found in the neighborhood of 100 meters a sharp maximum between two minima. They noted that the anomaly in μ_L is similar to that of the optical index of refraction in going through an absorption band. In attempting to explain this anomaly, they assumed a resonance response of the elementary magnetic particles of the iron. Similar anomalies were observed by Mitiaev.[8] Subsequent experiments by Wait,[2] Wait, Brickwedde and Hall,[3] Kreielsheimer,[7] and Woods[4] have not confirmed the existence of an anomaly in permeability in the neighborhood of 100 meters.

In this paper we are reporting values of apparent permeability μ measured on iron wires of different diameters for a frequency range corresponding to wave-lengths 54–1150 meters.

II. METHOD

These values of permeability were determined from the change in inductance of a specimen coil in an oscillating circuit resulting from the introduction of the sample. Changes in inductance were calculated from changes in capacitance measured by a heterodyne method described by Belz,[9] and by Wwedensky and Theodortschik[1] and later improved by Wait.[2] Essential features of the apparatus, exclusive of amplifier, power supplies, and a General Radio wavemeter, type 724-A, are shown in Fig. 1. A Western Electric 245 A tetrode was used in the tuned-grid test oscillator. The tank circuit contained two inductances L_1 and L_2 connected in series and so separated and shielded as to prevent both magnetic and electrostatic interaction. The specimen coil L_2 was shielded electrostatically from the specimen by longitudinal strips of tinfoil glued to the surface of a glass tube and grounded. This glass tube was enclosed by a second glass tube on which were wound twenty-six turns of No. 16 copper wire spaced to form a coil 16 cm long. This coil was mounted in a vertical position to facilitate the introduction and removal of the specimen by a pulley system. The tuning coil L_1 was wound on a standard plug-in coil form. To obtain the desired wave-length coverage, interchangeable coils were used for L_1. The tank circuit capacitance was supplied by the array of condensers C_1, C_2, C_{S1}, and C_{S2}. The last two were General Radio precision type condensers; the first two were of semiprecision type calibrated against the first two. One of the precision condensers was in the circuit when the specimen was in the specimen coil; the other was in when the specimen was out of the coil. A mercury switch S, operated by the pulley system that controlled the position of the specimen, effected this interchange of condensers. With this array of condensers, a change in capacitance of the precision condensers results in a much smaller change in the capacitance of the system. For example, a change of 4 $\mu\mu$f in the precision condensers resulted in a change of 0.01 $\mu\mu$f in the combination.

A Western Electric vacuum thermocouple and galvanometer were used at A to maintain the current in the specimen coil at a known and constant magnitude. The current was controlled

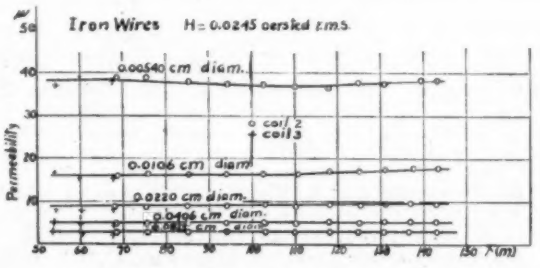

FIG. 2. Permeability as a function of wave-length in meters.

[8] W. K. Mitiaev, Zeits. f. Physik **38**, 716 (1926).
[9] M. H. Belz, Proc. Camb. Phil. Soc. **21**, 52 (1922); Phil. Mag. **44**, 479 (1922).

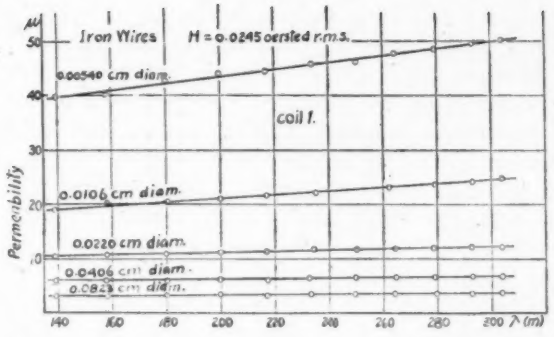

FIG. 3. Permeability as a function of wave-length in meters.

by adjustment of the screen-grid voltage E_{S1}, which was varied by means of a potential divider on the output of the filter of the rectifier.

With the circuit used, the d.c. component of the plate current does not magnetize the specimen; the d.c. component of the grid current produces negligible magnetic effect. Condenser bank, coils, and oscillator tube were in separate shielded compartments.

The comparison oscillator was designed to cover the same range of frequencies as the test oscillator. The tank circuit contained a tuning coil and a variable air condenser in parallel with a vernier condenser. The audio oscillator employed a single-tube circuit and operated at about 1000 c.p.s. The three oscillators were loosely coupled electrostatically through a shielded pick-up wire to the floating grid of a three-stage mixer-amplifier, the output of which was connected to a telephone headset. If the test oscillator were set at 1,001,004 c.p.s. and the comparison oscillator at 1,000,000 c.p.s., the audible beat tone has a frequency of 1004 c.p.s. If the audio oscillator at the same time were set at 1000 c.p.s., a second-order beat of 4 c.p.s. is heard. If the frequency of the test oscillator is gradually reduced to 1,000,000 c.p.s., the second-order beat frequency gradually reduces to zero. Frequency or wave-length calibration of the test oscillator was made by setting the test oscillator and comparison oscillator to zero-beat frequency and measuring the wave-length of the comparison oscillator by means of the loosely-coupled wave-meter.

Tests on the iron sample were carried out by setting the test oscillator at the desired wave-length with the sample out of the specimen coil. The comparison oscillator was set to produce a frequency higher than that of the test oscillator by an amount necessary to reduce the second-order beat frequency to zero. The introduction of the sample increases the inductance and reduces the frequency of the test oscillator. The frequency of the test oscillator was restored to its original value by such a change of tank capacitance as would bring the second-order beat frequency back to zero. By repeated trials, the settings of C_{S1} and C_{S2} were so adjusted that, upon the introduction of the specimen and the simultaneous interchange of C_{S1} and C_{S2}, no change in the frequency of the test oscillator existed. Wait[2] devised this arrangement to avoid effects of drift in the frequencies of the oscillators. In this procedure, change in inductance caused by the introduction of the sample is compensated by a change in capacitance so as to leave the frequency of the oscillating circuit unchanged. Under these conditions, the Kelvin formula relating frequency, inductance, and capacitance, leads to the equation

$$\Delta L/L = -\Delta C/C, \qquad (1)$$

in which ΔC represents the change in capacitance that will compensate for the change in inductance ΔL. In Eq. (1), C represents the total capacitance of the tank circuit, including that of the condensers and stray capacitance, and L represents the total inductance, including L_1, L_2, and any distributed inductance.

The total inductance L and the stray capacitance C_0 were determined for each coil combination by measuring the wave-length of the test oscillator corresponding to settings of C_2 covering its entire scale. Squares of wave-length were plotted against total capacitance of the condensers in circuit. From the slope of the linear graph, L was determined; from its intercept C_0 was found.

III. DESCRIPTION OF SPECIMENS

Five-centimeter lengths of chemically pure iron wire were used in making the samples. Each wire was enclosed in a sealed glass capillary tube. The test sample consisted of from one to twenty wires enclosed in a larger glass tube that moved freely in and out of the specimen coil. One end of the glass tube fitted into a Bakelite tube whose vertical motion carried the specimen each time to the same position in the coil.

IV. REDUCTION OF DATA

The inductance L_2 of the specimen coil was computed from its dimensions and number of turns by the use of a formula and tables of Nagaoka.[10] The computed inductance is 1.20

[10] Nagaoka, Bulletin 74, U. S. Bureau of Standards (Washington, D. C.).

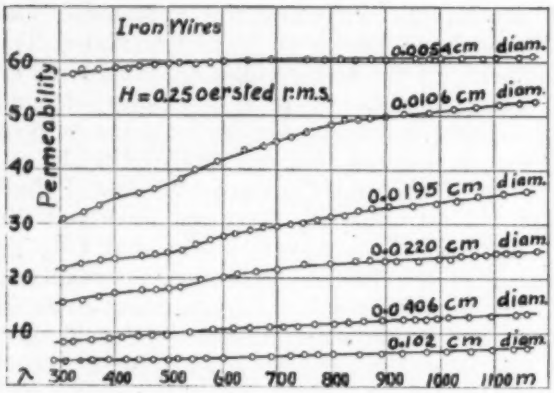

FIG. 4. Permeability as a function of wave-length in meters.

microhenrys. Since the specimen occupied only the middle third of the length of the specimen coil, it was in the uniform part of the field of the coil. Belz[9] derived an equation for computing the permeability under these conditions. We used the following modified form of Belz's formula:

$$\mu = 1 + \left(\frac{\text{Volume of specimen coil}}{\text{Volume of specimen wires}}\right) \times \left(\frac{L_1+L_2}{L_2}\right)\frac{\Delta C}{C}K, \quad (2)$$

in which $L_1+L_2=L$ the total measured inductance and C the total capacitance, including the stray capacitance C_0 of the oscillating circuit; and K is Nagaoka's correction factor for end-effects of the coil. The magnitude of the field intensity within the coil was computed by means of the usual formula for long solenoids.

V. RESULTS AND CONCLUSIONS

The dependence of the permeability μ upon the wave-length λ, in meters, is indicated by graphs of our results in Figs. 2–4. Data for Figs. 2 and 3 were obtained, for a constant $H=0.0245$ oersted, r.m.s., with the equipment shown in Fig. 1; those for Fig. 4 were obtained, for a constant $H=0.250$ oersted, r.m.s., with an earlier battery-operated set-up whose operation was similar to the later one. In the original set-up UV-199 triodes were used, and their tendency to drift in frequency makes the results given in Fig. 4 somewhat less reliable than those in Figs. 2 and 3. Diameters of wires are indicated on curves.

The permeability decreases with increase in frequency or decrease in wave-length. In contrast, Wait's results on wires of 0.0127-cm diameter indicate an increase in permeability with a decrease in wave-length. The wires used by Wait[2] were much longer than the magnetizing coil and were presumably in a non-uniform field. Moreover, his paper does not indicate that the magnetizing current was kept constant nor that the magnetic effect of the d.c. component of the plate current was eliminated. The presence of a d.c. magnetomotive force would reduce the measured values of μ. Wait's values of μ were of the order of one-half our values for comparable wire sizes.

A decrease in permeability μ with increase in frequency and increase in diameter of the wires is caused by the reduction in flux produced by eddy currents in the cross section of the wire. The demagnetizing effect of the eddy-current counter mmf increases with frequency and diameter and electrical conductivity of the wire. At longer wave-lengths and on wires of smaller diameter, the reduction in μ caused by eddy-currents decreases, and μ approaches the value of μ_L. At 1000 meters wave-length, the value of μ for the wire of 0.0054-cm diameter will be observed from Fig. 4 to be 61. Woods'[14] value of μ_L is 60.

Small inflections occur at about 500 meters in the curves for wires of diameters 0.0106, 0.195, and 0.0220 cm and at 110 meters for the wire of 0.0054-cm diameter. We do not know the cause of these variations, but we are inclined to attribute them to undiscovered systematic errors of measurement. On Fig. 2, a straight line drawn through the mean position of the points for the 0.0054-cm wire would probably represent the facts as accurately as the curve as it is drawn. Any apparent anomalies in our results are regarded as spurious. The small inflections observed were within the estimated accuracy of measurements of 5 percent.

Although these measurements were made at values of $H<1$ oersted, where the permeability is frequently assumed to be constant, a comparison of Figs. 3 and 4 at overlapping wave-lengths indicates an increase in permeability with increase in H even at these low field intensities. The data are too meager to be conclusive on this point.

Logarithmic plots of permeability against diameters of wires at specific wave-lengths indicate that the permeability μ varies inversely as the 0.9 power of the diameter, or to a rough approximation inversely as the diameter.

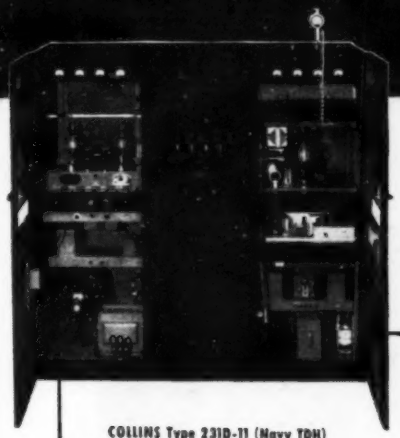

COLLINS Type 231D-11 (Navy TDH)
Multi-frequency transmitter

Output CW—5 KW; Output 'Phone—3 KW 100% modulated with a pair of Eimac 450TL tubes in class "B" audio; continuous coverage from 2 MC to 18.1 MC with 11 preset channels in that range and complete manual coverage throughout whole range. Capable of completely unattended remote control operation and of A1, A2 and A3 type emission. Audio characteristics: plus or minus three DB from 150 to 3,500 cycles. Total harmonic distortion less than 10%. The transmitter can be terminated into a 50 to 1,200 pure resistive load at zero degrees phase angle. 70 to 850 ohm load at plus or minus 45 degrees and 100 to 600 ohms at plus or minus 60 degrees.

COLLINS ENGINEERING AND EIMAC TUBES
achieve outstanding results

This Collins type 231D-11 (Navy TDH) radio transmitter is an outstanding demonstration of the value of capable engineering coupled with the intelligent choice and use of vacuum tubes.

It is the latest of a series of Collins Autotune, quick shift transmitters which were originally introduced in 1939, and which use Eimac tubes in the important sockets. In the 231D-11, two Eimac 750TL tubes in parallel make up the power amplifier, while a pair of Eimac 450TL tubes in class "B" are used as modulators for voice and MCW emission.

Mr. F. M. Davis, General Manager of the Collins Engineering Division, says: "Eimac tubes have been found to be reliable, rugged and capable of withstanding the severe overloads encountered during equipment tests, without damage." Statements like this, coming from such men as Mr. Davis, offer proof that Eimac tubes are first choice of leading engineers throughout the world.

Write for your copy of Electronic Telisis — a 64 page booklet fully illustrated — covering fundamentals of Electronics and many of its important applications. Written in layman's language.

Follow the leaders to

Eimac

REG. U. S. PAT. OFF.

TUBES

Eimac has received
8 ARMY-NAVY "E" AWARDS
for production efficiency
San Bruno 5, Salt Lake City 3

EITEL-McCULLOUGH, Inc., 956 San Mateo Ave., San Bruno, Calif.
Plants located at: San Bruno, California and Salt Lake City, Utah
Export Agents: Frazar & Hansen, 301 Clay Street, San Francisco 11, California, U. S. A.

Recent Applications of Physics

Prepared by CLARK GOODMAN, Associate Editor

Material to be included in this section should be submitted to Dr. Clark Goodman, Massachusetts Institute of Technology, Cambridge 39, Massachusetts.

Lightning Currents The magnitude and wave shape of the discharge currents in 46 direct lightning strokes measured at 25 different localities during the past five years have recently been reported by G. D. McCann of Westinghouse Electric and

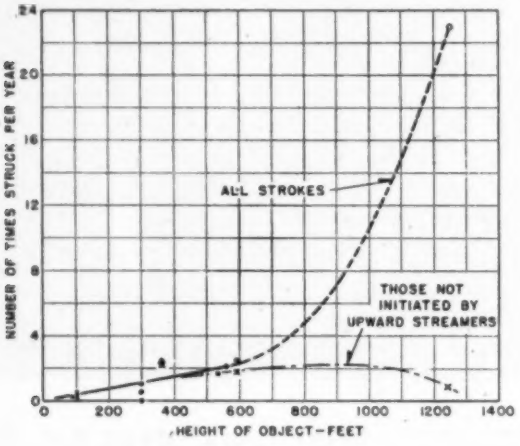

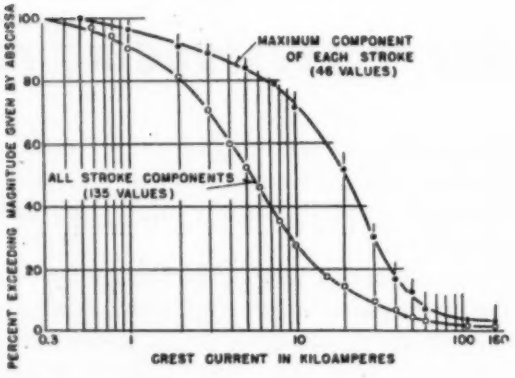

Manufacturing Company.[1] The structures ranged in height from 75 to 585 feet. The probability of being struck is approximately proportional to the height as seen in the solid curve of the upper graph. Laboratory model tests confirm this conclusion. The greater number of strokes to the 1250-foot structure, the Empire State Building, results from the more frequent occurrence of upward streamers from the building contacting charge centers in clouds that otherwise would produce strokes to ground by another path. Strokes to lower structures are usually initiated by single or multiple downward streamers. About 50 percent of all strokes are multiple. Time intervals between successive components as high as 0.5 second have been recorded with about 80 percent lying between 0.01 and 0.1 second. Of all recorded strokes, 96 percent started with a flow of negative charge from the cloud; 86 percent were entirely negative in polarity, and only 4 percent entirely positive. The principal range of total stroke charge is below 100 coulombs with 55 percent involving 10 coulombs or less. Ninety percent of the strokes are between 0.005 and 0.5 second in duration. The distribution of crest currents in individual stroke components is shown in the lower graph. The maximum current recorded is 160,000 amperes, while 75 percent exceed 10,000 amperes and 20 percent exceed 40,000 amperes.

[1] G. D. McCann, Preprint A.I.E.E. meetings (June 26–30, 1944).

Pop! Goes the Rivet Explosive rivets—in which the force of a minute explosive charge is controlled so accurately that the rivet shank is expanded within limits of 0.020 of an inch—are contributing greatly to the speed with which America's aircraft industry is turning out combat and transport planes.

The first explosive rivets had a small charge in the shank end, which, when exploded, expanded the end as effectively as if the rivet had been bucked by hand. Recently E. I. du Pont de Nemours and Company developed a rivet containing an explosive charge the full length of the shank. When this is detonated, the end expands into a barrel-shaped head and the shank fills the hole tightly, as shown in the sectional view. This eliminates close tolerance drilling and push-fitting the rivets into the holes.

The charge is composed of organic explosives and very finely divided aluminum which is used essentially to facilitate transfer of heat. The explosive is heat sensitive, firing at approximately 130°C, but it is relatively insensitive to shock and friction.

The rivets are fired within about 1½ to 3 seconds after the special electric heating iron is touched to the heads. In the accompanying photograph a Glenn Martin worker is installing these rivets in a B-26 bomb-bay door.

Millions of these rivets are being used to make dependable "blind" fastenings in the hard-to-get-at places. Virtually all of the production is now going into war uses,

Now at your

FINGER TIP

you have the solution of the most intricate simultaneous equations encountered in spectroscopic analysis

in minutes!

E.L.I. SPECTRO COMPUTER

PATENT APPLIED FOR

A development of the Research Department of Phillips Petroleum Company, outstanding manufacturer of automotive and aviation fuels, working in conjunction with Engineering Laboratories, Inc.

In the manufacture of high octane aviation fuels, synthetic rubber, butadiene and other critical war materials, quality control is being maintained by means of Mass and Infrared Spectrometers. By means of these devices accurate analysis can be made in minutes, instead of days.

The principal amount of time now required in multicomponent analysis by spectrophotometry is due to lengthy mathematical computations. Often hours are consumed in solving the more complicated equations encountered. Now, however, by means of the E. L. I. SPECTRO COMPUTER, routine problems involving eleven simultaneous equations in eleven unknowns can be solved in five minutes. The more complicated equations can be solved in fifteen minutes. The instrument is compact and simple in design. The operation is basically electrical following a mathematical method of iteration. It is so simple to operate that a high school student after a half hour's instruction can obtain foolproof results within the accuracy of the spectrometer data.

Designed primarily for solution of the type equations encountered in spectroscopic methods of analysis, this E. L. I. SPECTRO COMPUTER offers many applications. Your inquiry will bring full information.

U. S. ARMY AIR FORCES ★ ***APPROVED*** **INSPECTION RATING**

EQUIPMENT IN E.L.I. TRADE MARK REGISTERED **WORLD-WIDE USE**

Engineering Laboratories, Inc.

CONSULTING ENGINEERS & MANUFACTURERS

602-624 East Fourth Street **Tulsa 3, Oklahoma, U. S. A.**

but numerous peacetime applications are foreseen. The possibilities include their use in the construction of bus and passenger car bodies, refrigeration cabinets and lockers for the home and farm, in construction of prefabricated houses, and in the assembly of ships, radio units, and household appliances. All explosive rivets now are made of 17S-T aluminum alloy, but development work is under way toward adaptation of other metals, including soft iron, copper, monel metal, and stainless steel.

Hydration of Portland Cement Although Portland cement is one of the most important of building materials, its setting and hardening processes are not clearly understood. In fact, the theory proposed by LeChatelier in 1887 regarding the nature of the major reactions involved is still dominant in spite of considerable subsequent study of the problem. It is, of course, anticipated that a more exact understanding of the hydration processes would lead to

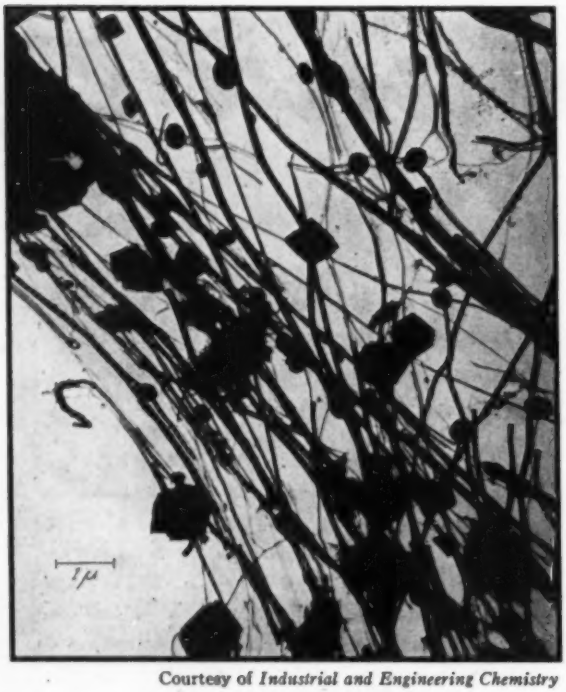

Courtesy of *Industrial and Engineering Chemistry*

improvements in the product. Toward this objective it has recently been established[1] that the crystal growth associated with setting and hardening can be followed by examination of specially prepared samples with the electron microscope. By comparing electron micrographs of pure compounds, presumed to be constituents of Portland cement, with similar photographs of artificial mixtures of these compounds and of Portland cements following hydration, valuable information has been obtained. Among the more practical results is that the strength of concrete apparently may be attributed to an abundance of crystals in the form of splines, needles, and fibers matted together and banded by the amorphous mass as seen in the accompanying micrograph of a Portland cement hydrated 18 days. Additional strength may be imparted by laminations and the strong surface forces of numerous platelike crystals.

[1] C. M. Sliepcevich, L. Gildart, and D. L. Katz, Ind. Eng. Chem. 35, 1178–1187 (1943).

New Booklets

Miniature Precision Bearings, manufacturers of miniature radial, pivot, and special bearings, precision parts and tools, has published a new Bulletin No. 44 showing complete and integrated line of miniature ball bearings for instrument, industrial, and special uses. The Bulletin is accompanied by a survey sheet which may be used by designers for obtaining engineering recommendation on any bearing application. Requests for further information should be addressed to Miniature Precision Bearings, Keene, New Hampshire.

Lectrofilm capacitors, available in case −60, −65, and −70 types, which are mechanically interchangeable with mica capacitors types CM60, 65, and 70 as listed in American War Standards Spec. C75.3, have been announced by the General Electric Company. Lectrofilm Capacitors are described in Bulletin GEA-4295 which is published by General Electric Company, Schenectady, New York, and is available there.

A new 4-page folder describing the Hitemp Dilatometer has been published by Harry W. Dietert Company, 9330 Roselawn Avenue, Detroit 4, Michigan, and will be sent upon request.

Walker-Jimieson, Radio and Electronic Distributors at 311 South Western Avenue, Chicago, Illinois, publish each month an Industrial Availability Booklet showing items available on priority for immediate delivery of stock. This booklet can be obtained free upon request by any engineers or purchasing agents. (October issue, 32 pages.)

As part of a movement under way to bring the Americas closer together in trade and harmony of friendship through an exchange of language knowledge, the Latin Americans learning English while North Americans study Spanish, the Pan American Society has prepared a free pamphlet which describes the words and endings of words and the similarity in the spellings of Spanish and English words. Applicants for the pamphlet on simplified Spanish should send their names and addresses to the Pan American Society, Box 315, Quito, Ecuador, South America.

Bronze with greatly increased strength and toughness can be made from common grades of tin and copper without the purchase of new or special equipment. The process is the result of several years of research and is now disclosed in the two latest publications of the Tin Research Institute, Nos. 120 and 121, which are reprints from the *Journal of the Institute of Metals* (Vol. 70, 1944, 127–147 and 275–289). A limited number of reprints will be available upon request from the Tin Research Institute, Fraser Road, Greenford, Middlesex, England.

Wenner Thermocouple Potentiometer, a 12-page catalog, describes the basic advantages which the potentiometer makes available. There is a discussion of the Wenner principle underlying the instrument design. There is also information about mechanical construction, including a description of important details, which helps to minimize and compensate for error resulting from parasitic e.m.f.'s. For Catalog E-33A(1), write to Leeds & Northrup Company, 4934 Stenton Avenue, Philadelphia 44, Pennsylvania.

A 16-page catalog, *Optical Pyrometer* (potentiometer type), recently reprinted with minor changes by the Leeds & Northrup Company, describes a portable instrument to measure temperatures of glowing objects. For more complete information, Catalog N-33D can be requested from Leeds & Northrup Company, 4934 Stenton Avenue, Philadelphia 44, Pennsylvania.